THESIS

COMPARATIVE S-FTIR ANALYSIS OF JAK INHIBITORS IN TF-1 CELLS AND EVALUATION OF KERRA™ EXTRACT FOR HCT116 COLON CANCER

JEERAPRAPA SIRIWASEREE

GRADUATE SCHOOL, KASETSART UNIVERSITY
Academic Year 2024

THESIS APPROVAL
GRADUATE SCHOOL, KASETSART UNIVERSITY

DEGREE: Doctor of Philosophy (Biochemistry)
MAJOR FIELD: Biochemistry
DEPARTMENT: Biochemistry

TITLE: Comparative S-FTIR Analysis of JAK Inhibitors in TF-1 Cells and Evaluation of Kerra™ Extract for HCT116 Colon Cancer

NAME: Miss Jeeraprapa Siriwaseree

THIS THESIS HAS BEEN ACCEPTED BY

THESIS ADVISOR
(Associate Professor Kiattawee Choowongkomon, Ph.D.)

THESIS CO-ADVISOR
(Ms. Buabarn Kuaprasert, Ph.D.)

DEPARTMENT HEAD
(Mr. Napapol Poopanitpan, Ph.D.)

DEAN
(Associate Professor Weeraphart Khunrattanasiri, Dr.rer.nat.)

THESIS

COMPARATIVE S-FTIR ANALYSIS OF JAK INHIBITORS IN TF-1 CELLS AND EVALUATION OF KERRA™ EXTRACT FOR HCT116 COLON CANCER

JEERAPRAPA SIRIWASEREE

A Thesis Submitted in Partial Fulfillment of
the Requirements for the Degree of
Doctor of Philosophy (Biochemistry)
Graduate School, Kasetsart University
Academic Year 2024

Jeeraprapa Siriwaseree : Comparative S-FTIR Analysis of JAK Inhibitors in TF-1 Cells and Evaluation of Kerra™ Extract for HCT116 Colon Cancer. Doctor of Philosophy (Biochemistry), Major Field: Biochemistry, Department of Biochemistry.
Thesis Advisor: Associate Professor Kiattawee Choowongkomon, Ph.D.
Academic Year 2024

This dissertation comprises two distinct research inquiries. The first inquiry analyzes the chemical signatures of TF-1 cells post JAK inhibitor treatment, specifically Ruxolitinib and Tofacitinib, using S-FTIR spectroscopy. JAK pathway deregulation is associated with myelofibrosis pathogenesis. Ruxolitinib demonstrated superior inhibitory efficacy over Tofacitinib, which targets JAK3. PCA successfully differentiated untreated and drug-treated cells, revealing biochemical changes in cellular components. The results affirm FTIR's efficacy in investigating drug-induced molecular changes, emphasizing JAK inhibitors' unique effects on cellular elements. The second investigation examines Kerra™ , a botanical extract from the Takxila scripture, on HCT116 colorectal cancer cells. This study evaluated the extract's effects on cancer cell viability and apoptosis through various assays. Apoptotic protein marker levels were quantified and elucidated the extract influenced the proteins and pathways by proteomics analysis. Kerra™ extract demonstrated a dose-dependent cytotoxicity, with higher concentrations leading to reduced cell viability in a 72-hour treatment period plus revealing early-late apoptosis characteristics. LC-MS/MS analysis identified 3,406 proteins. Pathway analysis indicated that Kerra™ extract induced apoptotic signaling and inhibited proliferation in cell lines via the EIF2 pathway. Regulatory proteins, including CDKN1A and MYC, were identified. Importantly, caspase 8 and 9 expression levels significantly increased in response to Kerra™ compared to Doxorubicin. These findings strongly support the extract's ability to induce apoptosis in HCT116 colon cancer cells. Its efficacy was confirmed through its dose-dependent cytotoxicity, apoptotic induction, and modulation of key proteins in death and proliferation pathways. This research highlights Kerra™ 's potential as a promising therapeutic entity in cancer treatment.

_____ _____ ____ / ____ / ____

Student's signature Thesis Advisor's signature

ACKNOWLEDGEMENTS

I am immensely grateful to Associate Professor Dr. Kiattawee Choowongkomon for allowing me to pursue my doctoral program. His extensive knowledge, expertise, and encouragement were invaluable and greatly contributed to the success of my thesis. I also appreciated my co-advisor, Dr. Buabarn Kuaprasert, for the support and respected guidance provided to me as I worked on the thesis and related publications. This achievement would not have been possible without the support of the Royal Golden Jubilee Ph.D. Program between the National Research Council of Thailand (NRCT) and the Synchrotron Light Research Institute (SLRI) (Grant no. PHD/0137/2561). Furthermore, I wish to express my gratitude for the valuable comments and feedback provided by the defense committees, which were instrumental in the successful completion.

I also express my sincere gratitude to Associate Professor Dr. Panan Kanchanaphum for his invaluable tutoring and support, particularly for facilitating my introduction to my advisor which enabled me to pursue my doctoral studies. I am deeply appreciative of the knowledge and guidance provided by my teachers. Additionally, I am thankful to my colleagues at KC lab, especially Dr. Siriluk Ratanabunyong, for their collaborative efforts, constructive feedback, and moral support during early-morning and late-night work sessions. I am also grateful to the research assistants, scientists, and officers from the Department of Biochemistry for their assistance and support.

Finally, I would be remiss in not mentioning my family, particularly my parents and siblings, for their unwavering support. Their constant belief in my abilities provided the encouragement and resilience necessary to persevere through favourable and adverse circumstances. Their influence has prevented despondency and steering me towards accomplishment.

Jeeraprapa Siriwaseree

TABLE OF CONTENTS

Page

ABSTRACT C

ACKNOWLEDGEMENTS ..... D

TABLE OF CONTENTS ..... E

LIST OF TABLE ..... F

LIST OF FIGURES ..... G

LIST OF PUBLICATION 9

LIST OF ABBREVIATIONS 10

SCOPE/STRUCTURE OF STUDY 11

INTRODUCTION 13

- Background and Rationale 14
- Objectives 15
- Contributions and Outcome of Research 15

PUBLICATIONS 17

- Publication 1 17
- Publication 2 43

CONCLUSION 69

RECOMMENDATIONS AND FUTURE WORK 70

FUNDING SOURCES 71

LITERATURE CITED 2

APPENDICES 3

- Appendix A 3
- Appendix B 6

CURRICULUM VITAE 100

LIST OF TABLE

Page

Table 1 The second derivative FTIR spectra band assignments for the vibration of functional groups that are found in untreated and drug-treated TF-1 cells.....31

Table 2 Upstream protein regulators predicted to be activated (positive value of activation z-score) or Inhibited (minus value of activation z-score) in HCT116 cells after Kerra™ extract treatment. 57

Table S3 Protein expression data. 6

LIST OF FIGURES

Page

Figure 1 TF-1 cells viability after treatment with Ruxolitinib and Tofacitinib at various concentrations. 22

Figure 2 2D interactions of Ruxolitinib and Tofacitinib complexed with (A and B) JAK1, and (C and D) JAK2. 23

Figure 3 (A)The average absorbance FTIR spectra of TF-1 cells in untreated conditions (blue), Tofacitinib treated cells (red), and Ruxolitinib treated cells (green). (B) Two-dimensional PCA score plot in PC1-2. (C) PCA corresponding loading plot PC1-2 indicating all samples biomarker differentiation. 27

Figure 4 The average of second derivative FTIR spectra characterize lipid regions in the wavelengths from 3,000 to 2,800 cm^{-1} of 60 spectra of untreated TF-1 cells (blue), 100 spectra of cells treated with 30.28 µM Tofacitinib (red), and 42 spectra of cells treated with 14.47 µM Ruxolitinib (green) after incubation for 72 h. 28

Figure 5 Average second derivative FTIR spectra characterize protein regions in wavelengths from 1,700 to 1,600 cm^{-1} of 60 spectra of untreated TF-1 cells (blue), 100 spectra of Tofacitinib treated (30.28 µM) cells (red), and 42 spectra of Ruxolitinib treated (14.47 µM) cells (green) after incubation for 72 h. 29

Figure 6 Average second derivative FTIR spectra characterize nucleic acids regions in wavelength from 1,300 to 1,000 cm^{-1} of 60 spectra of untreated TF-1 cells (blue), 100 spectra of 30.28 µM of Tofacitinib treated cells (red), and 42 spectra of 14.47 µM Ruxolitinib treated cells (green) after incubated for 72 h. 30

Figure 7 Cytotoxicity effect of Kerra™ extracts against HCT116 cells after 72 hours of exposure using MTT assay at the concentration ranging from 5 - 0.020 mg/mL in logarithmic scale. 53

Figure 8 Apoptosis cell characteristic analysis using Muse™ Annexin V assay. Two-dimensional diagram of viability and Annexin V-position cells in negative control (A), positive control (B) and Kerra™ extract (C) groups. 54

Figure 9 Differences in proteome expression by a volcano plot. The plot shows a negative natural log of the p values plotted against the base2 log values of the change in each protein between the Kerra extract with control group (Figure 9). Significantly differentially expressed protein were chosen by $p < 0.01$ and log2 fold change >2. The upregulated and down-regulated proteins are marked as red and blue dots, respectively. 55

Figure 10 The IPA analysis revealed the identification of canonical pathways. The threshold levels were indicated by the horizontal line. A negative z score indicates pathway inhibition, while a positive z score indicates pathway activation. White (transparent) bars signify "no activity" within the pathway 56

Figure 11 The level of caspase 8 and caspase 9 expression were determined. (A) The efficiency and accuracy of immune-based reactions with (black bar) and without apoptotic stimulant compound (white bar) in A549 and HeLa reference cell lines. (B) The effect of Kerra™ extract on the levels of caspase 8 and caspase 9 level in HCT116 cells was measured. The Dox-treatment group is represented by white bar, while the Kerra™ treatment group is represented by black bar. The error bars indicate ± S.D. 58

Figure 12 Protein upstream regulators and phytochemical in Kerra™ extract interaction prediction. Ligand protein mapping was constructed from 2-methoxy-xanthen-9-one, isorhapontigenin, betaine, anethole, and eicosatetraynoic acid with the upstream regulators. The predicted interactions were shown in the connecting line. .61

Figure S13 The docking energy scores of known drugs with the JAK1 and JAK2 proteins.....4

Figure S14 The binding pattern of known drugs within JAK1 and JAK2. (A) Ruxolitinib and Tofacitinib complexed with JAK1. (B) Ruxolitinib and Tofacitinib complexed with JAK2.....4

Figure S15 Summary of histograms showing interactions of Ruxolitinib and Tofacitinib complexed with JAK1 and JAK2.....5

LIST OF PUBLICATION

Page

1. Synchrotron Fourier Transform Infrared Microscopy Spectra in Cellular Effects of Janus Kinase Inhibitors on Myelofibrosis Cancer Cells……...17
2. Exploring the Apoptotic-Induced Biochemical Mechanism of Traditional Thai Herb (Kerra™) Extract in HCT116 Cells Using a Label-Free Proteomics Approach…….43

LIST OF ABBREVIATIONS

CDKN1A	= Cyclin-Dependent Kinase Inhibitor 1A
DMSO	= Dimethyl Sulfoxide
Dox	= Doxorubicin
FBS	= Fetal Bovine Serum
GM-CSF	= Granulocyte-Macrophage Colony-Stimulating Factor
IC_{50}	= The Half-Maximal Inhibitory Concentration
IL-3	= Interleukin-3
IPA	= Ingenuity Pathway Analysis
ISI	= Infrared Spectroscopy and Imaging
JAKs	= Janus Kinases
MCT	= Mercury-Cadmium-Telluride
MFI	= Median Fluorescence Intensity
PCA	= Principal Component Analysis
SD	= Standard Deviation
SEM	= Standard Error of the Mean
S-FTIR	= Synchrotron Fourier Transform Infrared Spectroscopy
SLRI	= Synchrotron Light Research Institute
STAT	= Signal Transducer and Activator of Transcription
TYK2	= Tyrosine Kinase 2

Comparative S-FTIR Analysis of JAK Inhibitors in TF-1 Cells and Evaluation of Kerra™ Extract for HCT116 Colon Cancer

SCOPE/STRUCTURE OF STUDY

This project contains two studies including the Janus kinase (JAK) inhibitor's effects on TF-1 myelofibrosis cancer cells and the apoptotic effects of the Kerra™ extract on HCT116 colorectal cancer cells.

The research paper titled "Synchrotron Fourier Transform Infrared Microscopy Spectra in Cellular Effects of Janus Kinase Inhibitors on Myelofibrosis Cancer Cells" aims to assess the chemical changes in cells following treatment with JAK inhibitors, shedding light on their potential for myelofibrosis therapy. The study utilizes synchrotron Fourier transform infrared (S-FTIR) spectroscopy to delve into the molecular-level impacts of these drugs on cellular biochemical components. By employing a fingerprint approach that combines S-FTIR data with in vitro cytotoxicity assays, the research unveils distinct patterns of cellular responses to the JAK inhibitors. The comparison of two inhibitors, Ruxolitinib and Tofacitinib, reveals that Ruxolitinib has a more pronounced inhibitory effect on TF-1 cells. Furthermore, the study involves calculating IC_{50} values and utilizing principal component analysis (PCA) to categorize cellular biochemical alterations under different treatment conditions. The research sheds light on the molecular changes induced by JAK inhibitors on TF-1 myelofibrosis cancer cells using advanced spectroscopic techniques, aiming to enhance understanding of their biochemical impacts and therapeutic potential.

The second publication was titled "Exploring the Apoptotic-Induced Biochemical Mechanism of Traditional Thai Herb (Kerra™) Extract in HCT116 Cells Using a Label-Free Proteomics Approach". This study delves into the mechanisms through which the Kerra™ extract triggers apoptosis in the HCT116 colorectal cancer cell line. It investigates the effects of the Kerra™ extract on cell viability and apoptosis in a dose-dependent manner. Additionally, the research aims to understand the biochemical mechanisms that regulate apoptotic markers such as caspase-8 and

caspase-9. The study utilizes a label-free proteomics approach to analyze changes in protein expression, shedding light on the molecular mechanisms and pathways impacted by the Kerra™ extract. These articles form an integral part of my graduation thesis.

INTRODUCTION

Cancer is the rapid creation of abnormal cells that grow from the transformation of normal cells into tumor cells. In general, cancer progresses from a pre-cancerous lesion to a malignant tumor that grows beyond and can invade bordering parts of the body and spread to other organs referred to as metastasis. Metastases are the main cause of death from cancer. These changes are the result of the interaction between a person's genetic factors and external agents. Global cancer statistics 2018: GLOBOCAN estimates of incidence and mortality worldwide for 36 cancers. In both sexes combined, lung cancer is the most diagnosed cancer (11.6% of the total cases) and the leading cause of cancer death (18.4% of the total cancer deaths), closely followed by female breast cancer (11.6%), the most commonly diagnosed cancer and the leading cause of cancer death [1].

The treatment to treat and manage cancer is available. The effectiveness of the treatment depends on the type of cancer, the location of the tumor, and the stage of its progression. Some traditional and widely used treatment options include surgery, radiation-based surgical knives, chemotherapy, and radiotherapy. Although chemotherapy is commonly used, it often comes with side effects. However, these treatments have not been able to significantly improve mortality rates or prolong survival time for metastatic cancer. In addition, drugs, biological molecules, and immune-mediated therapies are now being used for treatment.

New medications that target specific tumor pathways and characteristics are being researched to create a revolution in cancer treatment [2]. For instance, JAK inhibitors are a class of drugs that target the JAK/STAT signaling pathway which is the dysregulated cell signaling pathway that leads to tumor growth. Preclinical has shown tumor inhibition results, enhanced therapies' effects, and treating solid tumors in several clinical trials [3-5]. Nevertheless, some inhibitors found side effects and adverse events associated with infectious events among patients using these medications [6, 7]. Therefore, finding alternative methods that are more effective and less toxic is necessary. Traditional medicine is the first line of treatment that relies on the concern about the synthetic drug's safety and efficacy.

Natural products are increasingly identified as sources of pharmacological drugs and are used to treat various diseases, including cancers and neurological disorders [8].

The development of dependable and inexpensive technologies for the screening of individuals with cancer, for improving the early diagnosis of cancer and the prediction of treatment, and for prevention activities to reduce the incidence of cancer. For this reason, cancer biomarkers and molecular changes are important for discovering and validating cancer research [9]. The FTIR is a powerful tool for the study of biological systems. Its spectroscopy can consider molecular changes in cells exposed to antitumor drugs based on the S-FTIR spectrum [10]. Likewise, Proteomics analysis has become critical in biological alternated investigation. This technology has identified information, including protein targets and signaling pathways associated with cancer cell growth and cellular response.

Background and Rationale

First publication, JAKs are intracellular tyrosine kinases that play a crucial role in signal transduction for cytokines and growth factors via the JAK/STAT pathway. Dysregulation of JAKs can result in cancer and autoimmune diseases. Specifically, JAK2 mutations have been associated with myelofibrosis, a form of bone marrow cancer. Therefore, the inhibition of JAK2, such as with Ruxolitinib and Tofacitinib, is an important therapeutic option. Ruxolitinib selectively inhibits JAK1 and JAK2, while Tofacitinib is more specific to JAK3. Understanding the distinct mechanisms of these inhibitors is essential for optimizing treatment strategies for myelofibrosis. In this study, S-FTIR spectroscopy is used to analyze molecular changes in cancer cells following drug treatment, providing insights into the chemical fingerprints of cells and their responses to drugs. Previous research has shown that FTIR spectroscopy is effective in evaluating drug sensitivity in cancer cells and interactions of molecular components with anti-cancer drugs. This study aims to explore the specific effects of JAK inhibitors on TF-1 cells and to better characterize the impact of JAK2 inhibition, offering insights into the differing clinical effectiveness of the two drugs.

In the second publication, recent studies have shown a growing interest in utilizing natural products for cancer treatment due to their ability to impact multiple

pathways involved in cancer cell growth. This approach has shown promise in identifying new potential drugs that may be more effective than single compounds targeting specific markers. Specifically, the research emphasizes the importance of traditional herbs, such as the Kerra™ extract, which is a combination of various medicinal plants known for their potential in cancer treatment. Despite its historical use, there is a significant gap in our understanding of its efficacy and the mechanisms through which it affects cancer cells. Inducing apoptosis (cell death) in cancer cells is a crucial therapeutic strategy. Therefore, the study aims to investigate how the Kerra™ extract triggers this process in colon cancer cells through proteomics analysis. This method allows for a comprehensive exploration of protein changes in response to the Kerra™ extract, shedding light on the extract's effects on apoptosis and other cellular processes. This research underscores the potential of traditional medicine in providing effective and low-side-effect cancer treatments as an alternative to conventional therapies. By elucidating the apoptotic mechanisms induced by the Kerra™ extract, the study seeks to contribute to the development of safe and efficient cancer therapies.

Objectives

1. To evaluate the effects of JAK inhibitors, specifically Ruxolitinib and Tofacitinib, on erythroleukemia TF-1 cell line by S-FTIR spectroscopy.
2. To investigate how the Kerra™ extract induces apoptosis in HCT116 cells by exploring the biochemical pathways and mechanisms using proteomics.

Contributions and Outcome of Research

The first article successfully assessed the chemical fingerprints of TF-1 cells after treatment with Ruxolitinib and Tofacitinib using S-FTIR spectroscopy. Based on PCA can classify the biochemical alterations in treated versus untreated cells. It identified significant changes in lipid production, protein conformation, and nucleic acid levels, indicating how these inhibitors modify cellular biochemistry. These allowed for the identification of distinct molecular changes in response to the drugs, contributing to the understanding of their mechanisms of action. The findings suggest that FTIR spectroscopy can be a valuable tool for analyzing cellular responses

to drug treatments at the molecular level. The differences in the effectiveness of Ruxolitinib and Tofacitinib were found that Ruxolitinib had a two-fold higher inhibition effect on TF-1 cell lines compared to Tofacitinib. Ruxolitinib and Tofacitinib modulate the JAK/STAT signaling pathway that is shown to decrease STAT3 phosphorylation and induce apoptosis. This opens a broader understanding of myelofibrosis treatment and may help in developing more effective therapeutic strategies tailored to individual patient needs.

The second article indicated that the Kerra™ extract induced a higher level of late apoptosis and cell death compared to Doxorubicin (Dox) at IC_{50} concentration. The extract can activate apoptosis and suppress cell proliferation in HCT116 cells through the EIF2 signaling pathway. This finding is crucial as it elucidates the specific pathways involved in the apoptotic process triggered by the extract. The study identified 3406 proteins affected by the Kerra™ extract in cell lines. CDKN1A and MYC were predicted as upstream regulators in response to the Kerra™ extract. This extensive proteomic analysis provides a comprehensive overview of the biochemical changes induced by the extract, highlighting its potential as a therapeutic agent for colon cancer and understanding these regulatory proteins can help in developing targeted therapies that enhance the efficacy of the extract in inducing apoptosis in cancer cells.

PUBLICATIONS

Publication 1

Siriwaseree, J.; Sanachai, K.; Aiebchun, T.; Tabtimmai, L.; Kuaprasert, B.; and Choowongkomon, K. Synchrotron Fourier Transform Infrared Microscopy Spectra in Cellular Effects of Janus Kinase Inhibitors on Myelofibrosis Cancer Cells. **ACS Omega** 2022 7 (26), 22797-22803. DOI: 10.1021/acsomega.2c02404

Synchrotron FTIR microscopy spectra in cellular effects of JAK inhibitors on myelofibrosis cancer cells

Jeeraprapa Siriwaseree,[a] Kamonpan Sanachai,[b] Thitinan Aiebchun,[a] Lueacha Tabtimmai,[c] Buabarn Kuaprasert,[d] Kiattawee Choowongkomon [a,*]

[a]Kasetsart University, Faculty of Science, Department of Biochemistry, Bangkok 10900, Thailand

[b]Chulalongkorn University, Faculty of Science, Department of Biochemistry, Structural and Computational Biology Research Unit, Bangkok 10330, Thailand

[c]King Mongkut's University of Technology of North Bangkok, Faculty of Applied Science, Department of Biotechnology, Bangkok 10800, Thailand

[d]Synchrotron Light Research Institute (Public Organization), Nakhon Ratchasrima 30000, Thailand

*****E-mail: fsciktc@ku.ac.th, Tel: +662 5625444, Fax: + 66 25614627

Abstract

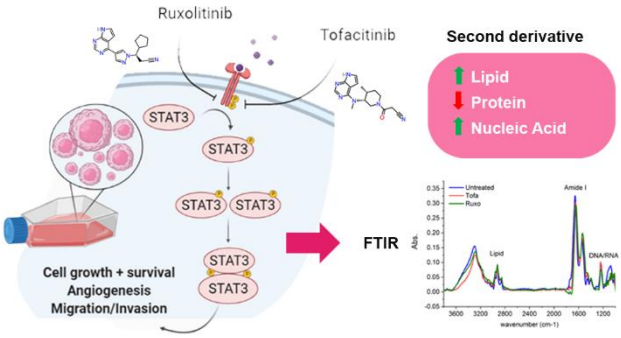

Janus kinases (JAKs) deregulation of the JAK/STAT pathway leads to myelofibrosis that can be treated by JAKs inhibitors including Ruxolitinib and Tofacitinib. Even though both inhibitors are effective against myelofibrosis, each of them has a different mode of action in the cells. Ruxolitinib is an inhibitor for selective JAK1/2 and Tofacitinib is an inhibitor for JAK3. This study evaluated the chemical fingerprints of TF-1 cells after JAKs inhibitor treatments by the Synchrotron Fourier transform

infrared microspectroscopy (S-FTIR) spectrum. Tofacitinib and Ruxolitinib treatments in TF-1 cells were applied with a chemical fingerprints approach in S-FTIR spectroscopy and in vitro cytotoxicity in a cell-based assay. Principal component analysis or PCA was utilized to classify three cell treatments with three biochemical alteration absorbances of lipids vibration by C-H stretching, protein amide I arise from C=O stretching, and P=O phosphodiester bond from nucleic acids. The results showed that the inhibition effect of Ruxolitinib on the TF-1 cell lines was two-fold higher than Tofacitinib. PCA distinguishes untreated and drug treatment by detected cellular biochemical alteration. The loading plots identify protein and nucleic acids were the different main components in disparate cell treatments. Tofacitinib separated from the others in lipid and nucleic acid. The second derivative spectra of three molecular components had decreased lipid production and accumulation, changes in secondary structures in proteins, and a high level of RNA overexpression in cell treatment. The JAKs inhibitors caused different spectroscopic biomarkers of the modifications of secondary protein conformation, stimulated cell lipid accumulation, and phosphorylation from untreated cells. The alteration of cellular biochemical components advises that the FTIR is a potential tool for used analyzing specific patterns of drug cellular responses at the molecular level.

Keywords: Synchrotron Fourier transform infrared microscopy (S-FTIR), Janus kinases (JAKs) inhibitors, Ruxolitinib, TF-1, Tofacitinib

Abbreviations: JAKs, Janus kinases; FTIR, Fourier-transform infrared spectroscopy; TYK2, Tyrosine kinase 2; STAT, Signal transducers and activators of transcription; IC_{50}, The half-maximal inhibitory concentration; GM-CSF, Granulocyte-macrophage colony-stimulating factor; IL-3, interleukin-3; DMSO, Dimethyl sulfoxide; FBS, Fetal bovine serum; SLRI, Synchrotron Light Research Institute; ISI, Infrared Spectroscopy, and Imaging; MCT, Mercury-cadmium-telluride; SEM, standard error of the mean; PCA, Principal component analysis

Introduction

Janus kinases (JAKs) are intracellular and nonreceptor tyrosine kinases family including, JAK1, JAK2, JAK3, and tyrosine kinase 2 (TYK2) that play signal transductions due to cytokines and growth factors[1]. These kinases are intermediaries between signal induction of cytokine and transcriptional factor phosphorylation, signal transducers and activators of transcription (STAT) passing through the JAK/STAT pathway. Therefore, JAK/STAT pathway deregulation can initiate cancer inflammation, and autoimmune diseases[2, 3].

JAK1 related to mutated sites has been associated with acute leukemia or B-cell lymphoma. JAK2 mutation is also allied with thrombocytosis, myelofibrosis, leukemia, and lymphoma, and JAK3 signaling increasing can develop T-cell acute lymphocytic leukemia[2, 4]. The tyrosine kinase domain location is in the JH1 domain at the C-terminal of the JAKs. This domain is controlled through a pseudokinase domain or JH2 that lacks Asp residue for phosphotransfer in the His/Arg/Asp motif of the catalytic loop in kinase activity. Hence, this domain is assumed to regulate the JH1 domain catalytic activity[5]. Among the JAKs, JAK2 is a critical target for the treatment of cancer disease. JAK2 inhibition can decrease the risk of bone marrow cancer due to the prevention of JAK2 activation.

Myelofibrosis cancer can be treated by JAKs inhibition[6]. Ruxolitinib and Tofacitinib are two FDA-approved drugs that widely used in clinical treatment of this cancer. These drugs interact in the ATP site of the JAKs and prevent JAKs activation. As a result, signal transduction cannot occur, and the risk of this cancer is decreased. Ruxolitinib is selective for JAK1/2 (The half-maximal inhibitory concentration (IC_{50}) for JAK1 = 3.3 and for JAK2 = 2.8 nM)[7], whereas Tofacitinib is more selective for JAK3 (IC_{50} = 34 nM) than JAK1/2 (IC_{50} = 81 and 80 nM, respectively)[8]. Ruxolitinib is effective for JAK1/2 inhibition, whereas Tofacitinib can inhibition of JAK1/3 more than JAK2. It is an interesting approach to investigate the binding pattern of both drugs with JAKs.

The FTIR is an effective tool for studying the biological systems by considering the effect of molecular changes in cells on antitumor drugs based on the FTIR spectrum[9]. Numerous FTIR chemical fingerprints between cancer cells and

drugs have been reported. The leukemic cell lines (K562) treated with an Akt1/2 kinase inhibitor (A6730) showed a noticeable change in the α-helix/β-strand conformation ratio[10]. A previous report revealed the capability of FTIR spectroscopy can evaluate the drug sensitivity in cells as well as interactions of different molecular components of anti-cancer drugs[11]. TF-1 cell line that originated from erythroleukemia in humans. These cells' proliferative are responsive to granulocyte-macrophage colony-stimulating factor (GM-CSF) or interleukin-3 (IL-3) through with JAK2/STAT signaling pathway activation[12]. Understanding the different inhibition patterns of drugs resulting from JAK2, based on the FTIR spectrum in cells treated with drugs, is important to better characterize the effect of JAK2 inhibition and the potential explanation for differences in clinical effectiveness.

In this study, the objective was to assess the chemical fingerprints of TF-1 cells after Tofacitinib and Ruxolitinib treatments. To achieve this, we applied a chemical fingerprints approach, using knowledge of both drugs in S-FTIR spectroscopy and *in vitro* cytotoxicity in a cell-based assay. These findings can be proposed that S-FTIR can be used for analyzing distinct patterns of cellular responses when drug-treated at the molecular level.

Results

3.1 Effect of Ruxolitinib and Tofacitinib on the TF-1 cell lines

We used the TF-1 cells to investigate the dose dependence of drug treatment using the Presto Blue assay. At 72 h, the IC50 of Ruxolitinib was 14.47±0.59 μM and Tofacitinib was 30.29±1.98 μM on TF-1 cells (**Figure 1**). These results showed that drugs can inhibit the viability of TF-1 cells, the inhibitory effect indicated that Ruxolitinib can inhibit TF-1 cells more than two-fold higher than Tofacitinib. However, the effect of both drugs on the TF-1 cells was further evaluated to consider molecular changes in cells by FTIR spectrum analysis.

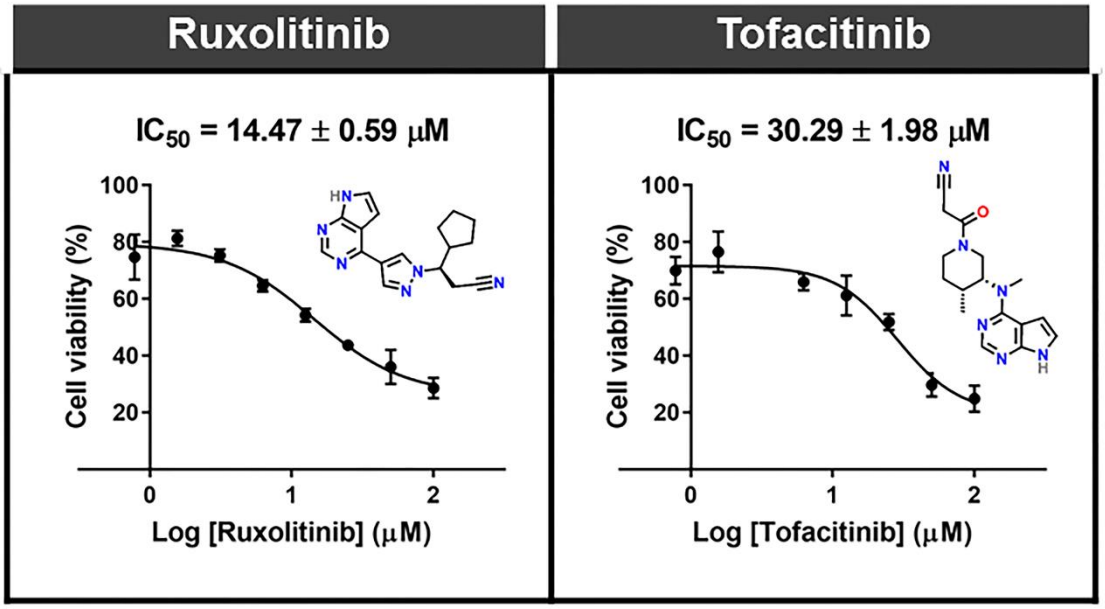

Figure 1 *TF-1 cells viability after treatment with Ruxolitinib and Tofacitinib at various concentrations.*

3.2 Molecular Docking

To demonstrate the interaction and binding mode of known drugs (Ruxolitinib and Tofacitinib) with JAK1 and JAK2, both compounds were individually docked into the binding pocket of the JAK1 and JAK2 proteins by using GOLD docking. The docking scores of Ruxolitinib in complex with both proteins (59.40 kcal mol^{-1} for JAK1 and 57.81 kcal mol^{-1} for JAK2) were higher than Tofacitinib (50.91 kcal mol^{-1} for JAK1 and 51.88 kcal mol^{-1} for JAK2) **(Figure S13)**. From these results confirmed the previously reports that the Ruxolitinib strongly interact with JAK1 than JAK2 whereas Tofacitinib strongly interact with JAK2 than JAK1. Moreover, the binding pattern and 2D interactions of all systems are illustrated in **Figure 2**. We found Ruxolitinib and Tofacitinib bound at the binding site with a similar pattern to JAK1/2; both compounds bound well with the deazapurine ring and stabilized through other interactions such as Pi-sulfur, Pi-alkyl, Pi-sigma, and van der Waals **(Fig. S14 and S15)**. Both drugs to be effective with JAK1 or JAK2 depending on the binding interactions and binding position inwards these proteins. The Glu957

and Leu959 are important interactions in the hinge region of JAK1[13], this interaction is determined to be important for the binding of inhibitors within the kinase protein. Therefore, Ruxolitinib strongly binding with JAK1 than Tofacitinib via the formation of two strong hydrogen bonds. Moreover, the Glu930 and Leu932 residues in the hinge region that are unique to JAK2[14], we found Ruxolitinib strongly binding with JAK1 than Tofacitinib via the formation of three strong hydrogen bonds.

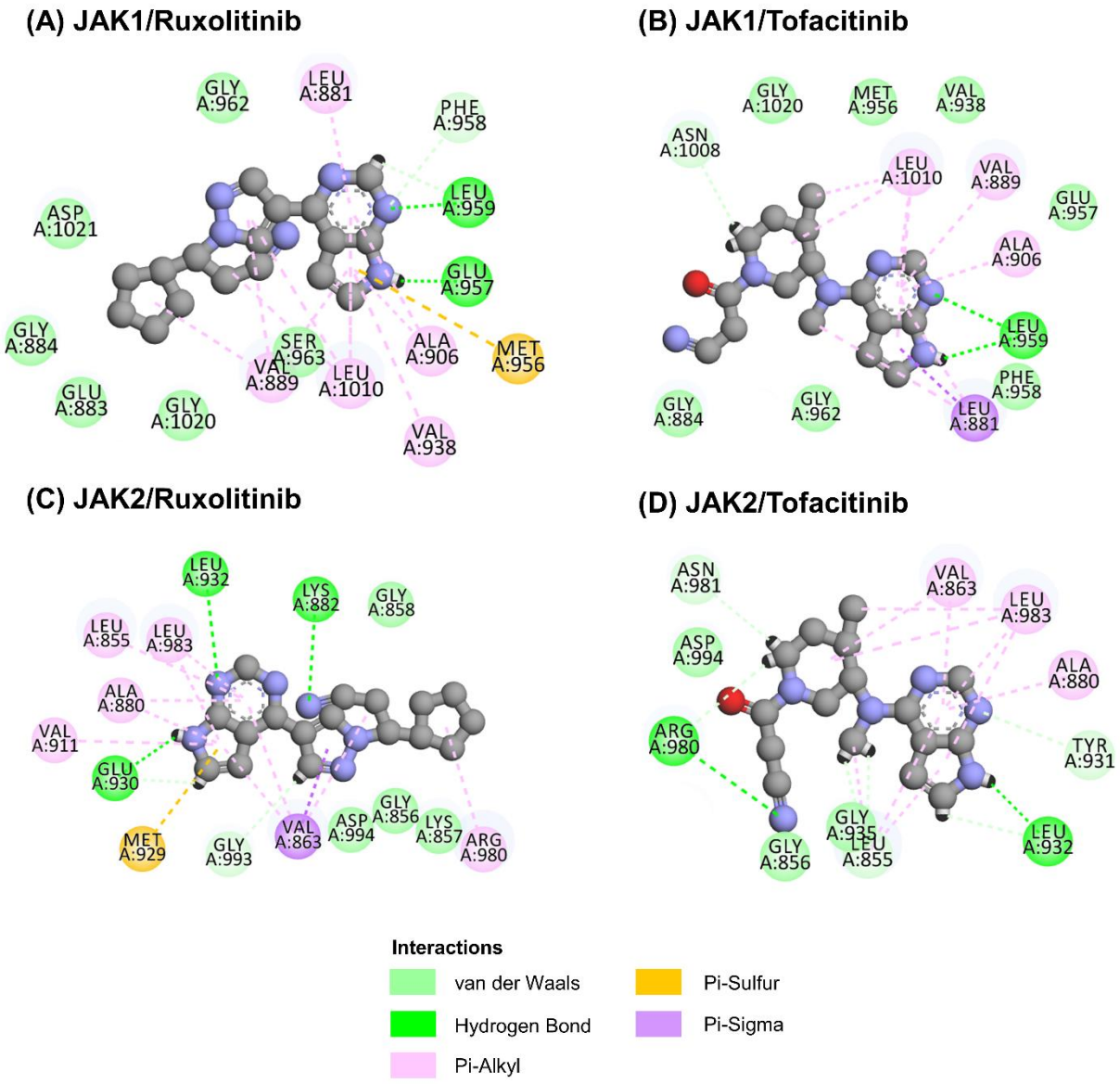

Figure 2 *2D interactions of Ruxolitinib and Tofacitinib complexed with (A and B) JAK1, and (C and D) JAK2.*

3.3 FTIR analysis

To further investigate if the different mode of actions between both drugs could affect in inhibit the cell differently, the FTIR was used to see differences in the biochemical cell responses. The overall FTIR spectrum was obtained from whole-cell lines between wavelength lengths 3,800-1,000 cm^{-1} in **Figure 3A**. The selected peaks at 2,923 cm^{-1}, 1,656 cm^{-1} and 1,238 cm^{-1} were assigned to C–H stretch, C=O stretch, and P=O stretch, respectively[15]. The selected spectral groups were adjusted using third polynomial order, eleven smoothing points, and linear baseline correction for finished Savitzky–Golay smoothing converted to second derivatives and EMSC by Unscrambler X 10.4. For an additional detailed comparison between different cell treatments, these average spectra were analyzed by PCA.

3.4 PCA distinguishes untreated and drugs treatment by detected cellular biochemical alteration

The goal was to distinguish the different cell treatments with biochemical alteration by PCA. PCA is a dimensionality-reduction method that uses multivariate exploratory analysis techniques allowing identification of the significant variables or wave numbers describing differences between samples. PCA could be achieved and represented two types of information including plot scores indicating class separation and loading plots for identification of the variables providing for clustering the responsible information[15]. The 2D score plots in **Figure 3B** distinctly show the three samples; PC-1 was sufficient to separate the TF-1 drug treatment from the untreated cells with an accuracy of 83% while PC-2 explained 5% total variance in the model. From **Figure 3C**, the loading plots identify various biochemical components by PC-1 and PC-2. The major components in the different treatment cells were differentiated at around 1,700-1,500 cm^{-1} for protein; it was reported that JAKs inhibitor-treated cells compared to untreated cells by PC-1 had higher signals amide I[16]. Previous research indicated that the range was around 3,000–2,800 cm^{-1} for CH_2 and CH_3 asymmetric/symmetric stretching in lipids, fatty acids, and proteins, and 1,300-1,000 cm^{-1} for PO_{2-} asymmetric stretching of DNA and RNA in PC-2 [17]. PC-2 loading scores showed Tofacitinib separated from the others with less lipid and a

higher level of nucleic acid accumulation. For further detailed analysis, the secondary derivative spectra were created and overlapped for comparison.

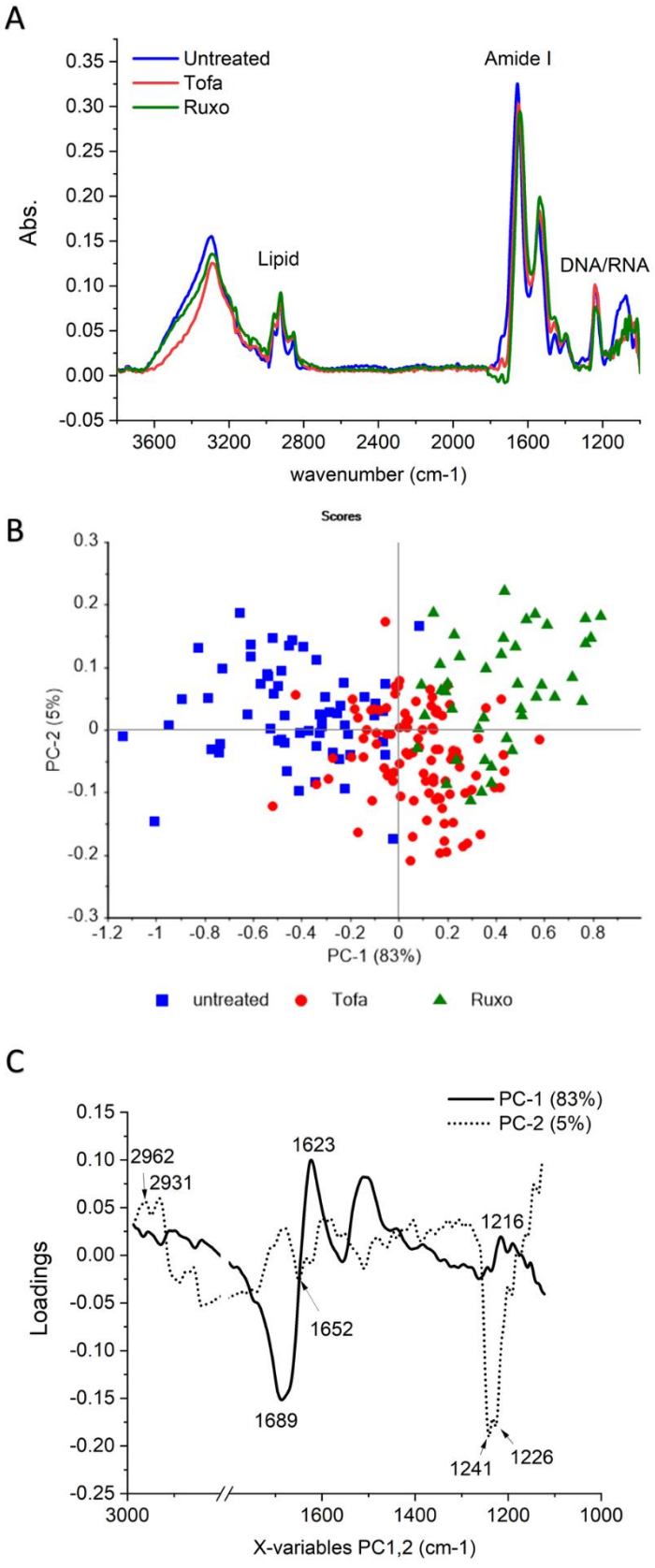

Figure 3 *(A)The average absorbance FTIR spectra of TF-1 cells in untreated conditions (blue), Tofacitinib treated cells (red), and Ruxolitinib treated cells (green). (B) Two-dimensional PCA score plot in PC1-2. (C) PCA corresponding loading plot PC1-2 indicating all samples biomarker differentiation.*

3.5 Cellular biochemical identification and differentiation detected by the S-FTIR

The average FTIR absorbance spectra of three samples were subsequently transformed to a second derivative to reduce baseline slopes and cover every single band in the unrefined spectra of samples. To identify the band and sub-band components, the spectra after the second derivative process of three major molecular components including lipid, protein, and nucleic acid are presented in **Figures 4-6.** The peak areas were assigned to the molecular vibrations in individual wavenumbers or IR frequencies that are summarized in **Table 1**.

3.5.1 FTIR spectra of treated cell display lipid alteration

The spectra in the region of 3,000–2,800 cm^{-1} detected vibrations of the C-H groups CH_2 in lipids and CH_3 from fatty acids, lipids and proteins using symmetric/asymmetric parameters. The average of three samples second derivative spectra exhibited high absorbance at 2,963 2,923 and 2,852 cm^{-1} **(Figure 4).** Untreated cells were stronger than the others for high lipid accumulation. After treatment with Tofacitinib and Ruxolitinib, the result was clearly observed indicating that both drug treatment decreases lipid production and accumulation. However, the absorbance of C-H symmetric stretching of CH_3 at 2,874 cm^{-1} was increased after drugs treatment.

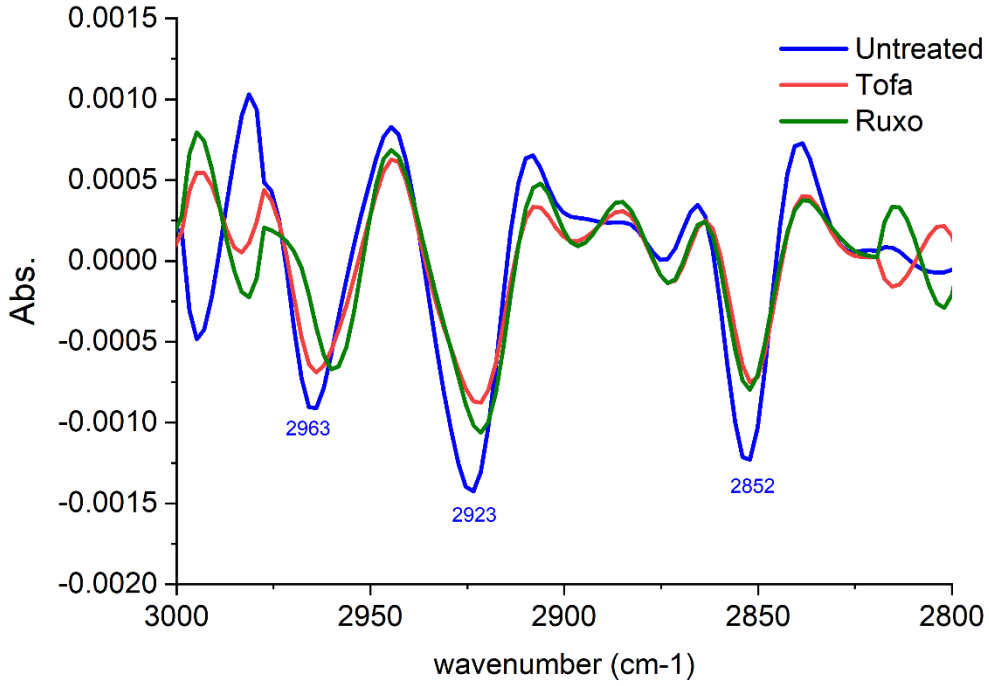

Figure 4 *The average of second derivative FTIR spectra characterize lipid regions in the wavelengths from 3,000 to 2,800 cm^{-1} of 60 spectra of untreated TF-1 cells (blue), 100 spectra of cells treated with 30.28 µM Tofacitinib (red), and 42 spectra of cells treated with 14.47 µM Ruxolitinib (green) after incubation for 72 h.*

3.5.2 FTIR spectra display treated cell changes of secondary structures in proteins.

The most apparent measurable differences of second derivatives are that they were surrounded by reflecting vibrations of protein amide I in 1,700-1,600 cm^{-1} (**Figure 5)**. The major absorptions of the amide I band from C=O stretching of the backbone, and the peptide backbone vibrations of the N-H bending, and C-N stretching were detected and assigned vibrations revealing the secondary structures changing in proteins. On this basis, infrared bands in the 1,660–1,650 cm^{-1} were defined to be the α-helices structure, β-sheets imposed in the wavelengths 1,640–1,620 cm^{-1}, in the 1,695–1,660 cm^{-1} region, determined to be β-turns and β-sheets structures. Furthermore, 1,650–1,620 cm^{-1} region to unordered structures[16, 18]. All the sample results showed that the absorption peaks appeared α-helix (1,656 cm^{-1}) and β-sheet (1,639 cm^{-1}) in the amide I. Although Tofacitinib and Ruxolitinib treated cells had remarkably reduced α-helices absorbance and an increase in the β-sheet peak at

1,639-1,633 cm^{-1}. Particularly, the aggregated peak at 1,630-1,620 cm^{-1} was increased in Tofacitinib treated cells. This implies that the intramolecular β-sheet structures collapsed into aggregated forms.

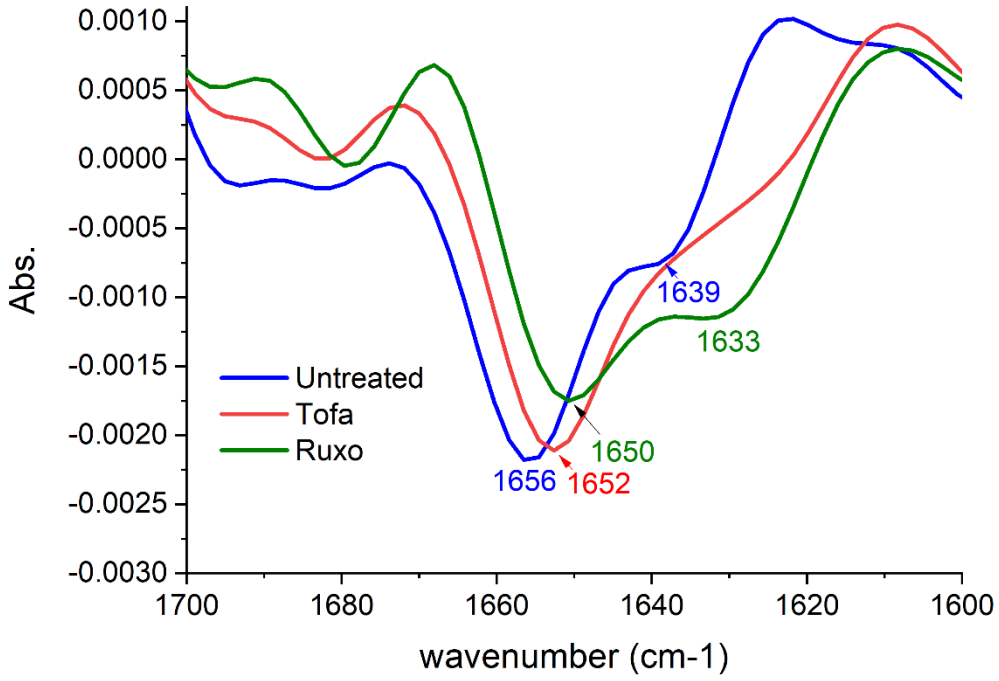

Figure 5 *Average second derivative FTIR spectra characterize protein regions in wavelengths from 1,700 to 1,600 cm^{-1} of 60 spectra of untreated TF-1 cells (blue), 100 spectra of Tofacitinib treated (30.28 µM) cells (red), and 42 spectra of Ruxolitinib treated (14.47 µM) cells (green) after incubation for 72 h.*

3.5.3 High level of RNA overexpression in cell treatment

Average second derivative FTIR spectra characterizing nucleic acid regions in wavelengths from 1,300 to 1,000 cm^{-1} are shown in **Figure 6.** Treated cells exhibited high synthesized nucleic acid levels at 1,243-1,238 cm^{-1} peaks together with 1,226-1,216 cm^{-1} related to asymmetrical stretching of PO_{2-} in the phosphodiester backbone of DNA or RNA: also, the high absorption of amide III band region at 1,191 cm^{-1}. In previous publications, the FTIR application establishes biomarkers for early screening of B-cell precursor lymphoblastic leukemia (BCP-ALL). The control group peak area at 1,241 cm^{-1} was identified as asymmetric/symmetric stretching of

PO_2^- (nucleic acids, phosphorylated proteins, and phospholipids)[19]. This correlates with the peak result of the treated cells which exhibited high synthesized nucleic acid levels at 1,243-1,238 cm^{-1}. As a result of both type I inhibitor effect mechanisms, Ruxolitinib decrease signaling can be associated with the accumulation of activation loop phosphorylation for preventing JAK2 dephosphorylation and ubiquitination[20].

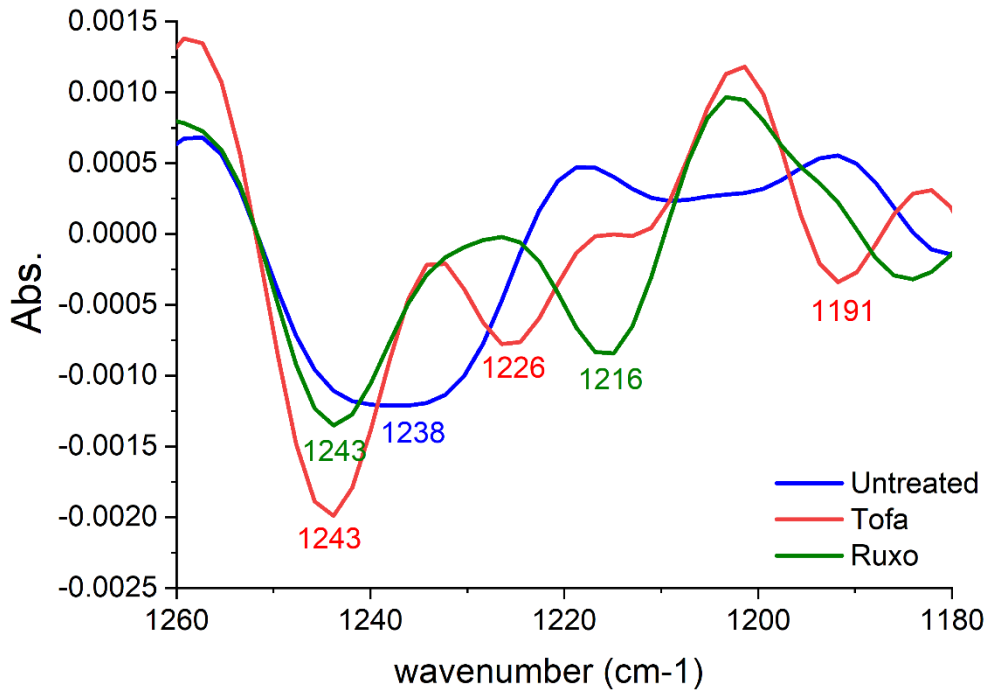

Figure 6 *Average second derivative FTIR spectra characterize nucleic acids regions in wavelength from 1,300 to 1,000 cm^{-1} of 60 spectra of untreated TF-1 cells (blue), 100 spectra of 30.28 µM of Tofacitinib treated cells (red), and 42 spectra of 14.47 µM Ruxolitinib treated cells (green) after incubated for 72 h.*

Table 1 *The second derivative FTIR spectra band assignments for the vibration of functional groups that are found in untreated and drug-treated TF-1 cells.*

Regions	Second derivative spectra (cm^{-1}) band	Band assignments
Lipid	2,963	C-H asymmetric stretching (CH_3) in fatty acids, lipids, and proteins[17]
	2,923	C-H asymmetric stretching (CH_2) in fatty acids, lipids, and proteins[17]
	2,874	C-H symmetric stretching (CH_3) in fatty acids, lipids, and proteins[17]
	2,852	C-H symmetric stretching (CH_2) in fatty acids, lipids, and proteins[17]
Protein	1,656-1,650	α-helix structure of amide I[17]
	1,639-1,633	β-sheet structure of amide I[17]
Nucleic acid	1,243-1,238	PO^-_2 asymmetric and symmetric stretching (phosphate I) (nucleic acids, phosphorylated proteins, and phospholipids)[17, 19]
	1,226-1,216	PO^-_2 asymmetric stretching (phosphate I)[17]
	1,191	Amide III band region[17]

Discussion

The JAK-STAT pathway is related to cellular processes such as cell division, proliferation, cell death, tumor formation, and immunity. The pathway information from chemical signals outside to the nucleus of the cell, results in the initiation of genes through a process called transcription[21]. Ruxolitinib and Tofacitinib **are** first-generation **and type I kinase inhibitors, which competitively** ATP binding site and represses the enzyme activity of JAK kinases, thus the effect of inhibitors is silencing the signal transduction and action of cytokine. As a result, signal transduction cannot occur, and the risk of this cancer is decreased. Therefore, FTIR is an effective tool that can study biological systems and consider the molecular changing of cells, subjected to antitumor drugs based on the FTIR spectrum[9].

This study, evaluate the chemical fingerprints of TF-1 cells after Tofacitinib and Ruxolitinib treatments. The TF-1 cells are proliferative responses to IL-3 or GM-CSF that can result in activation of the JAK2/STAT signaling pathway. Both JAKs inhibitor drugs are selective JAK inhibitors but Ruxolitinib is effective for JAK1/2 inhibition, whereas Tofacitinib causes a higher inhibition of JAK1/3 than JAK2[22]. This result corresponds to the higher inhibition of TF-1 cells by Ruxolitinib than Tofacitinib.

From the binding mode analyzed of known drugs (Ruxolitinib and Tofacitinib) with JAK1 and JAK2, we found that the docking scores of Ruxolitinib in complex with both proteins were higher than Tofacitinib **(Supplemental data figure 13)**. These results suggested that Ruxolitinib fits better with both proteins than Tofacitinib due to the fact that Ruxolitinib is a dual inhibitor against JAK1/2, whereas Tofacitinib is a dual inhibitor for JAK1/3[23]. Additionally, 2D interactions and the binding pattern bound well with the deazapurine ring at the ATP-binding site **(Supplemental data figure 14)**. In JAK1, the nitrogen atoms on the deazapurine ring of Ruxolitinib formed two hydrogen bonds (H-bonds) with Glu957 and Leu959, while Tofacitinib formed H-bonds with Leu959. For JAK2, we found that nitrogen atoms on the deazapurine ring and nitrile group formed H-bonds with Lys882, Glu930, Leu932 for Ruxolitinib and Leu932, Arg980 for Tofacitinib **(Figure 2)**. Apart from that, all compounds are stabilized through other interactions such as Pi-sulfur, Pi-sigma, Pi-

alkyl and van der Waals interaction; these interactions are called hydrophobic interactions (**Supplemental data figure 15**)

The goal was to evaluate the chemical fingerprints of TF-1 cells after Tofacitinib and Ruxolitinib treatments. FTIR analysis was performed and determined from the absorption (or transmission) versus wavelength (or frequency) of infrared radiation associated with vibrations of functional groups within the molecule, and chemical bonds between atoms undergoing various forms[24]. The second derivative spectra of three major molecular components including lipid, protein, and nucleic acid are presented (1) In the part of the lipid region is allocated for the phospholipid bilayer and organelle membranes of the cell. This consist of the fatty acid side chains that have repeated the moieties of CH_2- and CH_3- stretching vibration. (2) Protein region is designated the amide bonds of amino acids binding in proteins, and the peptide bond that provides the stretching vibration of amide I and bending vibration of amide II. (3) The region of nucleic acid is given for phosphodiester bonds binding to form DNA/RNA. Accordingly, the sensitized TF-1 cells of Ruxolitinib than Tofacitinib in the JAK/STAT pathway control can be observed and represent the FTIR spectrum. On the biological, the JAK/STAT pathway controls crucial cellular processes[25]. Ruxolitinib withdraw phosphorylated STAT3 and stimulated caspase-3 cleaving, enhanced apoptosis, and inhibited tumor growth[26]. As though, the inhibitors induced autophagosome accumulation and reduced the IL-6, IL-18, JAK2, TYK2, and AKT gene expression in multiple myeloma cells[27]. In previous publications, Han et al. offered the western blot result of Ruxolitinib treatment using ovarian cancer cells and explained the inhibiting of STAT3 phosphorylation[28]. For Tofacitinib, drug effect in JAK/STAT signaling inhibition as an anti-myeloma therapeutic. The result of western blotting demonstrates that decrease in STAT3 phosphorylation after treatment with 1 μM Tofacitinib[29]. *In Vivo*, Tofacitinib represses JAK-STAT pathways by downregulating the phosphorylation of STAT1, STAT3, STAT4, and STAT5 also decreases the expression of interferon-regulated and metalloproteinase genes in rheumatoid arthritis disease[30].

Conclusions

The study revealed that FTIR microspectroscopy and PCA analysis represent methods for classifying the biochemical pattern of untreated and treated TF-1 cells. The absorbance spectra of C-H lipids, C=O amide I protein, and the P=O phosphodiester bond from nucleic acids were detected. Possibly, Ruxolitinib and Tofacitinib treated cells induced the modifications of secondary protein conformation, stimulated lipid accumulation, and induced protein phosphorylation. These conclusions imply that FTIR can be a prospective tool for analyzing individual cellular response patterns in drug-treated cells at the molecular level.

Materials and Methods

2.1 Cell culture of TF-1 cell line

The human erythroleukemia TF-1 cells (ATCC CRL-2003, Manassas, VA, USA) were grown in a complete RPMI-1640 medium (Gibco, Thermo Fisher Scientific Inc., Waltham, Massachusetts, USA) supplemented with fetal bovine serum (FBS) (10% v/v) (Gibco), penicillin (100 U/mL), streptomycin (100 µg/mL) (Gibco) and GM-CSF (2 ng/mL) (Sigma-Aldrich, Merck KGaA, Darmstadt, Germany). Cells were incubated at 37 ˚C in a humidified incubator including CO_2 (5% v/v), and air (95% v/v).

2.2 Cytotoxicity

Tofacitinib and Ruxolitinib (Sigma-Aldrich) in dimethyl sulfoxide (DMSO) (Sigma-Aldrich) towards the TF-1 cells were determined using the PrestoBlue assay. The cell suspensions with a density of 50,000 cells/well were in a 96-well microplate seeding and 37 ˚C incubating overnight. After treatment with the drugs, the cells were 72 h incubating time. Subsequently, the cells were added to the PrestoBlue reagent (10 µL) (Invitrogen, Thermo Fisher Scientific Inc., Waltham, Massachusetts, USA), and incubated at 37 ˚C for 1 h. Finally, the absorbance of the resorufin was measured at 570 nm compared to the vehicle control by a microplate reader (Infinite M200 microplate reader, Tecan, Männedorf, Switzerland). The experiment was performed in triplicate independent experiments (n=9).

2.3 Molecular Docking

The crystal structure of JAK1 (PDB ID: 3EYG) and JAK2 (PDB ID: 3FUP)[14, 31] were obtained from the Protein Data Bank (PDB). The 3D structures of the drugs (Ruxolitinib and Tofacitinib) were downloaded in SDF format from the ZINC database. All docking tests were performed by GOLD docking software version 2020.1. The docking protocols of each system were set as 12 Å for sphere docking and GOLD score and ChemScore (rescore) for the scoring function. Then, docking into the ATP-binding pocket with 100 docking poses occurred. The binding between proteins and drugs was visualized using the Discovery Studio 2020 (Accelrys Inc.) and the UCSF Chimera package.

2.4 Sample preparation for S-FTIR

The TF-1 cells density of 300,000 cells/well was seeded in a 24-well microplate and incubated overnight at 37 ˚C. Afterward, the cells were replenished with a medium without drugs or a medium containing 2-fold concentrations of Tofacitinib or Ruxolitinib for a half-inhibitory concentration. After incubation for 72 h, cells were harvested by centrifuge at 300 g for 5 min. The pelleted cells were suspended and washed in NaCl (0.9% w/v) two times and then cells were fixed with formaldehyde (4% v/v) at 25 ˚C for 30 min. After decanting with formaldehyde, cells were washed three times and re-suspended with sterile distilled water (20 µL). The re-suspended cells (2 µL) were dropped onto 22 m-diameter × 1 mm-thickness calcium fluoride IR (CaF_2) windows for monolayer formation, then vacuum-dried and stored in a desiccator until spectra were acquired from FTIR analysis.

2.5 Synchrotron Fourier-transform Infrared spectroscopy

The S-FTIR experiments were accomplished at the BL4.1 Infrared Spectroscopy and Imaging (ISI), Synchrotron Light Research Institute (SLRI), Nakhon Ratchasima, Thailand. Samples were examined in the transmission mode of measurement using a Photon Energy range of 0.01-0.5 eV with a 36X Schwarzschild Objective, a Bruker Vertex 70 spectrometer coupled to a Bruker Hyperion 2000 microscope (Bruker Optics Ltd., Ettlingen, Germany) and a 100-micron narrow band mercury-cadmium-telluride (MCT) detector cooled with liquid nitrogen. Infrared spectra of samples were collected in the spectral range between 3,800-1,000 cm^{-1} using a 10X10 µm square aperture with a spectral resolution of 6 cm^{-1} in 40 to 100 scans. The instrument control

and spectral achievement were performed by OPUS 7.2 software (Bruker Optics Ltd., Ettlingen, Germany) and evaluated in the spectral range of 3,000-2,800 and 1,800-1,000 cm^{-1} for each sample group for PCA by Unscrambler 10.4 software (CAMO, Oslo, Norway). The absorbance of interesting molecules during vibrational modes was identified by spectral secondary derivative analysis. The absorbances of C-H stretching of lipids were detected between 3,000–2,800 cm^{-1}. The absorbances between 1,700–1,500 cm^{-1} from C=O stretching protein amide I and P=O phosphodiester bond from nucleic acids were detected in the absorbance of 1,300–1,000 cm^{-1}.

2.6 Statistical analysis

The IC_{50} values data are articulated as mean ± standard error of the mean (SEM), In the cytotoxicity experiments, significant differences were determined by comparing each treatment with the independent T-Test. $P < 0.05$ was counted as indicative of a statistically significant difference.

Acknowledgments

This work is supported by the Royal Golden Jubilee Ph.D. Program between the National Research Council of Thailand (NRCT) and the Synchrotron Light Research Institute (SLRI) (Grant no. PHD/0137/2561) and Kasetsart University Research and Development Institutes (KURDI (FF(KU)25.64)).

Conflict of interest

The authors declare no financial or commercial conflict of interest.

Data availability statement

Research data are not shared.

Author information

First Author

Jeeraprapa Siriwaseree, Department of Biochemistry, Faculty of Science, Kasetsart University, 50 Ngam Wong Wan Road, Chatuchak, Bangkok 10900, Thailand, E-mail: jeeraprapa.s@ku.th

The corresponding authors

Kamonpan Sanachai, Structural and Computational Biology Research Unit, Department of Biochemistry, Faculty of Science, Chulalongkorn University, 254 Phayathai Road, Pathumwan, Bangkok 10330, Thailand, E-mail: sanachaikamonpan@gmail.com

Thitinan Aiebchun, Department of Biochemistry, Faculty of Science, Kasetsart University, 50 Ngam Wong Wan Road, Chatuchak, Bangkok 10900, Thailand, E-mail: thitinan1906@gmail.com

Lueacha Tabtimmai, Department of Biotechnology, Faculty of Applied Science, King Mongkut's University of Technology North Bangkok, 1518 Pracharat 1 Road, Wongsawang, Bang Sue, Bangkok 10800, Thailand, E-mail: Lueacha.t@sci.kmutnb.ac.th

Buabarn Kuaprasert, Synchrotron Light Research Institute (Public Organization), 111 University Avenue, Muang District, Nakhon Ratchasrima 30000, Thailand, E-mail: buabarn@slri.or.th

Kiattawee Choowongkomon, Ph.D., Department of Biochemistry, Faculty of Science, Kasetsart University, 50 Ngam Wong Wan Road, Chatuchak, Bangkok 10900, Thailand, Tel: +662 5625444, Fax: + 66 25614627, E-mail: fsciktc@ku.ac.th

Supporting Information statement

Figure S13. The docking energy scores of known drugs with the JAK1 and JAK2 proteins

Figure S14. Binding patterns of known drugs within JAK1 and JAK2

Figure S15. Summary of histograms showing interactions of Ruxolitinib and Tofacitinib complexed with JAK1 and JAK2

References

(1) Stark, G. R.; Darnell, J. E. The JAK-STAT Pathway at Twenty. *Immunity* **2012**, *36* (4), 503-514. DOI: 10.1016/j.immuni.2012.03.013.

(2) O'Shea, J. J.; Holland, S. M.; Staudt, L. M. MECHANISMS OF DISEASE JAKs and STATs in Immunity, Immunodeficiency, and Cancer. *New Engl J Med* **2013**, *368* (2), 161-170. DOI: 10.1056/NEJMra1202117.

(3) Mascarenhas, J.; Mughal, T. I.; Verstovsek, S. Biology and Clinical Management of Myeloproliferative Neoplasms and Development of the JAK Inhibitor Ruxolitinib. *Curr Med Chem* **2012**, *19* (26), 4399-4413. DOI: Doi 10.2174/092986712803251511. Banerjee, S.; Biehl, A.; Gadina, M.; Hasni, S.; Schwartz, D. M. JAK-STAT Signaling as a Target for Inflammatory and Autoimmune Diseases: Current and Future Prospects (vol 77, pg 521, 2017). *Drugs* **2017**, *77* (11), 1261-1261. DOI: 10.1007/s40265-017-0772-7.

(4) Zhang, X. C.; Hu, F. Y.; Li, G.; Li, G. D.; Yang, X.; Liu, L.; Zhang, R. S.; Zhang, B. X.; Feng, Y. D. Human colorectal cancer-derived mesenchymal stem cells promote colorectal cancer progression through IL-6/JAK2/STAT3 signaling. *Cell Death Dis* **2018**, *9*. DOI: ARTN 25

10.1038/s41419-017-0176-3.

(5) Alicea-Velazquez, N. L.; Boggon, T. J. The Use of Structural Biology in Janus Kinase Targeted Drug Discovery. *Curr Drug Targets* **2011**, *12* (4), 546-555.

(6) Vainchenker, W.; Leroy, E.; Gilles, L.; Marty, C.; Plo, I.; Constantinescu, S. N. JAK inhibitors for the treatment of myeloproliferative neoplasms and other disorders. *F1000Res* **2018**, *7*, 82. DOI: 10.12688/f1000research.13167.1.

(7) Quintas-Cardama, A.; Vaddi, K.; Liu, P.; Manshouri, T.; Li, J.; Scherle, P. A.; Caulder, E.; Wen, X.; Li, Y.; Waeltz, P.; et al. Preclinical characterization of the selective JAK1/2 inhibitor INCB018424: therapeutic implications for the treatment of myeloproliferative neoplasms. *Blood* **2010**, *115* (15), 3109-3117. DOI: 10.1182/blood-2009-04-214957.

(8) Chrencik, J. E.; Patny, A.; Leung, I. K.; Korniski, B.; Emmons, T. L.; Hall, T.; Weinberg, R. A.; Gormley, J. A.; Williams, J. M.; Day, J. E.; et al. Structural and Thermodynamic Characterization of the TYK2 and JAK3 Kinase Domains in

Complex with CP-690550 and CMP-6. *J Mol Biol* **2010**, *400* (3), 413-433. DOI: 10.1016/j.jmb.2010.05.020.

(9) Gasper, R.; Vandenbussche, G.; Goormaghtigh, E. Ouabain-induced modifications of prostate cancer cell lipidome investigated with mass spectrometry and FTIR spectroscopy. *Biochim Biophys Acta* **2011**, *1808* (3), 597-605. DOI: 10.1016/j.bbamem.2010.11.033.

(10) Travo, A.; Desplat, V.; Barron, E.; Poychicot-Coustau, E.; Guillon, J.; Deleris, G.; Forfar, I. Basis of a FTIR spectroscopy methodology for automated evaluation of Akt kinase inhibitor on leukemic cell lines used as model. *Anal Bioanal Chem* **2012**, *404* (6-7), 1733-1743. DOI: 10.1007/s00216-012-6283-1.

(11) Denbigh, J. L.; Perez-Guaita, D.; Vernooij, R. R.; Tobin, M. J.; Bambery, K. R.; Xu, Y.; Southam, A. D.; Khanim, F. L.; Drayson, M. T.; Lockyer, N. P.; et al. Probing the action of a novel anti-leukaemic drug therapy at the single cell level using modern vibrational spectroscopy techniques. *Sci Rep-Uk* **2017**, *7*. DOI: ARTN 2649

10.1038/s41598-017-02069-5.

(12) Kitamura, T.; Tange, T.; Terasawa, T.; Chiba, S.; Kuwaki, T.; Miyagawa, K.; Piao, Y. F.; Miyazono, K.; Urabe, A.; Takaku, F. Establishment and characterization of a unique human cell line that proliferates dependently on GM-CSF, IL-3, or erythropoietin. *J Cell Physiol* **1989**, *140* (2), 323-334. DOI: 10.1002/jcp.1041400219.

Li, J.; Favata, M.; Kelley, J. A.; Caulder, E.; Thomas, B.; Wen, X. M.; Sparks, R. B.; Arvanitis, A.; Rogers, J. D.; Combs, A. P.; et al. INCB16562, a JAK1/2 Selective Inhibitor, Is Efficacious against Multiple Myeloma Cells and Reverses the Protective Effects of Cytokine and Stromal Cell Support. *Neoplasia* **2010**, *12* (1), 28-38. DOI: 10.1593/neo.91192.

(13) Keretsu, S.; Ghosh, S.; Cho, S. J. Computer aided designing of novel pyrrolopyridine derivatives as JAK1 inhibitors. *Sci Rep* **2021**, *11* (1), 23051. DOI: 10.1038/s41598-021-02364-2.

(14) Sanachai, K.; Mahalapbutr, P.; Choowongkomon, K.; Poo-Arporn, R. P.; Wolschann, P.; Rungrotmongkol, T. Insights into the Binding Recognition and Susceptibility of Tofacitinib toward Janus Kinases. *ACS Omega* **2020**, *5* (1), 369-377. DOI: 10.1021/acsomega.9b02800.

(15) Junhom, C.; Weerapreeyakul, N.; Tanthanuch, W.; Thumanu, K. FTIR microspectroscopy defines early drug resistant human hepatocellular carcinoma (HepG2) cells. *Exp Cell Res* **2016**, *340* (1), 71-80. DOI: 10.1016/j.yexcr.2015.12.007 From NLM.

(16) Gerwert, K.; Kötting, C. Fourier Transform Infrared (FTIR) Spectroscopy. 2010.

(17) Movasaghi, Z.; Rehman, S.; ur Rehman, D. I. Fourier Transform Infrared (FTIR) Spectroscopy of Biological Tissues. *Applied Spectroscopy Reviews* **2008**, *43* (2), 134-179. DOI: 10.1080/05704920701829043.

(18) Bellisola, G.; Sorio, C. Infrared spectroscopy and microscopy in cancer research and diagnosis. *Am J Cancer Res* **2012**, *2* (1), 1-21. PubMed.

(19) Chaber, R.; Kowal, A.; Jakubczyk, P.; Arthur, C.; Łach, K.; Wojnarowska-Nowak, R.; Kusz, K.; Zawlik, I.; Paszek, S.; Cebulski, J. A Preliminary Study of FTIR Spectroscopy as a Potential Non-Invasive Screening Tool for Pediatric Precursor B Lymphoblastic Leukemia. *Molecules* **2021**, *26* (4). DOI: 10.3390/molecules26041174.

(20) Tvorogov, D.; Thomas, D.; Liau, N. P. D.; Dottore, M.; Barry, E. F.; Lathi, M.; Kan, W. L.; Hercus, T. R.; Stomski, F.; Hughes, T. P.; et al. Accumulation of JAK activation loop phosphorylation is linked to type I JAK inhibitor withdrawal syndrome in myelofibrosis. *Sci Adv* **2018**, *4* (11), eaat3834-eaat3834. DOI: 10.1126/sciadv.aat3834 PubMed.

(21) Aaronson David, S.; Horvath Curt, M. A Road Map for Those Who Don't Know JAK-STAT. *Science* **2002**, *296* (5573), 1653-1655. DOI: 10.1126/science.1071545 (acccessed 2021/12/07).

(22) Kontzias, A.; Kotlyar, A.; Laurence, A.; Changelian, P.; O'Shea, J. J. Jakinibs: a new class of kinase inhibitors in cancer and autoimmune disease. *Curr Opin Pharmacol* **2012**, *12* (4), 464-470. DOI: 10.1016/j.coph.2012.06.008 PubMed. Schwartz, D. M.; Kanno, Y.; Villarino, A.; Ward, M.; Gadina, M.; O'Shea, J. J. JAK inhibition as a therapeutic strategy for immune and inflammatory diseases. *Nat Rev Drug Discov* **2017**, *17* (1), 78. DOI: 10.1038/nrd.2017.267 PubMed.

(23) Coricello, A.; Mesiti, F.; Lupia, A.; Maruca, A.; Alcaro, S. Inside Perspective of the Synthetic and Computational Toolbox of JAK Inhibitors: Recent Updates. *Molecules* **2020**, *25* (15). DOI: 10.3390/molecules25153321.

(24) Gaffney, J. S.; Marley, N. A.; Jones, D. E. Fourier Transform Infrared (FTIR) Spectroscopy. In *Characterization of Materials*, pp 1-33. Haris, P. I.; Chapman, D. Does Fourier-transform infrared spectroscopy provide useful information on protein structures? *Trends in Biochemical Sciences* **1992**, *17* (9), 328-333. DOI: https://doi.org/10.1016/0968-0004(92)90305-S.

(25) Lee, M.; Rhee, I. Cytokine Signaling in Tumor Progression. *Immune Netw* **2017**, *17* (4), 214-227. DOI: 10.4110/in.2017.17.4.214 PubMed.

(26) Dolatabadi, S.; Jonasson, E.; Lindén, M.; Fereydouni, B.; Bäcksten, K.; Nilsson, M.; Martner, A.; Forootan, A.; Fagman, H.; Landberg, G.; et al. JAK-STAT signalling controls cancer stem cell properties including chemotherapy resistance in myxoid liposarcoma. *Int J Cancer* **2019**, *145* (2), 435-449. DOI: 10.1002/ijc.32123 From NLM. Hu, Y.; Hong, Y.; Xu, Y.; Liu, P.; Guo, D. H.; Chen, Y. Inhibition of the JAK/STAT pathway with ruxolitinib overcomes cisplatin resistance in non-small-cell lung cancer NSCLC. *Apoptosis* **2014**, *19* (11), 1627-1636. DOI: 10.1007/s10495-014-1030-z From NLM.

(27) Kusoglu, A.; Bagca, B. G.; Ay, N. P. O.; Saydam, G.; Avci, C. B. Ruxolitinib Regulates the Autophagy Machinery in Multiple Myeloma Cells. *Anticancer Agents Med Chem* **2020**, *20* (18), 2316-2323. DOI: 10.2174/1871520620666200218105159 From NLM.

(28) Han, E. S.; Wen, W.; Dellinger, T. H.; Wu, J.; Lu, S. A.; Jove, R.; Yim, J. H. Ruxolitinib synergistically enhances the anti-tumor activity of paclitaxel in human ovarian cancer. *Oncotarget* **2018**, *9* (36), 24304-24319. DOI: 10.18632/oncotarget.24368 PubMed.

(29) Lam, C.; Murnane, M.; Liu, H.; Smith, G.; Wong, S.; Taunton, J.; Liu, J.; Mitsiades, C.; Hann, B.; Aftab, B.; et al. *Repurposing tofacitinib as an anti-myeloma therapeutic to reverse growth-promoting effects of the bone marrow microenvironment*; 2017. DOI: 10.1101/143206.

(30) Boyle, D. L.; Soma, K.; Hodge, J.; Kavanaugh, A.; Mandel, D.; Mease, P.; Shurmur, R.; Singhal, A. K.; Wei, N.; Rosengren, S.; et al. The JAK inhibitor tofacitinib suppresses synovial JAK1-STAT signalling in rheumatoid arthritis. *Annals of the Rheumatic Diseases* **2015**, *74* (6), 1311. DOI: 10.1136/annrheumdis-2014-206028.

(31) Williams, N. K.; Bamert, R. S.; Patel, O.; Wang, C.; Walden, P. M.; Wilks, A. F.; Fantino, E.; Rossjohn, J.; Lucet, I. S. Dissecting specificity in the Janus kinases: the structures of JAK-specific inhibitors complexed to the JAK1 and JAK2 protein tyrosine kinase domains. *J Mol Biol* **2009**, *387* (1), 219-232. DOI: 10.1016/j.jmb.2009.01.041.

Publication 2

Siriwaseree, J.; Yingchutrakul, Y.; Samutrtai, P.; Aonbangkhen, C.; Srathong, P.; Krobthong, S.; Choowongkomon, K. Exploring the Apoptotic-Induced Biochemical Mechanism of Traditional Thai Herb (Kerra™) Extract in HCT116 Cells Using a Label-Free Proteomics Approach. **Medicina** 2023, 59, 1376. https://doi.org/10.3390/medicina59081376

Article

Exploring the apoptotic-inducted biochemical mechanism of traditional Thai herbs (Kerra™) extracts in HCT116 cells using label-free proteomics approach

Jeeraprapa Siriwaseree [1,†], Yodying Yingchutrakul [2,†], Pawitrabhorn Samutrtai [3], Chanat Aonbangkhen [4], Pussadee Srathong [5], Sucheewin Krobthong [4,*], Kiattawee Choowongkomon [1,6,*]

[1] Department of Biochemistry, Faculty of Science, Kasetsart University, Bangkok, 10900, Thailand; e-mail: jeeraprapa_SR@hotmail.com

[2] National Center for Genetic Engineering and Biotechnology, NSTDA, Pathum Thani, 12120, Thailand; e-mail: yodying.yin@biotec.or.th

[3] Department of Pharmaceutical Sciences, Faculty of Pharmacy, Chiang Mai University, Chiang Mai, 50200, Thailand; e-mail: pawitrabhorn.s@cmu.ac.th

[4] Center of Excellence in Natural Products Chemistry (CENP), Department of Chemistry Faculty of Science, Chulalongkorn University, Bangkok 10330, Thailand; e-mail: (S.K.) sucheewin82@gmail.com, (C.A.) chanat.a@chula.ac.th

[5] Prachomklao College of Nursing, Phetchaburi, Faculty of Nursing, Praboromarajchanok Institute, Nonthaburi, Thailand; e-mail: pussadee@pckpb.ac.th

[6] Interdisciplinary Graduate Program in Genetic Engineering, Kasetsart University, Bangkok, 10900, Thailand

[†]Co-first author, these authors (Y.Y. and J.S) contributed equally to this work.

***** Correspondence: sucheewin82@gmail.com (S.K.) and kiattawee.c@ku.ac.th (K.C.)

Abstract

Background and Objectives: Natural products have proven to be a valuable source for the discovery of new candidate drugs for cancer treatment. This study aims to investigate the potential therapeutic effects of "Kerra™ ", a natural extract derived from a mixture of nine medicinal plants mentioned in the ancient Thai scripture named "Takxila Scripture", on HCT116 cells. Materials and Methods: In this study, the effect of the Kerra™ extract on cancer cells was assessed through cell viability assays. Apoptotic activity was evaluated by examining the apoptosis

characteristic features. Proteomics analysis was conducted to identify proteins and pathways associated with the extract's mechanism of action. The expression levels of apoptotic protein markers were measured to validate the extract's efficacy. Results: The Kerra™ extract demonstrated a dose-dependent inhibitory effect on the cells, with higher concentrations leading to decreased cell viability. Treatment with the extract for 72 hours induced characteristic features of early and late apoptosis, as well as cell death. LC-MS/MS analysis identified a total of 3,406 proteins. The pathway analysis revealed that the Kerra™ extract stimulated apoptosis and cell death in colorectal cancer cell lines and suppressed cell proliferation in adenocarcinoma cell lines through the EIF2 signaling pathway. Upstream regulatory proteins including cyclin-dependent kinase inhibitor 1A (CDKN1A) and MYC proto-oncogene, bHLH transcription factor (MYC), were identified. The expression of caspase 8 and caspase 9 was significantly elevated by the Kerra™ extract compared to the chemotherapy drug, Doxorubicin (Dox). Conclusions: These findings provide strong evidence for the ability of Kerra™ extract, to induce apoptosis in HCT116 colon cancer cells. The extract's efficacy was demonstrated by its dose-dependent inhibitory effect, induction of apoptotic activity, and modulation of key proteins involved in cell death and proliferation pathways. The study highlights the potential of Kerra™ as promising therapeutic agents in cancer treatment.

Keywords: traditional herbs; LC-MS/MS; colorectal cancer; caspase-8, caspase-9; CDKN1A; MYC

1. Introduction

The utilization of natural products for cancer treatment has gained prominence in recent years. Natural products have proven to be a valuable source for the discovery of new candidate drugs for cancer treatment. For example, Curcumin, a compound found in rhizomes of *Curcuma longa* (turmeric), has been shown to have antiproliferative and proapoptotic effects on various cancer cells including colon cancers, prostate cancers, and lung cancers [1-3]. Epigallocatechin gallate, a compound found in green tea, has been shown to inhibit the growth of various types of cancer cells such as ovarian cancers, head and neck Cancer [4,5]. Interesting,

combination of curcumin and epigallocatechin gallate exhibited potential anti-cancer activity inducing apoptosis in the various cancers [6]. Researchers are exploring compounds derived from natural products as potential alternatives for cancer treatment. One significant advantage of using crude natural products is their ability to target multiple pathways within cancer cells simultaneously. Cancer cells often activate multiple survival pathways, and natural products with their complex phytochemicals can effectively target these pathways, surpassing the effectiveness of single compounds that only focus on specific protein marker. Natural products typically contain various phytochemicals that can work together synergistically, resulting in a more potent therapeutic effect. This synergy adds to their potential as valuable treatments. Besides, utilizing crude herbal products for alternative cancer treatment offers several benefits, such as the ability to target multiple pathways, cost-effectiveness, and the combined effects of different compounds working together. These factors emphasize the importance of natural products in developing new and effective cancer treatments.

"Takxila", with the commercial name of "Kerra™ " from the ancient Thai scripture named "Takxila Scripture" was mixed of nine-ingredient medicinal plants such as *Pterocarpus santalinus*, *Santalum album*, *Momordica cochinchinensis*, *Citrus aurantiifolia*, *Dregea volubilis*, etc [7]. Each of these plants mentioned in the scripture has demonstrated significant potential in cancer therapeutics [8-12]. In addition, Kerra™ can inhibit inflammatory response and two enzymes in severe acute respiratory syndrome coronavirus 2 including main protease and RNA-dependent RNA polymerase [7]. However, while the mixture of these medicinal plants adheres to the "Takxila" formula for alternative cancer treatment, there remains a big knowledge gap in understanding its efficacy. In cancer therapeutic aspects, the natural process of cell death known as apoptosis is usually altered in several signaling pathways [13]. Therefore, the discovery of new traditional herbs with apoptotic activity can be an effective approach for treating cancer.

Apoptosis, or programmed cell death, plays a crucial role in the development and maintenance of tissue and organ health in multicellular organisms [14]. Caspases play a crucial role as key regulators of apoptosis and are part of the cysteine endo-protease family that mediates cell death and inflammation. In

mammals, caspases have been classified based on their well-defined biological functions in apoptosis, with caspase-3, -6, -7, -8, and -9. The biological process of caspase-mediated apoptosis involves two primary signaling pathways: intrinsic and extrinsic. Caspase-8 mediates the extrinsic pathway, while caspase-9 initiates the intrinsic pathway. Additionally, caspase-8 and -9 exert regulatory roles by activating downstream effector caspases, such as caspase-3, -6, or -7, which are responsible for stimulating various cellular apoptotic responses[15]. The apoptosis process helps to maintain a balance between cell division and cell death, by removing damaged or abnormal cells. In the context of cancer, apoptosis is an important consideration for therapeutic strategies [13]. Cancer cells are characterized by uncontrolled cell division and evasion of normal cell death mechanisms, these results in the growth of tumors. As a result, inducing apoptosis in cancer cells has been explored as a therapeutic approach. Generally, chemotherapy by using Doxorubicin (Dox) and radiation therapies often aim to induce apoptosis in cancer cells by causing DNA damage and triggering intrinsic apoptotic pathways, or by targeting specific pathways that regulate apoptosis [16,17]. However, it is important to note that resistance to apoptosis-inducing treatments can develop over time in cancer cells, reducing their efficacy. Additionally, non-cancerous cells or normal cells can also be affected, leading to adverse effects. Hence, traditional medicine utilizing various herbal remedies with potential apoptotic activity may provide an opportunity for alternative cancer treatment.

Proteomics analysis is a powerful tool that allows the comprehensive analysis of the entire protein complement of cells. To clarify the beneficial and adverse effects of these extracts, proteomics experiments are strongly required to evaluate their impact on cell lines or animal models. Proteomics has found extensive application in studying cellular responses and biochemical pathways concerning various natural products, such as diterpenoids from *Rabdosia rubrescens*, sesquiterpenoids from *Curcuma aromatica*, and iridoid glycosides from *Gardenia jasminoides* [18-20]. By analyzing the changes in protein expression, proteomics can provide a detailed understanding of the molecular mechanisms underlying the effect of external stimulants on cellular processes such as apoptosis [21,22]. In addition, proteomics analysis can be combined with other techniques, such as transcriptomics,

metabolomics and lipidomics, to provide a more complete picture of the molecular mechanisms underlying the effect of the external stimulants on cellular processes.

2. Materials and Methods

2.1 Kerra™ extract preparation and cell cytotoxicity evaluation

The Kerra™ was extracted by shaking the capsule powder in 95% ethanol at a ratio of 1:100 (w/v) for 24 hours at 37 ˚C. The extracted was filtered with the paper filter (Whatman, No. 41, pore size 20-25 μm) and concentrated at 40 ˚C by rotary evaporator (Buchi rotavapor R-210, BÜCHI Labortechnik, Flawil, Switzerland). Finally, the concentrated extract was dissolved in 100% DMSO (Merck KGaA, Germany). The human colorectal carcinoma cell line (HCT116) was bought from the American Type Culture Collection (ATCC; CCL-247). The cells were cultured in the complete growth media of modified McCoy's 5A medium (Gibco, Thermo Fisher Scientific Inc., Waltham, Massachusetts, USA) with 10% v/v fetal bovine serum (Gibco) and 1% v/v Antibiotic Antimycotic solution (100 units penicillin, 0.1 mg streptomycin and 0.25 μg/mL amphotericin B) (Gibco). Cultured cell lines were incubated at 37 ˚C and 5% CO_2. Cell cytotoxicity was determined based on MTT assay by the mitochondria dehydrogenase enzyme and cofactor reduction activity with the 3-[4, 5-Dimethylthiazol-2-yl]-2,5-Diphenyltetrazolium Bromide (MTT; Merck KGaA, Germany) forming purple color crystals of formazan. The density of HCT116 was seeding 1×10^4 cells/well or 1×10^5 cells/mL in 96 wells plate and left in an incubator for 24 hours for cell adherence. The cells were treated with samples for 72 hours in nine concentrations of two-fold serial dilution Kerra™ extract (5-0.020 mg/mL). The 0.1% DMSO was used as control condition. Cell cytotoxicity was assessed by measuring the absorbance at 570 nm and calculating the percentage of cell survival rate. Following from this calculation:

$$\text{Cell viability (\%)} = \text{Mean OD}_{\text{sample}}/\text{Mean OD}_{\text{blank}}\times100 \quad [23].$$

The experiments were conducted in three replications (n=3). The 50% cell proliferation inhibitory concentration (IC_{50}) was analyzed on a nonlinear regression dialog using GraphPad Prism 8 software (GraphPad Software Inc., San

Diego, California, USA). The resulting graph was presented in mean ± standard deviation (SD) of cell viability compared with the control.

2.2 Investigation of apoptotic events in HCT116 cells

The detection of apoptosis in HCT116 cells was conducted using the Muse™ Annexin V & Dead Cell Kit (MCH100105, EMD Millipore Co., , USA) following the manufacturer's guidelines [24]. Briefly, the cells were seeded in a 6-well plate at a density of 300,000 cells per well and allowed to incubate overnight at 37 °C. The experiments consisted of three experimental group including negative control (0.1% DMSO), positive control (0.1 μM Dox) and Kerra™ extracts (73 μg/mL). The cells were incubated in a 5% CO_2 incubator with 95% humidity for 72 hours. The treated cells were harvested, trypsinized and the commercial kit protocol was applied. The treated cells were harvested using trypsinization and resuspended in a fresh culture medium. The cells were then stained with the Muse® Annexin V & Dead Cell Kit (Luminex Corp., USA) and incubated in the dark at room temperature for 20 minutes. Fluorescence intensity was measured using flow cytometry with the Muse™ Cell Analyzer (Merck, Germany). The stained cells were categorized into four groups: live cells (annexin V-/7-AAD-), early apoptotic cells (annexin V+/7-AAD-), late apoptotic cells (annexin V+/7-AAD+), and necrotic cells (annexin V-/7-AAD+). The apoptotic values were expressed as percentages of healthy, apoptotic, and dead cells in the negative control, positive control, and Kerra™ extract conditions.

2.3 Sample preparation for label-free proteomics analysis

The treated HCT116 cells were prepared for proteomics using previously published protocol with minor modifications [25,26]. Briefly, the cells were lysed on-ice using a probe tip sonication at a frequency of 20 kHz and 80% amplitude for 2 seconds on, and 3 seconds off at the total of 15 seconds in 200 μL lysis buffer (0.2% TritonX-100, 2 mM TCEP, 5 mM sodium chloride, 10 mM HEPES-KOH, pH 8.0) with protease inhibitor cocktail. The protein solution was

collected by centrifugation at 15,000g for 30 minutes and subsequent to ice-cold 15% TCA/acetone precipitation (1:5 v/v) for 16 hours. After precipitation, the pallet protein was reconstituted in 0.5% RapiGest SF (Waters, UK), 5 mM NaCl in 5 mM ammonium bicarbonate. A total of 40 µg of protein were subjected to gel-free based digestion. Reduction sulfhydryl bonds by using 1 mM TCEP in 5 mM ammonium bicarbonate at 56 ^{o}C for 1 hour and alkylation of sulfhydryl groups by using 4 mM IAA in 5 mM ammonium bicarbonate at room temperature for 40 minutes in the dark. The solution was cleaned-up by desalting column (Zeba™ Spin Desalting Columns, 7K MWCO, 0.5 mL, ThermoFisher). The flow-through solution was enzymatically digested by Trypsin (Promega, Germany) at ratio 1:40 (enzyme: protein) ratio and incubated at 37^{o}C for 6 hours. The tryptic peptides were dried and stored at -20^{o}C until LC-MS/MS analysis.

2.4 LC-MS/MS configurations for proteomics analysis

The proteomics analysis was performed using a high-resolution SciEx 6600+ TripleTOF system (AB-Sciex, Concord, Canada) coupled with a nanoLC system, the UltiMate 3000 LC System (Thermo Fisher Scientific, USA), followed by previously publications with minor modifications [27]. Briefly, the dried tryptic peptides were reconstituted with 0.1% formic acid and 1.2 µg of protonated peptides were subjected to the nanoLC system. The mobile phases consisted of A) 0.1% formic acid in water and B) 95% acetonitrile with 0.1% formic acid. The samples were directly loaded onto a C18-reverse phase column (2 mm, 75 µm x 15 cm) and separated over a 155-minute period at a constant flow rate of 300 nl/min. The mass spectrum was acquired in data-dependent acquisition mode, with full scans over a mass range of 400-1600 *m/z*. The top 30 most abundant peptide ions with charge states ranging from 2 to 5 were selected for fragmentation. The dynamic exclusion duration was set at 18 seconds. The raw MS files were annotated with referenced protein sequences using the Paragon algorithm by ProteinPilot software [28]. The reviewed database used for the Paragon algorithm was assembled in FASTA format and retrieved from UniprotKB (https://www.uniport.org) on October 21, 2022 (species: *Homo sapiens*) [29].

2.5 Protein data and pathway enrichment analysis

To reduce the variability in the protein dataset, The normalization of protein intensity was performed using the NormalyzerDE [30], with quantile normalization applied to the relative expression data analysis after adding "1" to all expression values. To ensure high confidence data, only proteins identified with an FDR ≤1% and ≥10 peptides/protein were considered for the confidential protein list. The differentially expressed proteins were shown in volcano plot using a negative natural log of the *p*-values plotted against the base2 log values of the change in each protein between the Kerra™ extract (n=3) and negative control group (n=3). The effect of Kerra™ extract on pathway signaling cascade in HCT116 cells were analyzed using Ingenuity Pathway Analysis (IPA). All differentially expressed proteins were imported to the core analysis and analyzed to define the significantly changed protein signaling pathways and upstream regulators . The detailed procedures for IPA analysis and its parameters are described in previously report [31]. The analysis was performed by comparing all changed proteins against known canonical pathways within the IPA database (accessed on 18 May 2023). The activation and deactivation state of pathways and upstream regulator (any protein that can affect the expression of another protein) was analyzed based on the all differentially expressed proteins and adj. *p*-value (*z*-score). Major signal transduction pathways were reconstructed according to IPA results. Acceptable upstream regulator required to had *z*-score ≥ 1.5 and *p*-value < 0.01.

2.6 Immuno-based early apoptosis protein quantification

The level of apoptotic protein markers was measured using the MILLIPLEX® early apoptosis magnetic bead kit (48-669MAG). The levels of active Caspase-8 (Asp384) and active Caspase-9 (Asp315) were quantitated based on Luminex® xMAP® technology. Different passages of HCT116 cells were used in these experiments to confirm apoptotic events in the cells. The cells were cultured according to the specified protocols. Following treatment with Kerra™ extract at IC_{50} for 72 hours, the cells were washed with ice-cold buffered saline and disrupted with 0.3 mL of 1X MILLIPLEX® Lysis Buffer containing a protease inhibitor cocktail. To obtain lysed cells, the reaction was incubated at 50°C for 10 minutes with manual

mixing. The supernatant was collected by centrifugation at 14,000g at 16°C for 30 minutes. The protein concentration was measured using the BCA protein assay and adjusted with PBS to a concentration of 2 μg/μL. Prior to the experiment, the protein solution was further diluted in PBS at a 1:4 (v/v) ratio, resulting in a final concentration of 0.5 μg/μL. A total of 20 μL (10 μg) of the protein solution was subjected to the assay. For the magnetic beads, biotin-labeled detection antibody, streptavidin-PE, normalizing control proteins, and MILLIPLEX® cell lysates were prepared according to the manufacturer's instructions without any modifications. The efficiency and accuracy of immune-based reactions were qualified before the experiment. A549 cells stimulated with 5 μM camptothecin cell lysate were used as a positive control to confirm the expression profile of these apoptotic proteins, while HeLa cells treated with lambda phosphatase served as the negative control (no apoptotic characteristic cells) [32]. The quantification of protein levels was reported as the median fluorescence intensity (MFI) value along with the standard deviation, based on two biological replicate experiments and two replicate wells.

2.7 Statistical analysis

For the pairwise comparisons in proteomics analysis, a One-way analysis of variance (one-way ANOVA) at protein-level analysis with two multiple testing correction methods including the Bonferroni correction and the Benjamini and Hochberg FDR-correction was performed by ProteinPilot™ Software. For pathway analysis, A right-tailed Fisher’s exact test was used to calculate the significance of pathways and upstream regulator [33].

3. Results

3.1 Cell cytotoxicity

The cytotoxicity effect of Kerra™ extraction demonstrated the anti-cancer property. The extract exhibited a dose-dependent inhibitory effect as the concentration increased. After treated 72 hours, the viability of the HCT116 cells had slightly decrease the cell viability at a concentration of 39.06 μg/mL and completely inhibited from 156.25 to 5000 μg/mL (Figure. 7).

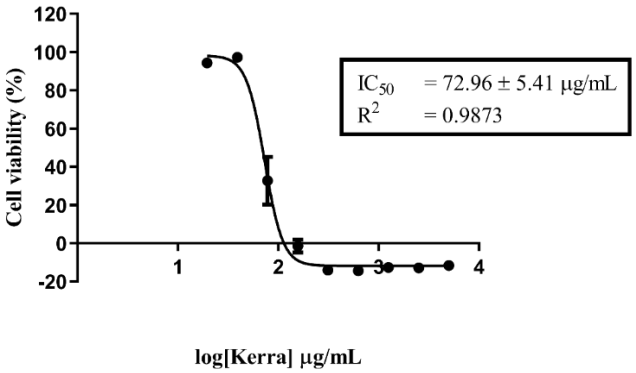

Figure 7 *Cytotoxicity effect of Kerra™ extracts against HCT116 cells after 72 hours of exposure using MTT assay at the concentration ranging from 5 - 0.020 mg/mL in logarithmic scale.*

The IC_{50} value of the Kerra™ extract was determined to be 72.96±5.41 µg/mL. In comparison, the positive control, Dox, exhibited an IC_{50} value of 0.059 µg/mL. These finding cleary indicate that the Kerra™ extract significantly affected the proliferation of HCT116 cells.

3.2 Kerra™ extract promotes apoptosis in HCT116 cells.

Flow cytometry was used to determine the apoptotic potential of Kerra extract, allowing the identification of healthy, early apoptotic, late apoptotic and death cells. To investigate the apoptotic effect, the cells were treated with the IC_{50} concentration of Kerra extract (73 µg/mL). The cell population profiles after treatments with negative control (0.1% DMSO), positive control (0.059 µM Dox), and Kerra extract (73 µg/mL) were shown in Figure 8A, 8B and 8C, respectively.

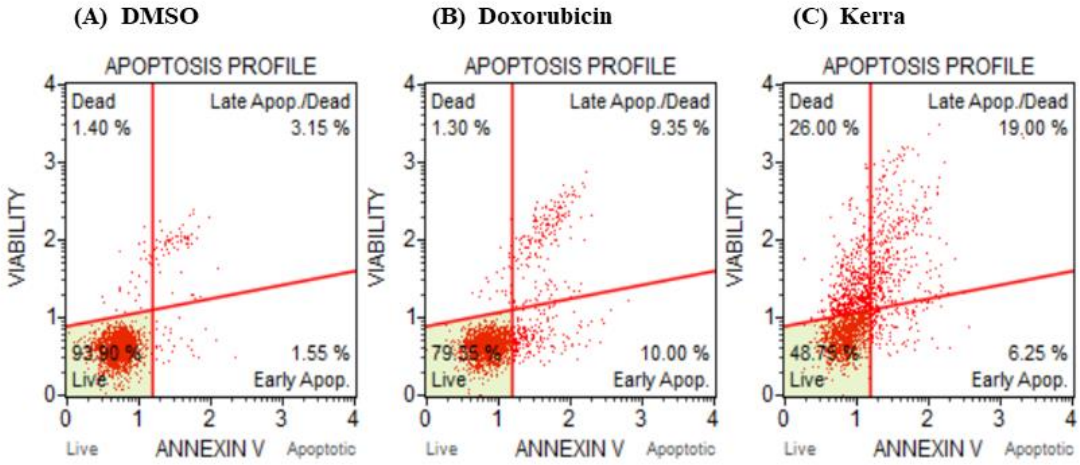

Figure 8 *Apoptosis cell characteristic analysis using Muse™ Annexin V assay. Two-dimensional diagram of viability and Annexin V-position cells in negative control (A), positive control (B) and Kerra™ extract (C) groups.*

When cells treated with Kerra™ extract for 72 hours showed the early apoptosis, late apoptosis, and cell death characteristic. The cells with Kerra™ extract treatment was compared with negative control cells, there was a significant difference in the percentage of healthy and apoptotic cells (p-value<0.01). The results showed Kerra™ extract increased total apoptosis by 21.55% compared to control. For confirm the experimental assay was corrected and properly, positive control was showed the increasing apoptotic cells in comparison to negative control. These findings imply that Kerra™ extract at 73 μg/mL can cause an increase in early and late apoptotic events in comparison to negative control cells (0.1% DMSO) in HCT116 cells.

3.3 Comparative proteomics analysis

In the LC-MS/MS based proteomics analysis of control and treatment conditions (IC_{50} of Kerra™ extract), a total of 18,448 unique peptides corresponding to 3406 individual proteins were identified. Among all identified proteins between Kerra™ extracts and control (0.1% DMSO), a total of 2196 (64%) and 1210 (36%) proteins were identified in high confidence (≤1% FDR, ≥2 unique peptides) and low

confidence (≥1% and ≤5% FDR, ≤2 unique peptides), respectively (Figure 9) (supplementary data 1).

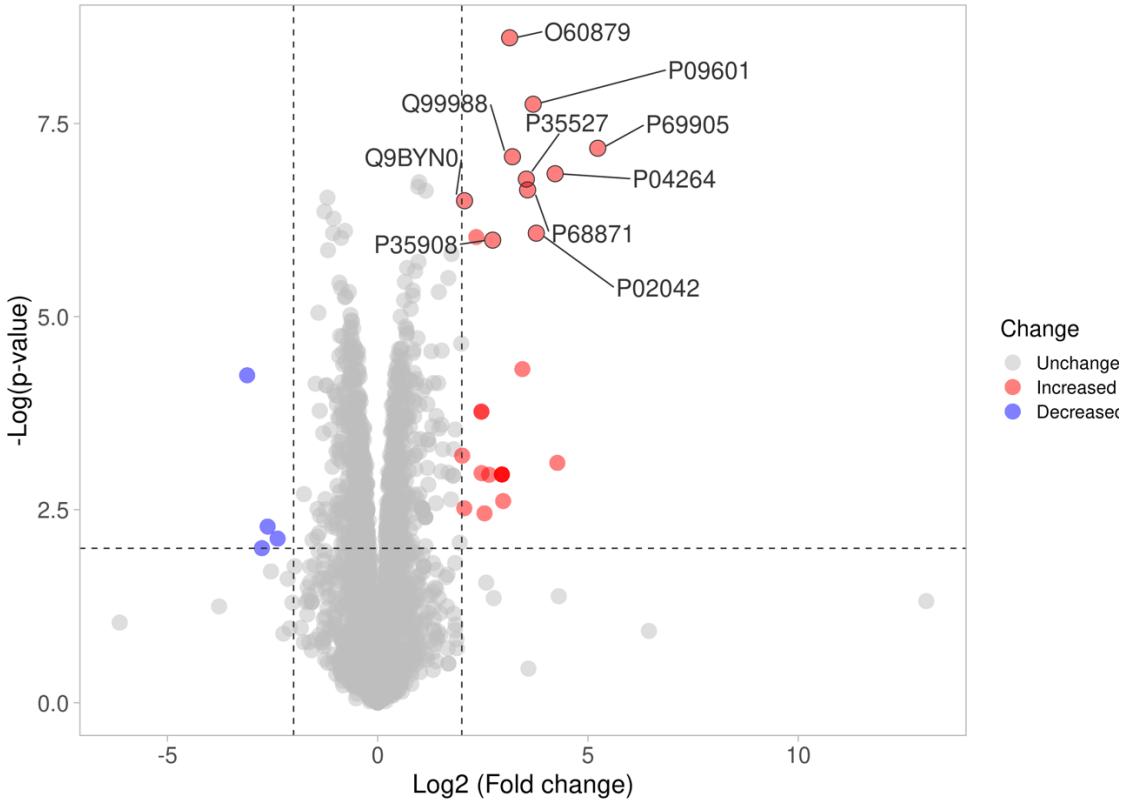

Figure 9 *Differences in proteome expression by a volcano plot. The plot shows a negative natural log of the p values plotted against the base2 log values of the change in each protein between the Kerra extract with control group (Figure 9). Significantly differentially expressed protein were chosen by p < 0.01 and log2 fold change >2. The upregulated and down-regulated proteins are marked as red and blue dots, respectively.*

3.4 The effect of Kerra™ extract on pathway signaling in HCT116 cells

Pathway signaling analysis of all proteome dataset in Kerra™ extract using IPA revealed various pathway were activated and inhibited. The analysis revealed Kerra™ extract stimulated apoptosis and cell death in colorectal cancer cell lines and suppressed cell proliferation of adenocarcinoma cell lines via EIF2 signaling pathway (Figure 10A).

(A)

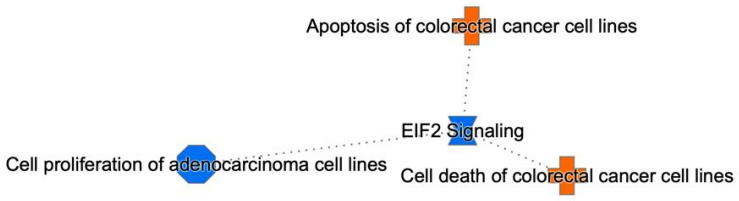

(B)

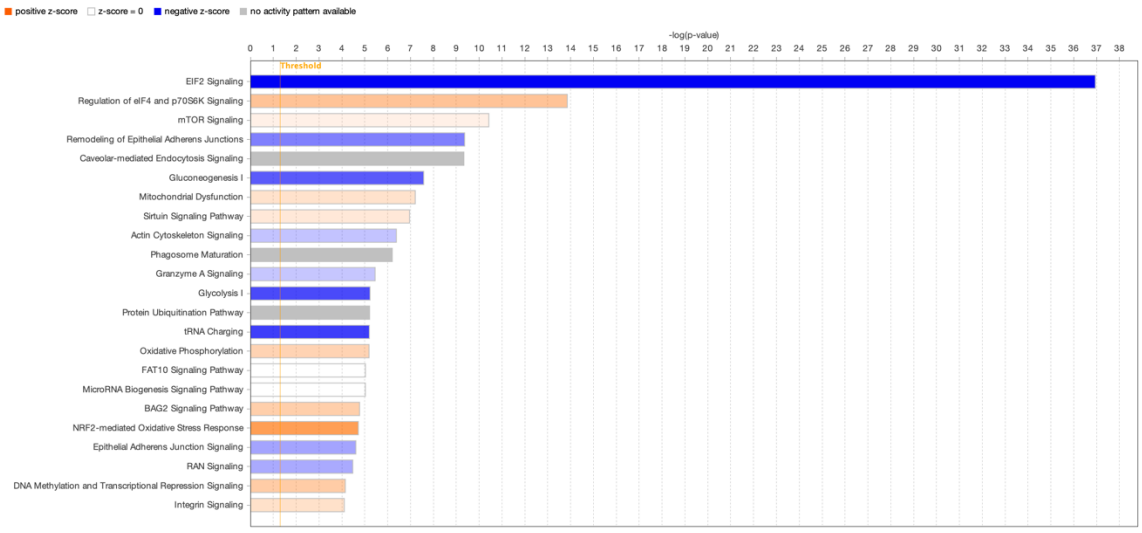

Figure 10 *The IPA analysis revealed the identification of canonical pathways. The threshold levels were indicated by the horizontal line. A negative z score indicates pathway inhibition, while a positive z score indicates pathway activation. White (transparent) bars signify "no activity" within the pathway*

For conical pathway signaling analysis, IPA revealed 9 significantly deactivated ($z \leq -1.5$ and $-\log(p\text{-value}) > 4$) and 9 significantly activated ($z \geq 1.5$, $-\log(p\text{-value}) > 4$) (Figure 10B). In terms of the prediction of upstream regulatory pathways in response of Kerra™ extract in HCT116 cells, there were 13 upstream regulators (Table 2). Among these regulators, cyclin dependent kinase inhibitor 1A (CDKN1A) and MYC proto-oncogene, bHLH transcription factor (MYC) exhibited the highest and lowest activation *z*-score, respectively.

Table 2 *Upstream protein regulators predicted to be activated (positive value of activation z-score) or Inhibited (minus value of activation z-score) in HCT116 cells after Kerra™ extract treatment.*

Upstream regulator	Molecular function	Activation *z*-score	*p*-value
MYC	Transcription regulator	-1.83	$1.19e^{-3}$
HIFA	Transcription regulator	-1.75	$1.45e^{-1}$
LONP1	peptidase	-1.23	$1.2e^{-8}$
TLR4	Transmembrane receptor	-1	$5e^{-3}$
THBS2	-	-1	$1.26e^{-3}$
KRAS	Enzyme	-0.29	$1.4e^{-2}$
SFN	-	-0.25	$9.18e^{-3}$
SMARCA4	Transcription regulator	0	$4.4e^{-2}$
NDRG1	Kinase	0.17	$1.27e^{-2}$
TP53	Transcription regulator	0.78	$3e^{-4}$
MXI1	Transcription regulator	1	$8.3e^{-3}$
GSTO1	Enzyme	1.99	$5.77e^{-1}$
CDKN1A	Kinase	2.73	$8.95e^{-2}$

3.5 Apoptosis protein level quantification

For confirmation the apoptotic-related proteins expression of Kerra™ extract induced apoptotic event, We used the immuno-based Luminex® assay, which allows the simultaneous detection of 2 apoptotic-related proteins that are markers of the apoptotic signaling pathways. There were caspase-8 (Asp384) and caspase-9 (Asp315). We used HeLa cells treated with lamda phosphatase for negative control (unstimulated cells) and A549 cells treated with 5 µM camptothecin for positive control (apoptotic cells). The results showed the all-apoptotic marker proteins in positive control were significantly higher abundance than negative control more than 100-folds (Figure 11A). These finding confirm us, the immuno-based Luminex® assay can be used to quantify the apoptotic protein in our experiment.

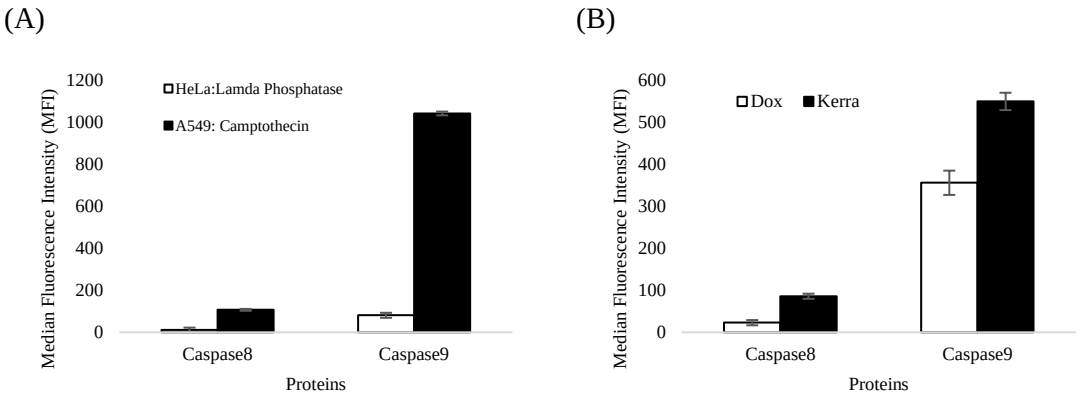

Figure 11 *The level of caspase 8 and caspase 9 expression were determined. (A) The efficiency and accuracy of immune-based reactions with (black bar) and without apoptotic stimulant compound (white bar) in A549 and HeLa reference cell lines. (B) The effect of Kerra™ extract on the levels of caspase 8 and caspase 9 level in HCT116 cells was measured. The Dox-treatment group is represented by white bar, while the Kerra™ treatment group is represented by black bar. The error bars indicate ± S.D.*

The efficiency and accuracy of immune-based reactions were assessed. It was observed that camptothecin significantly increased the levels of apoptotic marker proteins, including caspase 8 and caspase 9, by more than 10-fold compared to lambda phosphatase. These findings provide strong evidence that the immune-based assay used to quantify caspase 8 and caspase 9 was reliable and valid. The expression of apoptotic protein markers was significantly elevated by the Kerra™ extract, with caspase 8 and caspase 9 exhibiting increases of more than 3.7-fold and 1.5-fold, respectively, compared to Dox (Figure 11B).

4. Discussion

Interestingly, the Kerra™ extract exhibited a higher induction of late apoptosis and cell death in HCT116 cells compared to Dox at a concentration of 0.059 μM. Our results demonstrated that under Dox conditions, the percentage of HCT116 cells exhibiting total apoptosis characteristics was 20.65% (Figure 8B). Furthermore, the apoptosis levels in HCT116 cells could be further increased by raising the Dox

concentration to 1 or 10 μM [34]. Additionally, prolonged treatment with Dox also resulted in late apoptosis and cell death in HCT116 and MCF7 cells after an incubation period of 5 days [35]. Therefore, the observed apoptotic characteristics in these cells imply that certain phytochemical compounds present in the Kerra™ extracts have the ability to induce late apoptosis and cell death in HCT116 cells more effectively than Doxorubicin alone, specifically at this dosage. Dox is an anticancer drug widely used in chemotherapy for the treatment of various cancers[36]. It exerts its therapeutic effects by inducing various biological cellular changes, including cellular apoptosis. The effectiveness of Dox depends on both the dosage administered and the types of cells it targets[37,38]. This represents a research gap that needs to be addressed in future studies, aiming to identify the specific phytochemicals or combinations of phytochemicals responsible for inducing cell apoptosis. For confirmation apoptotic HCT116 cells can be induced by Kerra™ extracted, we done the Kerra™ extract treatment again with 2-fold higher concentration (146 μg/mL), the percentage of apoptotic cells also dramatically increased (data not shown). These findings suggest that the Kerra™ extract has the ability to induce cell apoptosis in HCT116 cells in a dose-dependent manner. However, the biochemical mechanisms underlying this effect are not yet fully understood, but the results of the study suggest that Kerra™ extract has potential as a therapeutic agent for colon cancer.

To gain better understanding in the effect of Kerra™ on cellular responses, studying the interaction between proteins is crucial for understanding their overall biological significance. Many proteins require interactions with specific partners to function properly. Therefore, analyzing the relationships between differentially expressed proteins is valuable in gaining insights into the integral biological roles of these proteins. To achieve this, we utilized the IPA tool to conduct network analysis, using microarray data from published literature as the basis for our investigation [39]. All the differentially expressed proteins were shown to be involved in 18 conical pathway networks. Based on the *z*-scores and *p*-values, the EIF2 signaling (*p*-value=$1.13e^{-37}$) was highest affected by Kerra™ extract treatment in the cells.

The current understanding of the upstream regulators influencing Kerra™ extracts on HCT116 cells remains limited. This study aims to enhance our

knowledge of the molecular function of Kerra™ extracts and its upstream regulators. The report emphasizes key protein regulators, such as CDKN1A and MYC. Previous studies have demonstrated that Curcumin can induce apoptosis by causing G1 cell cycle arrest in a human adenocarcinoma cell line, independently of TP53, while also simultaneously inducing CDKN1A expression [40]. Therefore, our finding revealed potential up-regulators as protein candidates for further investigation in relation to the development of Kerra™ extracts for colecteral cancer therapeutic approaches. In order to identify promising protein upstream regulators, we utilized previously obtained phytochemical data from the Kerra™ extracts [7]. We focused on the five most abundant phytochemicals: 2-methoxy-9H-xanthen-9-one, iso-rhapontigenin, Betaine, Anethole, and Eicosatetraynoic acid. To explore the interactions between these phytochemicals and upstream proteins, we employed the STITCH protein-ligand interaction tool (accessed on 21 May 2023) [41]. We discovered that betaine has a direct interaction with TLR4 (score=0.82), which is one of the candidate protein upstream regulators (Figure 12). However, the remaining four phytochemicals did not exhibit any interaction with the protein upstream regulators.

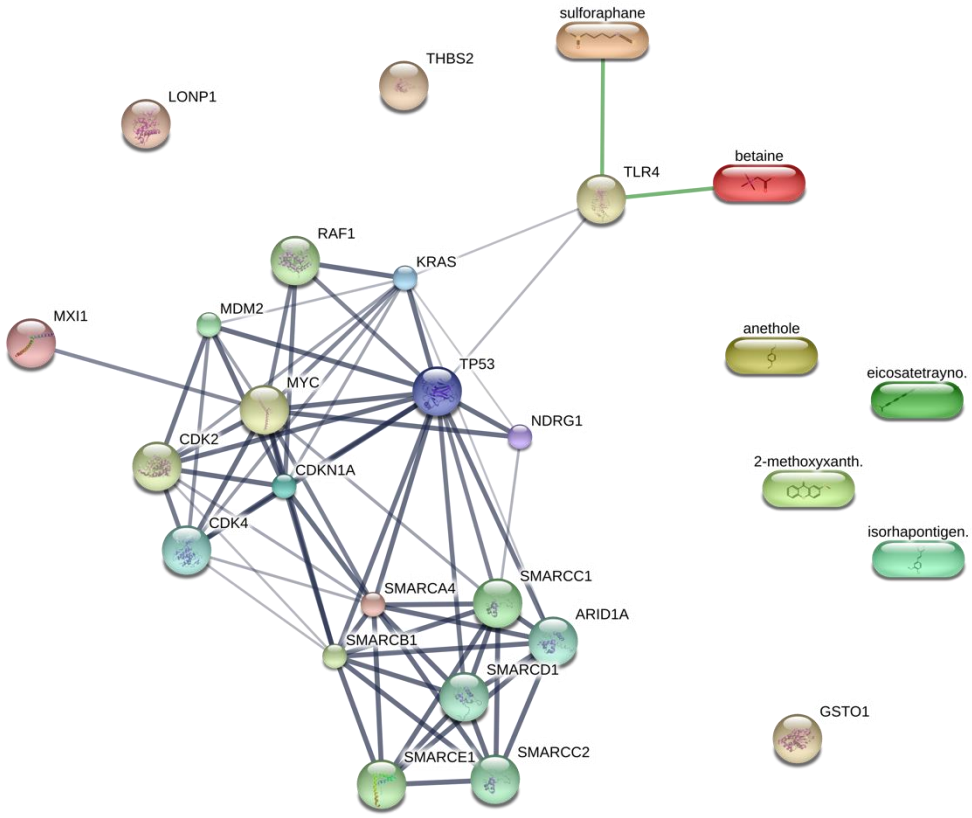

Figure 12 *Protein upstream regulators and phytochemical in Kerra™ extract interaction prediction. Ligand protein mapping was constructed from 2-methoxy-xanthen-9-one, isorhapontigenin, betaine, anethole, and eicosatetraynoic acid with the upstream regulators. The predicted interactions were shown in the connecting line.*

In addition, TLR4 also have direct interaction with KRAS and TP53 which they are candidate proteins in our results too. Our results showed TRL4 also interacts with KRAS and TP53, both of which are upstream candidate proteins identified in our results. We aimed to investigate the potential of integrating proteomics data, pathway analysis, and phytochemicals from Kerra™ extracts to study chemical compounds within biological pathways. Consequently, these findings serve to support our research and provide guidance for understanding the biochemical mechanisms of Kerra™ in HCT116 cells. It is suggested that the Kerra™ extract could potentially induce apoptotic events in HCT116 cells through the TLR4.

Apoptosis, a fundamental physiological process, plays a critical role in the normal development and maintenance of multicellular organisms. In humans, the cells exhibit two primary apoptotic pathways including the intrinsic pathway, which

involves Caspase-9 activation and is triggered by mitochondrial dysfunction, and the extrinsic pathway, which involves Caspase-8 activation and is initiated by the activation of cell surface receptors [42,43]. Immuno-based protein analysis revealed that both Caspase-8 and Caspase-9 were over-expressed under Kerra™ treatment condition compared to Dox. Furthermore, the expression pattern of these proteins correlated with characteristic biochemical changes associated with apoptosis (Figure 8). Based on these findings, we can infer that the Kerra™ extract may induce apoptosis in HCT116 cells through the regulation of Caspase-8 and Caspase-9

5. Conclusions

Kerra™ extract from the ancient Thai scripture affected on HCT116 cell viability. In addition, the extract also induced apoptosis in the cells. The Kerra™ extracts affected to various cellular proteins and biochemical pathways. Proteomics analysis revealed that 3406 proteins were affected by the Kerra™ extracts. Using pathway analysis, we found Kerra™ extract can activated apoptosis and cell death in colorectal cancer cell lines and suppressed cell proliferation of adenocarcinoma cell lines via EIF2 signaling pathway. CDKN1A and MYC were predicted as upstream regulator in response of Kerra™ extract in the cells. Therefore, these studies provide evidence for the ability of natural extracts to induce apoptosis in HCT116 colon cancer cells, demonstrating their potential as therapeutic agents for this type of cancer. Further research is needed to fully understand the mechanisms underlying these effects and to develop safe and effective therapies.

Supplementary Materials: The following supporting information can be downloaded at: www.mdpi.com/article/10.3390/medicina59081376/s1. Table S3: Protein expression data.

Author Contributions: Conceptualization, Jeeraprapa Siriwaseree, Yodying Yingchutrakul, Sucheewin Krobthong and Kiattawee Choowongkomon; Data curation, Jeeraprapa Siriwaseree and Pussadee Srathong; Formal analysis, Jeeraprapa Siriwaseree, Yodying Yingchutrakul and Pawitrabhorn Samutrtai; Funding acquisition, Sucheewin Krobthong and Kiattawee Choowongkomon; Investigation, Yodying Yingchutrakul; Methodology, Jeeraprapa Siriwaseree, Yodying

Yingchutrakul and Pussadee Srathong; Project administration, Sucheewin Krobthong and Kiattawee Choowongkomon; Resources, Chanat Aonbangkhen, Pussadee Srathong and Sucheewin Krobthong; Software, Jeeraprapa Siriwaseree; Supervision, Yodying Yingchutrakul, Pawitrabhorn Samutrtai and Chanat Aonbangkhen; Visualization, Pawitrabhorn Samutrtai; Writing – original draft, Jeeraprapa Siriwaseree and Yodying Yingchutrakul; Writing – review & editing, Yodying Yingchutrakul, Sucheewin Krobthong and Kiattawee Choowongkomon.

Funding: This work is supported by the Royal Golden Jubilee (RGJ) Ph.D. Programme by the National Research Council of Thailand (NRCT) and the Synchrotron Light Research Institute (SLRI) in the Royal Golden Jubilee Ph.D. Program scholarship (Grant no. PHD/0137/2561). K.C. wishes to thank the Kasetsart University Research and Development Institute (grant no. FF (KU)25.64). This project was financially supported by grants Innovation Policy Council by Program Management Unit for Human Resources and Institutional Development, Research and Innovation (PMU-B; grant number B05F640047). C.A. would like to thank the Development of Chula New Faculty Staff (Grant No. DNS_66_003_23_001_2), as well as the Fundamental Fund (FF66, Grant no. BCG66230008) through Chulalongkorn University Ratchadaphiseksomphot Endowment Fund, and the 29th Science and Technology Research Grant 2022 from Thailand Toray Science Foundation.

Institutional Review Board Statement: Not applicable

Informed Consent Statement: Not applicable

Data Availability Statement: Upon reasonable request, the corresponding author is willing to provide the data and materials supporting the results of this study.

Acknowledgments: -

Conflicts of Interest: The authors declare no conflict of interest. The funders had no role in the design of the study; in the collection, analyses, or interpretation of data; in the writing of the manuscript; or in the decision to publish the results.

References

1. Wang, J.-b.; Qi, L.-l.; Zheng, S.-d.; Wu, T.-x. Curcumin induces apoptosis through the mitochondria-mediated apoptotic pathway in HT-29 cells. *Journal of Zhejiang University SCIENCE B* **2009**, *10*, 93-102, doi:10.1631/jzus.B0820238.

2. Wu, L.; Xu, G.; Li, N.; Zhu, L.; Shao, G. Curcumin Analog, HO-3867, Induces Both Apoptosis and Ferroptosis via Multiple Mechanisms in NSCLC Cells with Wild-Type p53. *Evid Based Complement Alternat Med* **2023**, *2023*, 8378581, doi:10.1155/2023/8378581.

3. Piantino, C.B.; Salvadori, F.A.; Ayres, P.P.; Kato, R.B.; Srougi, V.; Leite, K.R.; Srougi, M. An evaluation of the anti-neoplastic activity of curcumin in prostate cancer cell lines. *Int Braz J Urol* **2009**, *35*, 354-360; discussion 361, doi:10.1590/s1677-55382009000300012.

4. Rodriguez Torres, S.; Gresseau, L.; Benhamida, M.; Fernandez-Marrero, Y.; Annabi, B. Epigallocatechin-3-Gallate Prevents the Acquisition of a Cancer Stem Cell Phenotype in Ovarian Cancer Tumorspheres through the Inhibition of Src/JAK/STAT3 Signaling. *Biomedicines* **2023**, *11*, doi:10.3390/biomedicines11041000.

5. Agarwal, A.; Kansal, V.; Farooqi, H.; Prasad, R.; Singh, V.K. Epigallocatechin Gallate (EGCG), an Active Phenolic Compound of Green Tea, Inhibits Tumor Growth of Head and Neck Cancer Cells by Targeting DNA Hypermethylation. *Biomedicines* **2023**, *11*, doi:10.3390/biomedicines11030789.

6. Chimento, A.; D'Amico, M.; De Luca, A.; Conforti, F.L.; Pezzi, V.; De Amicis, F. Resveratrol, Epigallocatechin Gallate and Curcumin for Cancer Therapy: Challenges from Their Pro-Apoptotic Properties. *Life (Basel)* **2023**, *13*, doi:10.3390/life13020261.

7. Seetaha, S.; Khamplong, P.; Wanaragthai, P.; Aiebchun, T.; Ratanabunyong, S.; Krobthong, S.; Yingchutrakul, Y.; Rattanasrisomporn, J.; Choowongkomon, K. KERRA, Mixed Medicinal Plant Extracts, Inhibits SARS-CoV-2 Targets Enzymes and Feline Coronavirus. *COVID* **2022**, *2*, 621-632, doi:10.3390/covid2050046.

8. Hossain, E.; Chakroborty, S.; Milan, A.; Chattopadhyay, P.; Mandal, S.C.; Gupta, J.K. In vitro and in vivo antitumor activity of a methanol extract of Dregea volubilis leaves with its antioxidant effect. *Pharm Biol* **2012**, *50*, 338-343, doi:10.3109/13880209.2011.600320.

9. Akhouri, V.; Kumar, A.; Kumari, M. Antitumour Property of Pterocarpus santalinus Seeds Against DMBA-Induced Breast Cancer in Rats. *Breast Cancer (Auckl)* **2020**, *14*, 1178223420951193, doi:10.1177/1178223420951193.

10. Santha, S.; Dwivedi, C. Anticancer Effects of Sandalwood (Santalum album). *Anticancer Res* **2015**, *35*, 3137-3145.

11. Wimalasiri, D.; Dekiwadia, C.; Fong, S.Y.; Piva, T.J.; Huynh, T. Anticancer activity of Momordica cochinchinensis (red gac) aril and the impact of varietal diversity. *BMC Complement Med Ther* **2020**, *20*, 365, doi:10.1186/s12906-020-03122-z.

12. Narang, N.; Jiraungkoorskul, W. Anticancer Activity of Key Lime, Citrus aurantifolia. *Pharmacogn Rev* **2016**, *10*, 118-122, doi:10.4103/0973-7847.194043.

13. Pfeffer, C.M.; Singh, A.T.K. Apoptosis: A Target for Anticancer Therapy. *Int J Mol Sci* **2018**, *19*, doi:10.3390/ijms19020448.

14. Rogers, C.; Alnemri, E.S. Gasdermins in Apoptosis: New players in an Old Game. *Yale J Biol Med* **2019**, *92*, 603-617.

15. Fischer, U.; Janicke, R.U.; Schulze-Osthoff, K. Many cuts to ruin: a comprehensive update of caspase substrates. *Cell Death Differ* **2003**, *10*, 76-100, doi:10.1038/sj.cdd.4401160.

16. Li, L.; Wang, S.; Zhou, W. Balance Cell Apoptosis and Pyroptosis of Caspase-3-Activating Chemotherapy for Better Antitumor Therapy. *Cancers (Basel)* **2022**, *15*, doi:10.3390/cancers15010026.

17. Lee, B.S.; Cho, Y.W.; Kim, G.C.; Lee, D.H.; Kim, C.J.; Kil, H.S.; Chi, D.Y.; Byun, Y.; Yuk, S.H.; Kim, K.; et al. Induced phenotype targeted therapy: radiation-induced apoptosis-targeted chemotherapy. *J Natl Cancer Inst* **2015**, *107*, doi:10.1093/jnci/dju403.

18. Wei, J.; Zhang, F.; Zhang, Y.; Cao, C.; Li, X.; Li, D.; Liu, X.; Yang, H.; Huang, L. Proteomic investigation of signatures for geniposide-induced hepatotoxicity. *J Proteome Res* **2014**, *13*, 5724-5733, doi:10.1021/pr5007119.

19. Zhang, D.; Qiao, W.; Zhao, Y.; Fang, H.; Xu, D.; Xia, Q. Curdione attenuates thrombin-induced human platelet activation: beta1-tubulin as a potential therapeutic target. *Fitoterapia* **2017**, *116*, 106-115, doi:10.1016/j.fitote.2016.11.016.

20. Wang, H.; Ye, Y.; Pan, S.Y.; Zhu, G.Y.; Li, Y.W.; Fong, D.W.; Yu, Z.L. Proteomic identification of proteins involved in the anticancer activities of oridonin in HepG2 cells. *Phytomedicine* **2011**, *18*, 163-169, doi:10.1016/j.phymed.2010.06.011.

21. Bai, Z.; Ye, Y.; Liang, B.; Xu, F.; Zhang, H.; Zhang, Y.; Peng, J.; Shen, D.; Cui, Z.; Zhang, Z.; et al. Proteomics-based identification of a group of apoptosis-related proteins and biomarkers in gastric cancer. *Int J Oncol* **2011**, *38*, 375-383, doi:10.3892/ijo.2010.873.

22. Lee, S.C.; Chan, J.; Clement, M.V.; Pervaiz, S. Functional proteomics of resveratrol-induced colon cancer cell apoptosis: caspase-6-mediated cleavage of lamin A is a major signaling loop. *Proteomics* **2006**, *6*, 2386-2394, doi:10.1002/pmic.200500366.

23. Kamiloglu, S.; Sari, G.; Ozdal, T.; Capanoglu, E. Guidelines for cell viability assays. *Food Frontiers* **2020**, *1*, 332-349, doi:https://doi.org/10.1002/fft2.44.

24. Khan, A.; Gillis, K.; Clor, J.; Tyagarajan, K. Simplified evaluation of apoptosis using the Muse cell analyzer. *Postepy Biochem* **2012**, *58*, 492-496.

25. Krobthong, S.; Yingchutrakul, Y.; Samutrtai, P.; Hitakarun, A.; Siripattanapipong, S.; Leelayoova, S.; Mungthin, M.; Choowongkomon, K. Utilizing Quantitative Proteomics to Identify Species-Specific Protein Therapeutic Targets for the Treatment of Leishmaniasis. *ACS Omega* **2022**, doi:10.1021/acsomega.1c05792.

26. Krobthong, S.; Yingchutrakul, Y.; Visessanguan, W.; Mahatnirunkul, T.; Samutrtai, P.; Chaichana, C.; Papan, P.; Choowongkomon, K. Study of the Lipolysis Effect of Nanoliposome-Encapsulated Ganoderma lucidum Protein Hydrolysates on Adipocyte Cells Using Proteomics Approach. *Foods* **2021**, *10*, 2157.

27. Krobthong, S.; Yingchutrakul, Y.; Visessanguan, W.; Mahatnirunkul, T.; Samutrtai, P.; Chaichana, C.; Papan, P.; Choowongkomon, K. Study of the Lipolysis Effect of Nanoliposome-Encapsulated Ganoderma lucidum Protein Hydrolysates on Adipocyte Cells Using Proteomics Approach. *Foods* **2021**, *10*, doi:10.3390/foods10092157.

28. Shilov, I.V.; Seymour, S.L.; Patel, A.A.; Loboda, A.; Tang, W.H.; Keating, S.P.; Hunter, C.L.; Nuwaysir, L.M.; Schaeffer, D.A. The Paragon Algorithm, a Next Generation Search Engine That Uses Sequence Temperature Values and Feature

Probabilities to Identify Peptides from Tandem Mass Spectra*. *Molecular & Cellular Proteomics* **2007**, *6*, 1638-1655, doi:https://doi.org/10.1074/mcp.T600050-MCP200.

29. Shilov, I.V.; Seymour, S.L.; Patel, A.A.; Loboda, A.; Tang, W.H.; Keating, S.P.; Hunter, C.L.; Nuwaysir, L.M.; Schaeffer, D.A. The Paragon Algorithm, a next generation search engine that uses sequence temperature values and feature probabilities to identify peptides from tandem mass spectra. *Mol Cell Proteomics* **2007**, *6*, 1638-1655, doi:10.1074/mcp.T600050-MCP200.

30. Willforss, J.; Chawade, A.; Levander, F. NormalyzerDE: Online Tool for Improved Normalization of Omics Expression Data and High-Sensitivity Differential Expression Analysis. *J Proteome Res* **2019**, *18*, 732-740, doi:10.1021/acs.jproteome.8b00523.

31. Degryse, S.; de Bock, C.E.; Demeyer, S.; Govaerts, I.; Bornschein, S.; Verbeke, D.; Jacobs, K.; Binos, S.; Skerrett-Byrne, D.A.; Murray, H.C.; et al. Mutant JAK3 phosphoproteomic profiling predicts synergism between JAK3 inhibitors and MEK/BCL2 inhibitors for the treatment of T-cell acute lymphoblastic leukemia. *Leukemia* **2018**, *32*, 788-800, doi:10.1038/leu.2017.276.

32. Luo, X.; Chi, X.; Lin, Y.; Yang, Z.; Lin, H.; Gao, J. A camptothecin prodrug induces mitochondria-mediated apoptosis in cancer cells with cascade activations. *Chem Commun (Camb)* **2021**, *57*, 11033-11036, doi:10.1039/d1cc04379j.

33. Murray, H.C.; Enjeti, A.K.; Kahl, R.G.S.; Flanagan, H.M.; Sillar, J.; Skerrett-Byrne, D.A.; Al Mazi, J.G.; Au, G.G.; de Bock, C.E.; Evans, K.; et al. Quantitative phosphoproteomics uncovers synergy between DNA-PK and FLT3 inhibitors in acute myeloid leukaemia. *Leukemia* **2021**, *35*, 1782-1787, doi:10.1038/s41375-020-01050-y.

34. Ravizza, R.; Gariboldi, M.B.; Passarelli, L.; Monti, E. Role of the p53/p21 system in the response of human colon carcinoma cells to Doxorubicin. *BMC Cancer* **2004**, *4*, 92, doi:10.1186/1471-2407-4-92.

35. El-Far, A.A.-O.; Godugu, K.; Noreldin, A.E.; Saddiq, A.A.; Almaghrabi, O.A.; Al Jaouni, S.K.; Mousa, S.A. Thymoquinone and Costunolide Induce Apoptosis of Both Proliferative and Doxorubicin-Induced-Senescent Colon and Breast Cancer Cells.

36. Minotti, G.; Menna, P.; Salvatorelli, E.; Cairo, G.; Gianni, L. Anthracyclines: molecular advances and pharmacologic developments in antitumor activity and cardiotoxicity. *Pharmacol Rev* **2004**, *56*, 185-229, doi:10.1124/pr.56.2.6.

37. Tacar, O.; Dass, C.R. Doxorubicin-induced death in tumour cells and cardiomyocytes: is autophagy the key to improving future clinical outcomes? *J Pharm Pharmacol* **2013**, *65*, 1577-1589, doi:10.1111/jphp.12144.

38. Kaufmann, S.H.; Earnshaw, W.C. Induction of apoptosis by cancer chemotherapy. *Exp Cell Res* **2000**, *256*, 42-49, doi:10.1006/excr.2000.4838.

39. Kramer, A.; Green, J.; Pollard, J., Jr.; Tugendreich, S. Causal analysis approaches in Ingenuity Pathway Analysis. *Bioinformatics* **2014**, *30*, 523-530, doi:10.1093/bioinformatics/btt703.

40. Saha, A.; Kuzuhara, T.; Echigo, N.; Fujii, A.; Suganuma, M.; Fujiki, H. Apoptosis of Human Lung Cancer Cells by Curcumin Mediated through Up-Regulation of “Growth Arrest and DNA Damage Inducible Genes 45 and 153&rdquo. *Biological and Pharmaceutical Bulletin* **2010**, *33*, 1291-1299, doi:10.1248/bpb.33.1291.

41. Szklarczyk, D.; Santos, A.; von Mering, C.; Jensen, L.J.; Bork, P.; Kuhn, M. STITCH 5: augmenting protein-chemical interaction networks with tissue and affinity data. *Nucleic Acids Res* **2016**, *44*, D380-384, doi:10.1093/nar/gkv1277.

42. Aral, K.; Aral, C.A.; Kapila, Y. The role of caspase-8, caspase-9, and apoptosis inducing factor in periodontal disease. *Journal of Periodontology* **2019**, *90*, 288-294, doi:https://doi.org/10.1002/JPER.17-0716.

43. Boice, A.; Bouchier-Hayes, L. Targeting apoptotic caspases in cancer. *Biochimica et Biophysica Acta (BBA) - Molecular Cell Research* **2020**, *1867*, 118688, doi:https://doi.org/10.1016/j.bbamcr.2020.118688.

CONCLUSION

In conclusion, the differential effects of JAK inhibitors Ruxolitinib and Tofacitinib on myelofibrosis cancer cells study revealing Ruxolitinib is more effective due to its selective inhibition of JAK1 and JAK2 and stronger binding interactions. The synchrotron Fourier transform infrared (S-FTIR) spectroscopy technique provided valuable insights into the biochemical alterations induced by these treatments, highlighting the potential for analyzing cellular responses to cancer therapies. These findings underscore the importance of understanding the specific mechanisms of action of JAK inhibitors to enhance treatment strategies for myelofibrosis and other related malignancies.

Another study, the Kerra™ extract from traditional Thai herbs demonstrates its significant impact on HCT116 colon cancer cells, particularly in inducing apoptosis and affecting cell viability. A comprehensive proteomics analysis revealed that the extract influences cellular proteins and biochemical pathways, specifically activating apoptosis and suppressing cell proliferation via the EIF2 signaling pathway. Key proteins such as CDKN1A and MYC were identified as upstream regulators responding to the extract. These findings highlight the potential of natural extracts like Kerra™ as therapeutic agents in cancer treatment, warranting further research to elucidate the underlying mechanisms and develop safe, effective therapies for colorectal cancer.

RECOMMENDATIONS AND FUTURE WORK

Based on the effects of JAK inhibitors on myelofibrosis cancer cell findings in the first paper. It could investigate deeper into the specific molecular mechanisms by which these JAK inhibitors exert their effects, including the downstream signaling pathways affected and the role of other cellular components in mediating these responses. Furthermore, the efficacy of additional JAK inhibitors beyond Ruxolitinib and Tofacitinib could be explored, assessing their selectivity and effectiveness against various JAK isoforms in myelofibrosis and other hematological malignancies.

Further studies in the second paper are needed to identify the specific phytochemicals in the Kerra™ extract that respond to inducing cell apoptosis regarding the detailed understanding of the upstream regulators influencing the extract's effects on HCT116 cells. Additionally, should focus on isolating these compounds and understanding their contributions to the observed biological effects. It could elucidate these mechanisms and validate the therapeutic potential of Kerra™ extract in clinical settings, particularly for colorectal cancer treatment.

FUNDING SOURCES

This work is supported by the Royal Golden Jubilee PhD Program between National Research Council of Thailand (NRCT) and the Synchrotron Light Research Institute (SLRI) (Grant no. PHD/0137/2561; 4.C.KU/61/A.1.O.XX)

LITERATURE CITED

1. Bray, F., et al., *Global cancer statistics 2018: GLOBOCAN estimates of incidence and mortality worldwide for 36 cancers in 185 countries.* CA: A Cancer Journal for Clinicians, 2018. **68**(6): p. 394-424.
2. Rehman, S., *An Overview of Cancer Treatment Modalities*. 2018.
3. Qureshy, Z., D.E. Johnson, and J.R. Grandis, *Targeting the JAK/STAT pathway in solid tumors.* Journal of Cancer Metastasis and Treatment, 2020. **6**: p. 27.
4. Johnson, D.E., R.A. O'Keefe, and J.R. Grandis, *Targeting the IL-6/JAK/STAT3 signalling axis in cancer.* Nature Reviews Clinical Oncology, 2018. **15**(4): p. 234-248.
5. Sabaawy, H.E., et al., *JAK/STAT of all trades: linking inflammation with cancer development, tumor progression and therapy resistance.* Carcinogenesis, 2021. **42**(12): p. 1411-1419.
6. Hoisnard, L., et al., *Adverse events associated with JAK inhibitors in 126,815 reports from the WHO pharmacovigilance database.* Scientific Reports, 2022. **12**(1): p. 7140.
7. Samuel, C., et al., *A Review on the Safety of Using JAK Inhibitors in Dermatology: Clinical and Laboratory Monitoring.* Dermatol Ther (Heidelb), 2023. **13**(3): p. 729-749.
8. Hossain, M.S., et al., *Herb and Spices in Colorectal Cancer Prevention and Treatment: A Narrative Review.* Frontiers in Pharmacology, 2022. **13**.
9. Bellisola, G. and C. Sorio, *Infrared spectroscopy and microscopy in cancer research and diagnosis.* American journal of cancer research, 2012. **2**(1): p. 1-21.
10. Gasper, R., G. Vandenbussche, and E. Goormaghtigh, *Ouabain-induced modifications of prostate cancer cell lipidome investigated with mass spectrometry and FTIR spectroscopy.* Biochim Biophys Acta, 2011. **1808**(3): p. 597-605.

APPENDICES

Appendix A

Supplementary of Publication 1

Synchrotron FTIR microscopy spectra in cellular effects of JAK inhibitors on myelofibrosis cancer cells

Additional figures as mentioned in the text

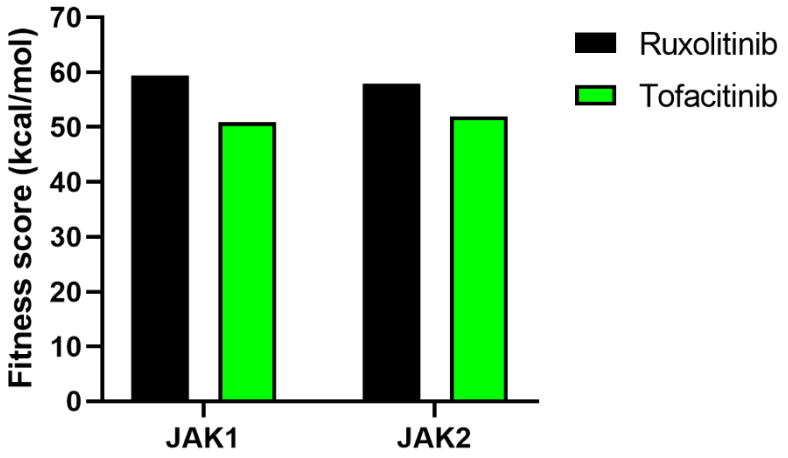

Figure S13 The docking energy scores of known drugs with the JAK1 and JAK2 proteins

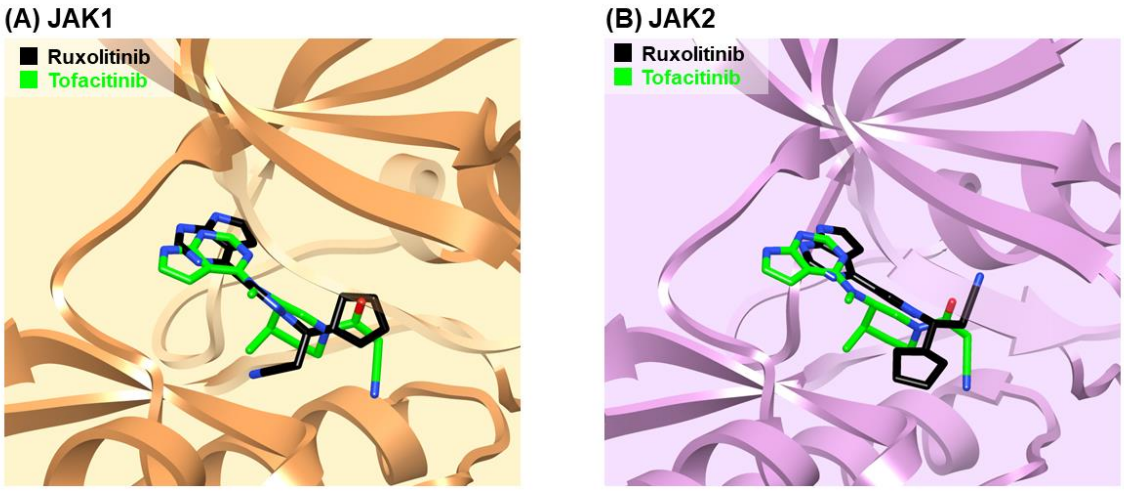

Figure S14 The binding pattern of known drugs within JAK1 and JAK2. (A) Ruxolitinib and Tofacitinib complexed with JAK1. (B) Ruxolitinib and Tofacitinib complexed with JAK2.

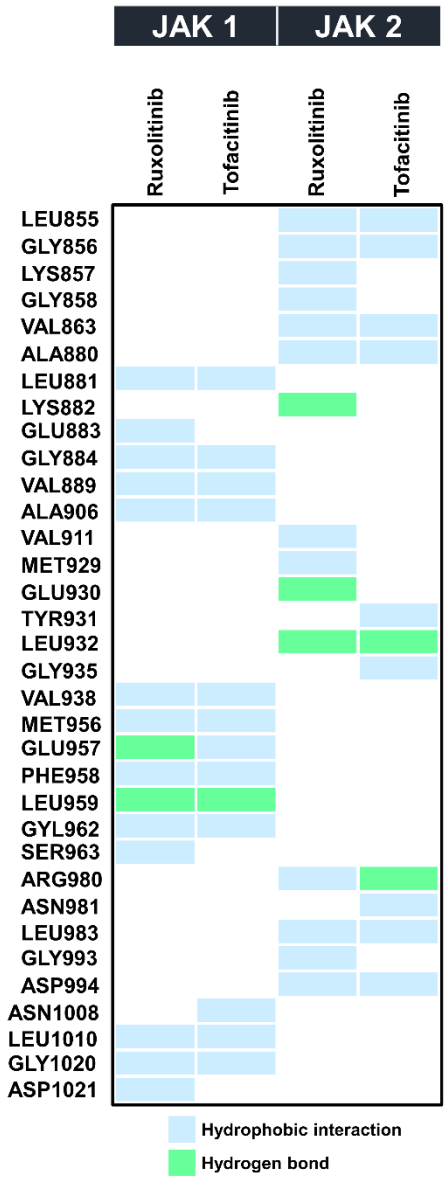

Figure S15 Summary of histograms showing interactions of Ruxolitinib and Tofacitinib complexed with JAK1 and JAK2

Appendix B

Supplementary of Publication 2

Exploring the Apoptotic-Induced Biochemical Mechanism of Traditional Thai Herb (Kerra™) Extract in HCT116 Cells Using a Label-Free Proteomics Approach

Table S3 Protein expression data.

Identifier	logFC	adj.P.Val
O60879	3.137425	8.61E+00
P09601	3.697033	7.75E+00
P69905	5.232422	7.18E+00
Q99988	3.203848	7.07E+00
P04264	4.219399	6.85E+00
P35527	3.53482	6.78E+00
P37235	0.983752	6.74E+00
Q99653	0.962597	6.68E+00
P68871	3.564752	6.64E+00
P84074	1.14114	6.63E+00
Q86Z14	-1.19563	6.54E+00
Q9BYN0	2.064807	6.50E+00
O95447	-1.26506	6.36E+00
Q9NQU5	-1.05164	6.27E+00
Q8WUM4	-0.77576	6.11E+00
Q14152	-1.06138	6.08E+00
P02042	3.77113	6.08E+00
Q96B67	2.344123	6.03E+00
P16401	-0.87083	6.02E+00
P35908	2.734303	5.99E+00
Q05639	-1.18024	5.86E+00
Q13501	1.757506	5.81E+00
Q92674	0.96995	5.71E+00
Q14201	0.700504	5.63E+00
O15525	0.891621	5.59E+00

Q9UIS9	1.679684	5.50E+00
O15479	0.648347	5.45E+00
P46777	-0.91112	5.44E+00
Q7Z406	-0.86946	5.37E+00
P02768	0.83087	5.34E+00
P11940	-0.68662	5.32E+00
P13645	1.45333	5.32E+00
P01130	0.83313	5.27E+00
P60842	-0.75824	5.26E+00
P50991	-0.77934	5.25E+00
P10321	0.628191	5.21E+00
P08758	0.784245	5.10E+00
Q01082	-1.41047	5.05E+00
Q04637	-0.64712	5.02E+00
P46782	0.546464	5.00E+00
P07195	-0.62249	4.95E+00
P50914	-0.61173	4.94E+00
P12270	0.659526	4.87E+00
P50990	-0.64718	4.86E+00
P38919	-0.58043	4.85E+00
O43291	0.682083	4.84E+00
O00148	-0.67621	4.82E+00
Q5BKZ1	0.696545	4.79E+00
Q15758	0.686393	4.76E+00
P62826	-0.62929	4.76E+00
P35749	-0.89353	4.75E+00
P26641	-0.832	4.74E+00
P07711	0.946446	4.72E+00
Q13838	-0.61351	4.70E+00
P49368	-0.70781	4.66E+00
P02649	1.985407	4.65E+00

P18124	-0.57015	4.63E+00
Q13310	-0.6334	4.61E+00
P23526	-0.5411	4.60E+00
Q7RTV0	0.570012	4.59E+00
P49736	-0.65072	4.58E+00
O00422	0.511346	4.58E+00
O76015	0.54995	4.57E+00
P07737	-0.73127	4.57E+00
Q92597	0.848623	4.57E+00
Q99547	1.520307	4.56E+00
Q99873	-0.6385	4.56E+00
P10909	1.276335	4.55E+00
P61981	-0.46744	4.55E+00
Q99832	-0.82854	4.54E+00
Q15181	-0.54395	4.54E+00
O60885	0.841274	4.53E+00
P26373	-0.4811	4.53E+00
P62917	-0.59268	4.50E+00
Q92692	0.472595	4.49E+00
P07478	-0.91566	4.49E+00
P63173	-0.52016	4.47E+00
Q01658	0.512166	4.47E+00
P23396	-0.46397	4.46E+00
Q15102	-0.53979	4.46E+00
Q9H254	0.557014	4.45E+00
Q12797	0.641891	4.43E+00
O00303	-0.76969	4.41E+00
P14174	-0.61449	4.40E+00
Q9GZQ8	0.493744	4.38E+00
P18669	-0.82086	4.38E+00
O15212	-0.69359	4.37E+00

Q6UX04	0.585046	4.35E+00
Q9H3N1	0.447306	4.34E+00
Q9P1Z2	3.441129	4.32E+00
Q13765	-0.50284	4.31E+00
P13667	-0.46067	4.31E+00
Q14676	0.553622	4.30E+00
O95294	0.590574	4.30E+00
Q16658	-0.63448	4.29E+00
Q9UBB5	0.510833	4.29E+00
Q07020	-0.44843	4.28E+00
Q86X29	0.431761	4.27E+00
P17676	0.861766	4.27E+00
Q8N163	-0.61434	4.27E+00
P27635	-0.63477	4.25E+00
P55010	0.414899	4.25E+00
Q9UBS4	0.632729	4.25E+00
O15481	-3.10436	4.24E+00
Q8TCS8	0.484393	4.23E+00
Q9Y3U8	-0.42956	4.22E+00
P01116	0.494513	4.22E+00
Q02790	-0.6893	4.20E+00
P31949	0.924819	4.19E+00
P06744	-0.60119	4.19E+00
O75376	-0.48072	4.19E+00
Q9Y265	-0.53384	4.18E+00
Q99613	-0.67219	4.18E+00
P42167	0.477091	4.18E+00
Q14114	0.782085	4.18E+00
Q9UJZ1	0.785887	4.17E+00
Q9H3K6	-0.56908	4.17E+00
P62805	-0.85629	4.15E+00

Q13751	1.435475	4.14E+00
P04259	1.330112	4.14E+00
Q99848	0.401314	4.14E+00
P52306	0.906361	4.14E+00
A8TX70	-1.4774	4.13E+00
Q9Y6W5	0.428186	4.13E+00
P00338	-0.68774	4.12E+00
P11908	-1.22155	4.11E+00
P60891	-1.22155	4.11E+00
Q9NPA0	0.465603	4.11E+00
P35241	-0.55121	4.10E+00
P10809	1.130089	4.10E+00
Q6NZY4	0.629085	4.10E+00
P11021	0.587167	4.09E+00
P31153	-0.63528	4.07E+00
Q9H814	-0.79558	4.07E+00
Q14789	0.679211	4.07E+00
Q12789	1.070488	4.04E+00
P12532	0.51697	4.03E+00
P47897	-1.03815	4.03E+00
P17931	0.414239	4.01E+00
P02792	0.636685	4.01E+00
O00154	-0.79483	4.00E+00
P16949	-0.46231	4.00E+00
Q9UHB6	0.412933	3.982211
O95373	-0.99303	3.979481
Q9GZR7	-0.96306	3.978224
Q6P161	0.609206	3.963507
Q9H147	0.731863	3.959841
P30041	-0.42302	3.957543
P84077	-0.44173	3.950352

Q9H773	-0.57663	3.94554
P55786	-0.45414	3.937501
P04406	-0.485	3.936164
O15173	0.430574	3.931024
P17275	0.714018	3.930961
P13473	0.449507	3.922618
P59998	-0.53234	3.921695
Q03405	0.860443	3.919175
Q03135	-0.40486	3.89768
Q96S55	0.868421	3.89386
P62258	-0.66499	3.892641
P50213	0.382221	3.889825
O15234	-0.73925	3.889262
P08865	-0.5476	3.883117
O14944	0.561878	3.882063
O15372	-0.69299	3.881613
P46781	-0.53644	3.872736
P15880	-0.46447	3.870252
P50395	-0.45461	3.866171
P48507	1.182908	3.866053
P55884	-0.97159	3.861719
P60468	0.366146	3.858933
Q9NXV2	0.987709	3.856083
Q01844	0.335613	3.852979
Q14137	-0.46772	3.830229
P17987	-0.72816	3.828119
Q9Y224	0.542996	3.821282
P43307	0.616363	3.815326
P00491	-0.86316	3.79067
P40925	-0.54701	3.790107
Q96QD8	-1.37852	3.781254

Q13428	0.41333	3.77997
Q13033	0.6083	3.770646
P62906	-0.44277	3.769201
Q6FI13	2.466004	3.769194
Q16777	2.466004	3.769194
Q13740	0.369697	3.767395
Q13242	0.41988	3.764093
P21583	-0.80625	3.745249
P62847	-0.84835	3.744665
P40429	-0.60967	3.732181
Q9NPI1	0.704648	3.731925
O95297	0.419027	3.730214
P63313	-0.4764	3.729615
Q12907	0.446201	3.728096
Q14061	-0.55772	3.71748
O00220	0.647817	3.716599
Q5XKE5	1.395462	3.712463
P04156	0.744029	3.709928
Q96IY1	0.864318	3.709525
Q9NX58	0.418481	3.706949
Q14919	0.440774	3.701121
P43487	-0.50837	3.697667
P68133	0.659831	3.694425
P04080	-0.6898	3.694335
P49327	-0.94188	3.692973
P22234	-0.90592	3.690593
Q96QC0	0.580941	3.678619
P49207	-0.45376	3.678337
Q9UIG0	0.711044	3.676162
P62829	-0.44587	3.675547
Q6NXG1	0.368795	3.672169

P62266	-0.68752	3.668229
P52565	-0.61117	3.664003
P62495	-0.58362	3.661105
P25208	0.523155	3.654272
Q96A33	0.492909	3.650219
P78347	-0.55068	3.645356
Q02878	-0.53707	3.644158
P36578	-0.81379	3.643588
Q93045	-0.40629	3.642763
P17693	0.509842	3.632447
Q07065	0.581592	3.630367
Q96FS4	0.396766	3.617756
Q15424	0.590291	3.610726
Q9UDY4	0.35751	3.606313
O75832	1.516213	3.600158
P19623	-0.8011	3.596101
P62241	-0.60681	3.585214
P08559	-0.70536	3.584482
P18077	-0.45989	3.583017
Q9BRT2	1.299314	3.580633
P19256	0.764723	3.575742
P61088	-0.32663	3.569174
Q96JB5	0.546871	3.567884
O95171	-0.54667	3.562043
O00264	0.400255	3.555557
Q9Y6M7	1.46369	3.55126
Q96A72	-0.65799	3.548264
O75821	-0.39219	3.547965
P33316	-0.32424	3.542316
Q6NSI4	-0.41995	3.538536
Q5T4S7	1.84749	3.537962

O14763	0.658824	3.536764
Q9Y262	-1.12448	3.535752
Q01813	-0.55701	3.534183
Q9Y2R5	-0.5575	3.52662
Q5JTV8	0.345301	3.526348
P02545	0.340421	3.524534
P54652	0.430089	3.519177
P63027	0.451969	3.512891
Q9BZF1	-0.53789	3.510317
P18621	0.312449	3.508867
P17096	0.424771	3.492946
Q9NYJ1	-1.29623	3.491249
P46779	-0.44497	3.480785
P40926	-0.36549	3.465305
Q92785	0.447091	3.464312
Q9HCM1	0.545285	3.463986
Q14185	0.545285	3.463986
P61353	-0.44582	3.453563
Q71UM5	-0.38776	3.453181
Q9HB71	-0.46832	3.441905
Q9P0J1	-0.83572	3.433403
O96008	-0.57936	3.431708
O15355	-0.52902	3.431089
P50454	-0.45221	3.424853
Q7Z794	0.405589	3.422282
P02788	0.876632	3.417409
P31947	1.013635	3.413984
P62244	-0.37916	3.409875
P16104	1.197758	3.406098
Q8IUE6	1.197758	3.406098
Q15056	-0.32796	3.403359

P35240	-0.38027	3.399877
Q96HY6	0.561668	3.397387
P04439	0.418712	3.389196
Q13045	0.401061	3.38223
P45973	0.40138	3.381018
P07477	-0.8713	3.380743
Q13435	0.416717	3.378985
Q13126	-0.92734	3.377938
P07602	0.635706	3.37213
P61313	-0.59285	3.369231
Q9UQB8	0.364652	3.367722
Q16584	0.44503	3.366824
Q9Y230	-0.56302	3.359609
Q96P16	0.428454	3.352068
Q96T88	-0.45535	3.349891
Q8IUZ0	1.216596	3.342409
P26038	-0.4209	3.340942
Q99439	-0.45642	3.327499
P13489	-0.49984	3.324677
P62979	-0.3932	3.314447
O43396	0.358198	3.314267
P52292	0.481986	3.311244
P25788	-0.46299	3.310833
P00367	-0.37721	3.306283
P42677	-0.39	3.301219
Q8NC56	0.419612	3.298914
Q9NS69	-0.42412	3.293371
Q9UHD1	-0.81786	3.287969
P06703	1.805518	3.283543
P48163	1.550904	3.28255
Q14197	0.33509	3.280091

O60841	-0.52871	3.275895
Q9BZZ5	-0.92751	3.270776
Q9UNN8	0.393526	3.264827
O60216	-0.71307	3.259763
P35658	-0.98127	3.257547
Q9Y399	-0.40782	3.253624
Q15075	0.98894	3.246872
P60900	-0.50633	3.243861
P43034	0.638165	3.242856
P84243	-0.61564	3.233375
P23921	-0.90228	3.231059
P55795	0.502514	3.230432
O43670	-0.37664	3.217259
Q70UQ0	0.899826	3.216852
Q9NY61	0.467172	3.21364
Q969H8	-0.50725	3.21173
P35249	0.293328	3.207351
P09455	-0.49556	3.2071
Q13162	-0.3444	3.20504
Q15528	0.877857	3.201396
P49915	-0.55908	3.200923
Q86T82	2.009551	3.19946
Q8IXK0	0.47908	3.194251
Q9Y3A6	0.604533	3.191236
Q8IYB3	0.393632	3.190108
P35580	-0.42095	3.188769
Q9Y2B0	-0.34908	3.187814
Q09028	0.335001	3.17813
P06748	0.744839	3.172953
P10515	-0.33584	3.169727
P31942	0.348602	3.169056

Q15046	-0.67072	3.162407
Q14258	-0.606	3.161773
Q14204	-0.93591	3.161162
Q14203	0.321793	3.160944
P84098	-0.39248	3.157745
P61326	-0.71158	3.152436
O00330	0.440032	3.151374
Q86VM9	0.594134	3.150613
Q9P035	-0.58749	3.146744
Q9HCN8	0.401743	3.145935
P14868	-0.50726	3.135293
Q15008	-0.29935	3.12792
Q15435	-0.86808	3.126544
Q6UN15	0.532517	3.12147
P51398	-0.4839	3.116871
P12004	-0.33364	3.111142
Q86UD0	4.27173	3.106125
P18846	0.61748	3.098036
O95816	0.468823	3.086962
O94925	-0.41441	3.086895
P30613	-0.42737	3.081575
P25786	-0.31569	3.078185
P00505	-0.4027	3.078071
P62888	-0.36365	3.077359
P83731	-0.26527	3.075398
P98175	0.427446	3.069973
Q00059	0.399997	3.068886
Q8WTV0	0.334899	3.068647
O75683	0.361031	3.059508
O43491	-0.52285	3.057185
P26358	-1.0771	3.055677

Q6FI81	-0.29543	3.049012
Q9UBQ5	-0.44274	3.043067
Q5JRX3	0.535522	3.042503
Q86TS9	1.182265	3.040849
Q02818	0.390664	3.038478
P46778	-0.53498	3.027749
O43709	0.478041	3.026898
Q969X1	0.897682	3.026397
O00505	-0.45759	3.0236
P60228	-0.68671	3.019863
Q92598	-0.5753	3.013527
P61956	-0.31824	3.010567
Q15233	-0.50008	3.005092
P07355	0.739658	3.004862
P11166	0.424594	3.00454
P07814	-0.55369	3.000867
Q8NC51	0.385096	2.999652
Q8WZA9	1.506103	2.995054
P28799	-0.38218	2.990771
Q03252	0.24667	2.98793
P01111	0.331736	2.984218
Q15005	0.406441	2.981866
P12236	-0.29526	2.980934
P48506	1.683162	2.978408
Q71DI3	2.4698	2.97335
P51970	0.281461	2.969328
O75381	0.3037	2.962874
Q15004	-0.40949	2.961744
P62304	-0.49078	2.961283
P38159	0.330823	2.960133
Q9NYL9	0.321611	2.956319

P78386	2.954143	2.955705
P78385	2.954143	2.955705
O43790	2.954143	2.955705
Q14533	2.954143	2.955705
Q7Z3Y9	2.649129	2.951562
P52926	0.63314	2.949011
Q99594	-0.54832	2.945431
Q15561	-0.54832	2.945431
P28347	-0.54832	2.945431
Q15562	-0.54832	2.945431
P78329	1.793496	2.941395
Q9HBI6	1.793496	2.941395
Q8NBJ5	-0.53572	2.940732
P01112	0.352666	2.937021
Q00325	-0.29712	2.930218
Q9H5V8	0.373879	2.927942
Q15388	0.393591	2.925415
P60866	0.289736	2.925049
Q7L0Y3	-0.40843	2.923516
Q9BVJ6	0.312377	2.915465
Q96GQ7	-0.70951	2.914449
P63244	-0.55664	2.914083
P62753	-0.37313	2.908201
O43920	0.57484	2.90392
Q9BV68	-0.50204	2.903405
P25205	-0.51493	2.899472
Q15717	-0.40052	2.897739
O14653	0.361254	2.891653
Q9HBM6	0.363621	2.89007
P31946	-0.39016	2.889842
P09669	0.279773	2.883707

O43869	0.516438	2.88368
Q8NH04	0.516438	2.88368
Q9ULX6	0.261113	2.876589
O95292	0.281243	2.873737
P27824	0.6718	2.873417
P78344	0.567735	2.865722
O75934	0.471088	2.85897
P16403	0.503447	2.858359
Q86U42	0.267353	2.853988
P62857	-0.25872	2.842984
Q9Y291	0.534318	2.839767
O75251	-0.40333	2.839658
Q9H2U2	-0.33084	2.839235
P23284	-0.23989	2.835319
O95817	0.393539	2.835146
P13929	-0.26678	2.826458
P62937	1.204331	2.825105
Q13243	0.253149	2.819709
Q13158	0.409617	2.816857
P22392	-0.26538	2.815583
O00566	0.488132	2.811685
P37837	-0.72068	2.811008
P27708	-0.95718	2.809564
P10606	0.283657	2.80104
Q9NQH7	-0.40216	2.800935
Q14244	0.400866	2.799434
P29373	-0.5026	2.795802
Q9NYF8	0.245159	2.793651
P49585	0.392044	2.786802
P62306	-0.38455	2.779779
Q9NSD9	-0.45154	2.779134

P30084	-0.30092	2.777498
Q9BXY0	-0.54127	2.772506
P26639	-0.75457	2.770907
P22087	-0.44952	2.767702
P12081	-0.43634	2.764174
Q99471	-0.38706	2.75424
P15151	0.607981	2.742877
O14818	-0.42425	2.742511
Q10567	-0.54206	2.739276
P61163	-0.89801	2.737192
O75131	-0.50542	2.728904
Q92841	-0.3648	2.728758
P07237	-0.67175	2.721944
Q16543	-0.30057	2.721042
Q15366	-0.27759	2.719934
Q9BYC8	0.708025	2.716245
Q4G176	-0.5963	2.708179
P49790	0.6519	2.708037
P09972	-0.41614	2.702899
Q14019	-0.28567	2.702414
Q16850	-1.75465	2.701578
P52597	0.992472	2.700428
P62424	-0.56642	2.697143
P36542	-0.26511	2.696847
O14893	0.868993	2.69547
Q15459	-0.56507	2.694338
P06493	-0.54786	2.693825
O75528	0.713653	2.671782
P09012	0.336055	2.66988
P14927	0.371622	2.669513
P68032	0.423713	2.663615

P62736	0.423713	2.663615
P63267	0.423713	2.663615
P32969	-0.39011	2.661251
O75534	-0.53493	2.659122
Q9UKV3	0.316799	2.657578
P05026	0.404407	2.65425
O43823	0.430092	2.65092
Q9H0E9	0.927466	2.648416
Q96GY0	0.688609	2.648063
P46459	-0.32579	2.637045
O95400	0.489473	2.637008
P55273	0.417359	2.636875
P20645	0.274379	2.636455
Q9BQ70	-1.24305	2.636362
Q8NEW0	1.742964	2.633243
P01893	0.326577	2.628863
Q14108	0.44075	2.619255
P08648	0.399579	2.618867
Q9NV96	0.692548	2.615387
P02647	2.98331	2.612008
P31350	-0.60309	2.610939
O14974	0.394083	2.610318
Q8NFH3	0.288928	2.601817
P25440	0.500418	2.600739
Q9UFW8	0.329929	2.599083
O95167	-0.37716	2.597973
Q9UIJ7	0.366037	2.597735
P04083	0.219711	2.594009
O15014	0.724567	2.592619
P49459	0.301653	2.592083
P00390	0.405382	2.591613

Q562R1	-0.86344	2.588383
Q9ULV4	-0.95702	2.58789
Q01081	0.349926	2.587657
Q8NBJ7	-0.26545	2.585406
Q16531	-0.39289	2.584077
P22626	0.272565	2.584066
Q96S52	1.386635	2.583807
Q9BT09	-0.70277	2.583026
O96000	0.327604	2.579618
P33992	-0.91175	2.577423
O43665	-0.36029	2.57515
Q99828	0.854733	2.574004
P50750	0.266861	2.570955
Q9NYV4	0.266861	2.570955
Q969Y2	0.561261	2.567608
Q6P5R6	0.298614	2.566575
P34932	-0.38269	2.564535
P22102	-0.55771	2.559245
Q9Y639	0.313815	2.553507
P22307	0.257627	2.549954
P15311	-0.80018	2.547937
Q96EU6	-0.55472	2.545841
P08174	0.615855	2.542921
Q9Y5L4	-0.25431	2.541339
P54317	0.374332	2.541122
P60604	0.420093	2.540883
P18754	-0.42101	2.540565
P04075	-0.59728	2.530132
O00151	-0.2567	2.526726
P33778	1.049617	2.524602
P57053	1.049617	2.524602

O60814	1.049617	2.524602
P58876	1.049617	2.524602
Q5T8P6	0.242485	2.518968
Q8N135	2.059092	2.518711
P62277	-0.25799	2.511596
P08195	1.038841	2.511484
Q92546	-1.429	2.510408
Q16563	0.312805	2.507054
Q9NQ50	0.279456	2.505723
Q86X55	-1.22953	2.505321
P30050	-0.23827	2.504406
P35244	-0.87891	2.503393
Q5T9L3	-0.94354	2.500992
Q16778	1.071252	2.497196
P06899	1.071252	2.497196
P23527	1.071252	2.497196
P62807	1.071252	2.497196
Q93079	1.071252	2.497196
Q9UK76	-0.48858	2.497136
Q14671	-0.75861	2.493143
P35579	-0.87299	2.492724
O75439	-0.24209	2.491782
Q9Y3D7	0.368139	2.489211
O14737	-0.34229	2.486532
P63167	-0.75588	2.481194
Q9NX63	0.224551	2.47942
Q9BSY4	-0.98345	2.478894
P56182	0.485814	2.475311
P46776	-0.2538	2.47398
P31939	-0.71654	2.47378
Q9UK22	0.37249	2.472687

Q9H410	0.540493	2.463779
Q99497	-0.26431	2.463197
Q4VC05	0.540884	2.462777
Q9C0J8	-0.60201	2.462567
Q969Q0	-0.26948	2.462087
Q04941	0.305443	2.462002
P61254	-0.37228	2.455232
Q7Z6E9	2.53985	2.453072
Q92520	-0.26564	2.452353
Q8WYQ5	0.640283	2.452109
P21333	-0.44247	2.451705
P13987	0.225749	2.44914
O43776	-0.6126	2.447858
P48729	-0.48871	2.444977
Q5T8D3	0.509289	2.443575
P12235	-0.26576	2.443149
P26196	-0.39835	2.441289
O43818	-0.38861	2.439137
P54920	-0.59771	2.43565
P28290	-0.51929	2.435534
Q14166	-0.81375	2.434034
P04920	0.788784	2.428294
Q6UB35	-0.27791	2.427809
Q9BUJ2	-0.38883	2.426092
Q496H8	-1.37152	2.424805
Q93050	0.374605	2.41661
Q9UBL6	-0.3245	2.416323
Q8IVT2	0.229092	2.409356
P33240	0.332552	2.405113
P62256	0.275553	2.403234
Q99877	1.132434	2.403015

Q99879	1.132434	2.403015
Q5QNW6	1.132434	2.403015
Q99880	1.132434	2.403015
P12268	-0.60034	2.401266
Q8WZ42	-0.31107	2.387057
Q9Y6E2	-0.49209	2.385845
Q86YP4	0.247269	2.384252
P08574	0.317315	2.383595
P07384	-0.54652	2.382323
P48047	0.207391	2.376318
Q3B7T1	-1.016	2.376169
Q9BYD3	-1.27182	2.369195
Q04323	-0.50917	2.364703
P30086	-0.21005	2.357883
Q96PU4	-0.33533	2.357188
Q9UJU6	-0.2903	2.352683
Q04837	0.416529	2.352231
P13995	0.305309	2.34965
Q92522	-0.27664	2.344121
P29084	0.420469	2.338797
P20042	0.271409	2.338215
L0R8F8	0.602347	2.337532
P13284	0.568005	2.33723
P15559	0.885134	2.334336
Q9Y6C9	-0.39732	2.330325
Q8N7H5	0.517927	2.32826
Q96FZ7	0.408554	2.325536
Q9UNX3	-0.30859	2.323232
P33991	-0.53169	2.321678
P61024	-1.09213	2.320833
Q92667	-0.78848	2.320431

Q9ULX3	-0.39755	2.316906
Q9UPT5	-0.95943	2.316862
O15145	-0.52557	2.313
Q9UBB4	-0.41689	2.311095
P62249	-0.25359	2.307776
O15400	0.307568	2.307509
Q92900	-0.60297	2.304073
Q5JRA6	0.515092	2.299238
Q9H7Z7	0.389837	2.296292
P07947	0.232389	2.295675
P49590	-0.33448	2.293158
P07858	-0.25597	2.292178
Q9NYB9	0.345619	2.285466
P49419	-0.42552	2.284843
O14980	-0.44764	2.283583
P24941	0.211154	2.282244
Q00526	0.211154	2.282244
P11586	-2.61721	2.281348
P63098	-1.07718	2.280854
P62701	-0.30441	2.280163
P16220	0.496163	2.278451
P26006	0.299025	2.266499
Q96B36	-0.57507	2.264792
P07339	0.204734	2.261145
P05067	0.548391	2.260511
Q5VZE5	-0.96688	2.258004
P42126	-0.31303	2.257375
P49750	0.348999	2.251277
P04040	-0.49252	2.249534
P15924	-0.41014	2.249257
P55081	0.394274	2.249183

Q13438	0.540819	2.239045
Q9Y2D5	0.768792	2.23896
P61604	0.473818	2.236948
O75525	0.218162	2.231938
P05388	-0.32849	2.227688
Q8NF91	-0.44598	2.226023
O15305	-0.23845	2.222785
O75533	-0.68482	2.215612
P62314	-0.23512	2.214949
P62913	-0.31186	2.210776
Q92499	-0.79785	2.209995
P35080	-0.26722	2.207015
Q9Y5J9	-0.26124	2.206934
O14639	-0.68095	2.206346
P61247	-0.28158	2.201729
P17568	0.198081	2.200266
P11766	-1.39359	2.197711
Q9BTC0	0.507781	2.192834
P17535	0.552551	2.19059
P38117	-0.29374	2.190324
P40227	-0.55034	2.189605
Q9C0C2	0.624512	2.186747
Q96NC0	0.208034	2.178624
Q9GZL7	-0.58187	2.175641
P10109	-0.23694	2.173676
Q01518	-0.51534	2.173604
Q14696	-0.51212	2.170288
Q5UCC4	0.385398	2.167484
Q969G3	0.317137	2.167147
P51151	0.41815	2.162898
Q07955	0.225839	2.159052

Q16891	-0.45573	2.158461
Q9Y5B9	-0.24892	2.156509
P56537	-0.28957	2.150863
Q9Y2R4	-1.44176	2.150104
Q96DH6	-0.802	2.14847
Q15390	0.540985	2.145949
Q14978	0.474326	2.140574
P60903	0.220073	2.133636
P62081	-0.32319	2.129536
Q7Z417	0.177762	2.126644
Q8IY67	-2.38005	2.125433
O15031	0.281171	2.123321
P09496	-0.21949	2.123196
Q2TAY7	-0.29519	2.118293
P32322	-0.29276	2.11824
Q13557	-0.3551	2.11758
O95365	0.666835	2.115518
P83881	-0.27734	2.109469
Q7KZ85	-1.54819	2.10734
Q13444	-0.25733	2.10696
Q13405	0.260984	2.106609
Q9H0H5	0.32864	2.106321
Q99714	-0.38862	2.105191
P49411	-0.3031	2.105061
P54105	-0.21902	2.104536
P53396	-0.71973	2.0994
P62280	-0.51796	2.09517
Q15043	-0.61955	2.095031
Q9Y2W1	0.253469	2.090215
Q7Z7H5	0.295161	2.08986
Q9NZL4	-0.50597	2.088708

P49591	-0.56764	2.087435
P48443	0.814894	2.086553
Q8N5K1	0.347657	2.085595
Q9UQ80	-0.45098	2.085109
Q9UKK9	-0.2805	2.084754
P12956	-0.60303	2.078858
P10253	0.636072	2.076965
Q96C36	-0.22081	2.072554
Q16527	1.951084	2.072313
Q8NDX5	0.538876	2.071837
Q14974	0.615036	2.070024
P53634	-0.41714	2.067358
O94888	-0.48235	2.065013
Q01469	-0.30142	2.062443
Q04760	-0.31744	2.062241
Q9C004	0.339653	2.06217
Q16718	0.202435	2.062014
Q9UHF1	-0.86162	2.059071
P56556	-0.26607	2.057157
P55060	-0.79586	2.057016
O95208	0.362899	2.055138
P61513	-0.39251	2.048634
O00165	0.33681	2.046746
P23497	0.712008	2.046595
Q9H0C8	-0.67575	2.043509
P18031	-0.45003	2.041988
Q12962	0.284451	2.040759
O00299	-0.3592	2.039512
Q09666	0.77828	2.038002
O75616	0.303155	2.035775
Q1KMD3	-0.3604	2.034846

P08729	-0.24417	2.029722
O95999	1.1386	2.027474
Q9Y6H1	0.226924	2.025408
O00410	-0.38957	2.023301
Q5U5X0	0.391595	2.022858
P51608	0.468315	2.015367
P67936	0.399367	2.014825
Q9NY12	0.403318	2.014148
P33176	-0.35681	2.013339
Q15007	0.342371	2.01258
Q92547	0.238044	2.011918
P07910	-0.18989	2.01183
Q9GZT3	-0.27749	2.010391
P17655	-0.32005	2.009804
P08621	0.302453	2.008284
P37802	-0.28537	2.00745
Q9BVP2	-0.32501	2.002367
Q9Y4W2	-2.75348	2.001799
P43026	0.294511	1.992417
Q9Y2V2	-0.47436	1.991217
Q8N5A5	0.374013	1.988109
P26885	-0.4474	1.98797
P00558	-0.21472	1.985322
O00762	-0.23818	1.981941
P46940	-0.53379	1.979797
P11279	0.210318	1.978181
Q96ST2	0.226619	1.977224
Q96B49	-0.61269	1.976366
P51148	-0.34942	1.970697
Q9UBE0	-0.63777	1.967313
O15269	-0.49064	1.966913

Q9H9P8	-1.40676	1.965893
Q9Y5J1	-1.2575	1.965547
Q969L2	0.267945	1.963665
Q96FJ2	-0.82977	1.959597
Q9BVK6	0.296412	1.959551
O43681	-0.48601	1.956561
P08579	0.38749	1.955297
O60664	-0.50319	1.951716
P78536	0.812333	1.950533
P50895	-0.3601	1.950195
P84085	-0.24661	1.949955
Q8WXI9	0.806002	1.948508
P35221	0.269099	1.94659
Q96R06	0.892822	1.946421
Q9NRP2	0.267886	1.945311
P55036	0.210129	1.941437
P09960	-0.4152	1.938284
Q08378	-0.53297	1.936886
Q9H488	0.221498	1.934432
O14686	0.221498	1.934432
P31937	0.321156	1.933663
Q9UHR5	0.333568	1.929902
Q9UHX1	-0.38961	1.929452
Q9P258	-0.32883	1.926184
P02656	0.672024	1.923091
O00170	-0.75445	1.922672
O15240	0.734996	1.920724
Q8IWX8	1.067386	1.918451
Q14980	-0.39803	1.917867
Q9NZM5	0.296744	1.910794
Q9BXJ9	-1.05192	1.910747

Q16186	-0.49239	1.908794
P07108	-0.17523	1.9071
P00167	-0.58518	1.904606
Q9H4A6	0.404958	1.903213
Q00403	0.595207	1.901327
O94842	0.415882	1.901143
Q8WYQ3	-0.446	1.897241
Q15545	0.935689	1.895657
Q16630	-0.53873	1.895642
Q8WYP5	-0.28823	1.895307
Q9H307	0.320809	1.895085
P46109	-0.30576	1.891738
Q14847	-0.21922	1.888591
P20618	-0.40751	1.888377
P29992	-0.81063	1.886369
O75976	0.291495	1.886098
Q9NSE4	-0.33804	1.884515
P35998	-0.29888	1.878723
P0DPB6	-0.18829	1.876367
Q08170	0.173973	1.871756
P67870	0.242974	1.870344
P11233	0.249845	1.868067
Q9NTJ5	0.723011	1.865354
O43765	-0.16323	1.863471
P32119	-0.24708	1.863169
Q9H0L4	0.317829	1.856921
P13674	0.323265	1.856692
Q16204	-0.25028	1.856
Q15642	-0.33767	1.855805
Q92542	0.493916	1.852576
P82932	0.411604	1.852128

P42166	0.19568	1.850815
P62854	-0.57559	1.845345
O43513	0.772422	1.8421
P61970	-1.28139	1.841749
Q9GZR2	0.515018	1.838281
Q14697	-0.52855	1.834146
Q12874	0.213011	1.827651
P23743	-1.00088	1.818737
P63010	-0.41878	1.815889
Q02543	-0.62098	1.814513
Q9NZ01	-0.36454	1.813287
O95218	0.159332	1.810524
O75369	-0.38884	1.810355
Q9NZJ7	1.841869	1.809452
Q15843	0.583554	1.808758
Q9NQG1	1.315528	1.808667
Q9H936	-0.20865	1.807751
P60174	-0.29787	1.805995
P63104	-0.3804	1.805545
Q9Y3I0	-0.33166	1.804368
P21108	-0.24233	1.803181
Q12906	-0.25129	1.801968
P53007	-0.45313	1.798269
Q15125	-0.33636	1.798105
Q96PC5	0.374958	1.791246
P35222	-0.31104	1.788912
Q14315	-0.29508	1.785705
Q96BR5	-0.89539	1.781739
P20290	-0.94727	1.780003
Q7L2H7	-1.503	1.779655
Q9BW91	0.646396	1.779528

Q8WUM0	-0.33286	1.774601
P07951	0.395279	1.769209
Q15349	-1.97577	1.767387
P61244	0.41551	1.766514
P0DP25	1.096063	1.765219
P0DP24	1.096063	1.765219
P0DP23	1.096063	1.765219
P49321	-1.60979	1.761431
P63220	-0.2017	1.758523
Q9NPJ6	0.478074	1.757025
O76094	-0.61486	1.75326
P22314	-0.31638	1.753072
P63096	-0.21622	1.750667
A0A142I5B9	-0.2211	1.750281
Q9NTZ6	-0.74037	1.75022
P62263	-0.20877	1.745002
Q16594	0.477762	1.741903
P14923	-0.33181	1.74189
Q14684	0.26213	1.740223
Q13885	0.312118	1.737909
P24534	0.223255	1.737719
P51809	-1.28448	1.737142
P50502	-0.18196	1.73317
Q9BV40	0.284858	1.732106
P43304	-0.24083	1.73107
Q04917	0.200877	1.728264
Q9Y3T9	-0.29601	1.726755
Q9H1I8	1.400362	1.720312
Q9NX55	-0.48944	1.718187
P46379	-1.00012	1.714152
P36543	-0.5442	1.713212

P61923	-0.47515	1.711494
Q7RTS3	0.198025	1.71145
Q9UMS0	-0.21159	1.710526
P06454	0.222606	1.707321
Q96HR3	0.582651	1.705535
P25787	-0.55113	1.703288
P62140	-0.29812	1.702459
P48444	-0.24183	1.701416
O14880	-2.53821	1.701006
P61158	-0.279	1.699733
P68400	-1.05823	1.699502
P06280	0.702527	1.693054
P13010	-0.75878	1.693036
P05023	0.234029	1.690118
Q9Y3C1	0.152778	1.688882
Q13111	0.406939	1.688815
Q14573	-0.50239	1.687687
P52434	-0.65984	1.687066
Q8NE71	-0.48326	1.685575
Q92734	-0.59258	1.684257
P54725	-0.18965	1.682437
Q12846	1.064781	1.681973
Q9Y5U9	-0.25864	1.67881
P41252	-0.86677	1.678762
P36551	-0.37085	1.678396
Q8TB36	0.287096	1.674177
P20339	-0.29729	1.668394
Q15819	-0.14881	1.667975
Q6P2E9	-0.52153	1.667766
P36954	0.223639	1.664236
P17844	-0.25698	1.661285

Q04721	0.608762	1.660175
O43837	-0.56679	1.658923
Q86UK5	1.662162	1.658212
P06733	-0.37757	1.657326
O00625	0.986964	1.657187
P82933	-0.45835	1.657068
Q7Z5L9	-0.36734	1.656968
O43660	-0.37685	1.656913
P15531	-0.19832	1.655714
O15371	-0.71311	1.64998
Q8NBT2	-0.24387	1.647069
P42892	0.223109	1.646602
Q06481	0.519836	1.64596
P23246	-0.32332	1.644827
P50151	-0.19079	1.640801
Q9NVA2	-0.44613	1.63871
Q14141	-0.44613	1.63871
Q9BRA2	-0.18315	1.637631
Q96AQ6	0.353878	1.634145
Q15836	0.192051	1.631577
P50416	-0.24312	1.629995
P25789	-0.34482	1.625688
P82094	0.921825	1.625271
P26583	-0.30444	1.624893
Q86VP6	-1.132	1.624878
O75688	1.619246	1.624755
P47756	-0.30042	1.623848
P45974	-0.65168	1.622587
P38432	0.300951	1.622219
P61020	-0.31656	1.619858
Q03001	-1.27735	1.619748

Q15050	0.286825	1.618829
P28331	-0.32599	1.618441
Q9BTE3	-1.02029	1.616686
Q8WTS6	-0.23263	1.614712
O15446	0.184152	1.613971
P36405	-0.23273	1.612962
O43464	0.189853	1.610777
Q7RTP6	0.189853	1.610777
Q8IUF8	-1.34715	1.610151
Q00796	-0.32982	1.609313
Q92736	-0.22293	1.609176
Q96J92	-2.13871	1.605333
O00754	0.29131	1.602942
Q9NTK5	-0.34742	1.60013
Q9Y266	-0.16253	1.5986
Q86Y82	0.232351	1.597177
Q12788	-0.39867	1.596402
P49720	-0.59926	1.596301
Q9C0C9	-1.39279	1.59406
Q02809	-0.54888	1.591903
P51991	0.389184	1.586338
Q9NV06	-0.76251	1.58546
Q86XK2	0.40876	1.584233
P61160	-0.36963	1.584073
Q8NEY8	0.166971	1.583845
P08962	0.200759	1.583286
P00846	-0.27382	1.5823
Q7L014	-0.33438	1.58035
Q9H1A7	0.531537	1.578656
P52435	0.531537	1.578656
Q32MZ4	0.613115	1.57762

P30622	0.286944	1.577484
Q9Y6Y8	-0.94644	1.57682
Q9NXE8	0.356325	1.576749
Q96FF9	0.176416	1.573123
P25685	0.219684	1.56977
P98179	0.153819	1.567829
P52907	-0.31381	1.567152
Q9NRG9	-0.48916	1.564857
P31150	-0.32846	1.564639
Q96HC4	-0.29323	1.564026
Q86Y79	0.422108	1.563245
Q9NP72	-0.28042	1.562854
Q9NVH1	-0.66711	1.562843
P19367	-1.60609	1.562831
P10599	0.955364	1.560592
O43752	0.405705	1.560471
Q14839	-0.26965	1.558981
P35606	-0.2399	1.556807
Q9Y2Z0	-0.33271	1.556275
Q99996	2.579352	1.555637
P35232	0.726664	1.555385
O75083	-0.40493	1.554926
O75494	0.301887	1.55459
O75937	0.278542	1.550548
P30040	-0.22225	1.549164
Q9Y6M1	-0.32727	1.54831
P13747	0.254036	1.547935
Q96HP0	0.569193	1.545684
P78371	-0.38863	1.54393
Q9Y608	0.690886	1.543594
P54707	0.205429	1.542654

Q96RD7	0.915383	1.536196
P33993	-0.48988	1.53572
P63261	-0.49971	1.53469
P60709	-0.49971	1.53469
Q92844	0.547968	1.533265
Q16637	-0.42678	1.532953
Q8IWE2	-1.20926	1.53258
Q9NYB0	0.250554	1.531973
P82650	-0.33221	1.527554
P14866	-0.24365	1.52411
Q9BRP8	0.603807	1.523543
O14672	-0.22848	1.5103
Q99470	1.011569	1.507414
Q9BXK5	0.305667	1.506259
P46937	-0.71068	1.499935
Q9NRX2	0.164802	1.49758
O43242	-1.66634	1.49517
Q7Z4V5	0.15476	1.493778
P62760	-0.38631	1.493257
P14854	0.139696	1.493163
P29401	-0.41042	1.491512
P48723	1.357692	1.491411
Q12792	-1.25221	1.491142
Q96A26	0.142894	1.48781
Q99598	0.757224	1.487047
Q5T1R4	0.150579	1.485028
Q15691	-0.35039	1.48306
O95295	0.300589	1.480918
Q86SX6	-0.14921	1.479728
Q8N5F7	0.234822	1.478942
Q9NUP9	-0.35571	1.477692

Q00613	-0.30131	1.476944
O60506	-0.30027	1.476172
O14979	0.514491	1.474876
P13984	0.313046	1.474661
Q7Z7K6	-0.36715	1.474277
Q8NHZ8	0.476511	1.473607
P35052	1.38934	1.472625
O75152	0.196696	1.472287
O95721	0.242661	1.470569
P19338	0.205147	1.470001
Q969Z0	-0.6611	1.469221
O00231	-0.53918	1.468687
Q9P015	-0.5382	1.468124
Q96BZ8	-1.4549	1.464699
Q9P0J7	0.734184	1.464256
P23368	-0.29644	1.462754
Q9C005	0.336805	1.462102
Q9HD15	-0.27992	1.460569
P30153	0.168275	1.457026
P00387	-0.13244	1.455414
Q96IU4	-1.013	1.45536
O60232	-0.62908	1.455016
Q14651	0.177989	1.452979
O15260	-0.38776	1.452706
Q9BRT3	-0.21571	1.452687
P08238	-0.72347	1.451065
O15382	-0.55783	1.447527
P21912	0.146399	1.444152
Q15906	0.290409	1.43574
P02549	1.315608	1.435512
P23434	-0.21191	1.432796

Q99733	-0.3124	1.432506
Q9UDW1	-0.2957	1.432125
P11717	0.233255	1.42967
Q9Y2X3	-0.23348	1.428864
P43243	-0.27798	1.428165
O15144	-0.44437	1.426803
P12830	0.230744	1.424587
P56211	-0.39841	1.422971
Q9P0U1	0.141361	1.422861
Q99729	0.216168	1.42058
Q9NXR1	0.458478	1.417658
Q9P2J5	-0.59434	1.415969
O00571	-0.27693	1.415488
Q12849	0.726135	1.414651
O14950	0.153979	1.412757
O00483	0.297002	1.410904
P52272	-0.4124	1.405074
Q8IXM3	0.326778	1.401738
P53367	-0.76557	1.400471
Q9BW71	-0.32938	1.400071
Q9H6S3	0.139915	1.39971
Q02487	0.693378	1.399489
O95302	-0.20684	1.397082
Q8NFU3	-0.28594	1.395515
Q15428	-1.15147	1.394183
Q9P2D6	-1.62541	1.394101
Q8IVM0	1.240897	1.3925
Q8NFC6	0.963009	1.392377
P36957	-0.13107	1.392287
P67812	0.208378	1.391942
P48436	-0.22566	1.390743

P78417	0.129774	1.388981
P28676	1.16545	1.38852
O95865	-0.46082	1.386751
O75390	-0.31935	1.383622
P18085	-0.14757	1.381965
P05198	-0.16391	1.380861
O43181	0.163493	1.380337
Q8IYG6	4.305077	1.37983
O60828	0.142491	1.379716
P30043	0.313802	1.379006
Q9BRJ6	0.260056	1.378966
Q7L2E3	-0.36932	1.3773
P02533	-0.16082	1.376235
Q9UN86	0.12924	1.374713
P04844	0.428573	1.373502
Q9NQP4	-0.21033	1.371622
Q96C19	-0.17902	1.370637
P30044	-0.16387	1.368191
P63208	0.13076	1.367733
Q99536	-0.16796	1.367204
Q71U36	-0.58755	1.365937
Q13404	-0.14447	1.364916
P03886	0.759659	1.364287
Q13427	0.223054	1.364152
P55265	-0.57412	1.363842
Q9NVP1	-0.32019	1.362965
Q9ULX9	0.870506	1.362617
P36776	-0.44531	1.362323
P41223	-1.19007	1.361515
P15927	-1.01101	1.361326
Q16576	0.138181	1.360144

Q9NP92	0.616931	1.359939
Q9H0U3	0.389139	1.359031
O14744	-0.24595	1.357269
Q16595	0.142215	1.357014
Q6IAA8	0.172621	1.35635
Q7L576	1.455033	1.356345
O14579	0.613192	1.355903
Q96T58	2.759191	1.354907
P54136	-0.63435	1.354787
Q9H3K2	0.32893	1.354558
Q99623	-0.22319	1.352038
Q08380	0.132119	1.351437
P07305	0.158896	1.348978
Q9NP77	0.197549	1.346947
Q96DI7	-0.35309	1.346922
P34897	-0.35024	1.346886
Q3KQU3	0.567613	1.346819
A0JLT2	0.533066	1.343421
P53621	-0.42347	1.342222
P49406	-0.233	1.341705
Q9Y512	-0.29929	1.337632
Q8TCT9	0.267605	1.336313
P54577	0.148901	1.335061
P06737	-0.68315	1.330649
Q86SQ4	0.954242	1.330303
O00273	-0.15574	1.328921
Q5RKV6	0.254516	1.32742
Q9Y2S7	-0.62283	1.326236
O60610	-0.57624	1.325719
P30533	-0.29382	1.325681
Q99643	-1.65271	1.324728

P26599	-0.42819	1.323299
P80303	0.445592	1.321823
Q14247	0.168465	1.318994
Q9NVS9	-0.41382	1.318058
O43615	-0.21867	1.317188
Q13535	13.0442	1.316599
P39023	-0.58752	1.316115
P0DMV9	0.519321	1.315955
P0DMV8	0.519321	1.315955
Q13573	0.167598	1.315356
Q8TED1	0.451541	1.313547
P55327	-0.18067	1.310097
Q9H8Y8	0.293424	1.309609
P52789	-1.70185	1.304528
O94776	-1.5655	1.304012
Q13330	-1.5655	1.304012
Q9BTC8	-1.5655	1.304012
O95342	0.847789	1.303521
O43819	-0.76983	1.299743
Q13085	-0.90032	1.29884
O95782	-0.45761	1.297582
P28074	-0.1734	1.297207
Q9NPL8	-2.02686	1.29676
P05114	0.262624	1.296546
Q53EU6	0.83614	1.296026
P67809	-0.21355	1.296019
Q5W111	0.895022	1.294148
Q9Y4Y9	-0.52146	1.29108
P00441	-0.37258	1.28549
P82664	-0.63438	1.285033
Q9UKX7	0.187287	1.283741

P15374	-0.22751	1.283466
Q9Y3F4	-0.31497	1.281307
Q92769	-0.29896	1.28076
Q9Y3B7	0.307913	1.278397
Q10713	-0.27629	1.278033
Q9BPW8	-0.49903	1.276384
Q8NBN7	-0.37251	1.27627
P21926	0.220601	1.273396
O75330	0.404937	1.269802
O95757	-0.38586	1.268747
Q96B54	0.267135	1.266265
O95239	-0.54157	1.26615
P28066	0.149797	1.265931
Q12824	-0.44484	1.264552
P10644	0.19781	1.263983
Q5M775	-0.31144	1.26274
Q13114	0.761887	1.26214
Q8N1F7	-0.28698	1.261941
P17980	0.290081	1.261254
Q9P032	0.217807	1.260148
O15054	0.611126	1.258701
P09234	-0.16518	1.257899
P54819	0.43387	1.257598
P63000	-0.1689	1.257068
Q9UBI6	0.251341	1.254996
Q00610	-0.3569	1.254618
O95248	-0.97935	1.253532
P30626	0.199171	1.253505
Q9UQ35	0.259647	1.253374
P25398	-0.2115	1.253262
P98172	0.415498	1.252483

P61086	-0.41558	1.250863
O95433	-0.49084	1.250645
P78316	-0.37964	1.249051
Q96S66	1.651121	1.248825
P98171	-3.77178	1.247915
Q9UPN4	0.25276	1.244514
Q8TCU4	-0.1604	1.24373
Q6NYC8	0.1721	1.243161
O75436	-0.6632	1.243113
O14925	0.797219	1.24306
Q96RT1	0.136285	1.242837
O43617	0.510719	1.239741
Q8IV48	-0.83856	1.238966
Q14566	-0.48541	1.237218
O14519	-0.83458	1.2366
P53999	-0.15621	1.234701
Q96KP4	-0.42288	1.233775
P42704	-0.33625	1.233099
Q9GZS3	1.321595	1.230593
Q9P2E9	-0.19385	1.230418
O95197	-0.16767	1.22863
Q13907	-0.23468	1.228018
Q9Y5U2	0.626595	1.226811
O43768	-0.1854	1.224752
Q9BTT0	-0.21659	1.224489
Q14186	0.656224	1.221814
Q2NL82	0.461817	1.221667
Q9H2H8	-1.19638	1.220014
P05556	0.538521	1.218673
P37198	0.162548	1.218369
O43809	-0.22875	1.218078

Q13177	-0.14917	1.216501
Q9Y2A7	0.436511	1.215938
Q9GZZ1	-0.84636	1.215291
Q8N183	0.198426	1.210066
O14561	-0.14362	1.209416
O95801	0.2978	1.208889
P49588	-0.23119	1.203741
O15392	-0.25101	1.20303
P25705	-0.23789	1.201854
Q99460	-0.26762	1.199779
Q92945	-0.15841	1.191879
Q9NSI2	-0.24925	1.191675
P61457	0.481359	1.190704
Q96E29	1.098613	1.188023
P34931	0.502528	1.18769
P62891	-0.28146	1.187567
O94919	-0.17291	1.1868
Q9UMY4	0.150849	1.186471
Q13277	0.754369	1.186182
O00567	-0.20753	1.181397
Q96PK6	-0.1542	1.180768
P48634	0.249644	1.180604
Q9Y676	-0.28352	1.180444
O75347	-0.20208	1.176929
P23528	-0.11437	1.175423
P09211	0.177257	1.173554
P52758	0.13426	1.172395
Q9Y3A4	1.201557	1.171428
Q9P2B2	0.163207	1.169337
Q16795	-0.36903	1.165974
P31930	-0.2459	1.164486

Q9NQC3	-0.29322	1.16364
Q86U86	1.482795	1.161779
O60568	-1.0411	1.15999
Q02952	0.453214	1.159273
O00116	-0.35046	1.158655
P53985	-0.37579	1.158638
Q06323	-0.15784	1.157934
Q96EY8	0.174175	1.157141
P10619	0.256118	1.156729
P29590	0.176792	1.155554
P33947	1.806748	1.154427
P30154	0.130053	1.151076
P11177	-0.20789	1.150211
P07919	0.278361	1.149061
O00159	-0.32158	1.146076
Q53HL2	0.334302	1.145844
Q08211	-0.26176	1.145301
Q9Y5V0	0.166195	1.14359
P33681	-1.67433	1.143028
P52948	0.21447	1.141829
Q5VYS8	0.694425	1.137584
P46199	0.694425	1.137584
P09622	-0.34964	1.137415
Q9NYM9	0.170809	1.135627
Q6IBS0	-0.70284	1.135379
Q9NVI7	-0.22018	1.132883
Q32P51	-0.32293	1.131901
P21796	-0.44246	1.128912
P51572	0.115874	1.127053
Q9H6F5	0.116764	1.125711
Q8TEM1	-0.21177	1.124741

O15511	-0.12314	1.123201
O60499	-0.13253	1.121032
P61221	-0.5345	1.118906
P62837	-0.14581	1.117182
P61077	-0.14581	1.117182
Q14493	0.752934	1.116538
Q9UNX4	-1.23775	1.114025
P53384	-0.36959	1.114018
Q01780	-1.00901	1.113254
P62745	0.211016	1.113224
Q9H0S4	-0.23105	1.112519
P61225	0.269292	1.109764
O00629	-0.15585	1.10672
Q01105	-0.23783	1.105515
P48509	0.125784	1.103079
P55957	-0.40937	1.102741
Q9UNZ2	-0.20396	1.101802
P26368	-0.16879	1.101332
Q8N9N8	0.128213	1.100871
Q07812	0.273083	1.10053
P09493	0.136446	1.09736
Q14126	0.608918	1.096993
Q96HQ2	-0.5758	1.095853
P11441	-0.25129	1.09573
Q02978	-0.34173	1.095048
P62491	0.139641	1.095045
Q86SF2	0.847586	1.092052
Q9NPD8	-0.33499	1.091927
Q01664	-0.32912	1.090837
P28482	-1.2835	1.090019
Q8N0V3	0.226825	1.089559

P07099	0.389537	1.089504
Q9UMS4	-0.29835	1.087803
Q15637	0.181789	1.086391
Q9BYT8	1.334381	1.08554
Q96BP2	0.238274	1.085397
Q06830	-0.11523	1.084481
P50552	-0.25952	1.084316
Q9P2B4	1.131899	1.082719
P19105	0.127337	1.081622
O60313	0.504706	1.081622
P53618	-0.27123	1.081046
O43290	0.206823	1.080703
Q16540	-0.3887	1.078623
Q13503	0.457305	1.077632
Q13951	-0.75754	1.075823
Q9BV86	-0.35182	1.075262
Q16181	-0.41253	1.0722
P52655	0.666691	1.071438
O14646	-0.52972	1.070339
O60488	-0.41924	1.070133
P13797	0.12885	1.069549
P99999	0.139299	1.067129
O00244	-0.46014	1.066736
Q08J23	-0.62499	1.065624
Q99459	0.199014	1.060714
P39019	0.100196	1.059173
Q9H0U6	-0.30803	1.058771
Q99627	-0.37054	1.05803
Q9H2H9	1.099929	1.057969
A0FGR8	-0.5287	1.056975
Q9NXH9	0.913279	1.056616

P46100	-0.54191	1.055579
Q12888	0.168147	1.050458
Q9NYU2	-0.51837	1.048266
Q9UER7	0.438222	1.046612
P05387	-0.102	1.046009
Q15287	0.178341	1.044259
Q9UNF0	-0.18117	1.044187
Q8N5N7	0.143762	1.043608
P14678	-0.17716	1.041542
P63162	-0.17716	1.041542
Q13283	-0.16394	1.040316
Q9GZU8	-0.2246	1.039711
P17858	-1.01723	1.038847
O43677	-6.13477	1.038743
P17028	0.308785	1.038529
Q86U28	-0.46055	1.037274
P54709	0.114072	1.035521
Q9Y3B4	-0.46033	1.033481
Q8N6N3	-0.4445	1.027344
Q9Y3E0	0.718762	1.026564
Q96HE7	-0.38545	1.026042
P07686	0.173466	1.02544
O76021	-0.54176	1.02293
P62333	0.115777	1.021452
Q75N03	0.866378	1.01873
P05091	0.346079	1.016821
Q96NT0	1.854255	1.012909
Q96HR8	0.454529	1.011747
Q14008	-0.27516	1.010118
Q9Y6D0	1.034174	1.00902
Q9H845	-0.39598	1.008772

Q9BUN8	-0.38855	1.008564
P11216	-0.57536	1.008239
P47895	-0.25228	1.008218
P15407	0.315394	1.007212
Q8IUD2	-1.01249	1.006912
P11142	-0.28267	1.00681
Q6PIU2	-0.18619	1.00612
Q16625	0.334865	1.005315
P25490	0.352217	1.004764
Q8WTT2	-0.99931	1.003036
Q9H7E9	-0.21129	1.001951
Q9Y3D5	0.317716	1.00108
Q9NP81	-0.38207	0.999983
P21589	0.152296	0.999873
P52952	-0.14529	0.999138
P39656	0.157764	0.998103
O00584	0.241743	0.998092
Q14344	-0.12954	0.998073
Q9BRJ2	0.571307	0.99329
P62253	-0.42058	0.993207
P12814	-0.36484	0.993127
Q9HD33	-0.33249	0.991932
P15954	0.292986	0.991539
Q9Y624	0.146278	0.990941
P50542	0.385991	0.99032
P43897	-0.32274	0.990029
O75607	-0.24705	0.988883
Q96JM3	-0.4843	0.988554
P46087	-0.12258	0.988271
P57105	0.193358	0.987999
P56181	-0.29859	0.987729

P46531	0.257072	0.987374
P06753	0.132793	0.982371
Q9H3Z4	0.147963	0.981729
O75643	-0.29693	0.981465
Q12904	-0.22115	0.98022
P35754	0.137883	0.979993
O94992	0.297218	0.979466
P10155	0.571069	0.978059
Q92979	-0.13986	0.975653
Q9UBU9	-0.35866	0.975038
Q6QNY1	0.330394	0.974043
P37108	0.137337	0.972615
P43246	-1.12552	0.972493
Q13895	-0.3401	0.972389
Q9H4M9	-0.2807	0.971337
Q9NZN3	-0.2807	0.971337
O95793	0.125534	0.971281
Q01970	-0.18656	0.97111
Q15436	-1.27614	0.970303
Q9Y673	0.411864	0.969539
Q4LE39	-1.82975	0.96908
Q14728	0.598883	0.968991
Q9Y5Y6	-0.24169	0.964803
Q96EL2	-2.09111	0.964009
Q9NRF9	0.119509	0.962944
P51153	0.114002	0.962627
P09525	0.25774	0.961693
P62195	0.630838	0.958571
P82909	0.142678	0.958155
P29317	0.161724	0.957427
Q8WVC0	0.351205	0.956447

Q9BXP5	0.215942	0.956149
Q8N1G4	-0.24127	0.953699
Q9H5K3	1.015114	0.953621
Q13526	-0.1107	0.953519
Q9BZE4	-0.33679	0.952906
Q9BY77	0.187414	0.951584
Q9UBR2	0.137618	0.951259
P06730	-0.17514	0.950961
P78318	-1.03987	0.950705
P30520	-0.35228	0.950524
Q9Y281	-0.11565	0.949298
Q9Y241	0.234679	0.947588
Q9BTM9	-0.70731	0.947269
Q8N357	1.34006	0.946193
P35270	0.143203	0.945437
Q9H9J2	-0.16046	0.944266
Q8N6H7	-1.15064	0.942919
Q92575	0.23697	0.941002
P28288	-0.64352	0.940766
Q8IZA0	1.836188	0.940604
O00541	-0.20996	0.940325
P61758	-0.09672	0.938532
Q96B26	0.806187	0.938111
Q15019	-0.63134	0.936664
Q9NVJ2	-0.21013	0.935994
P40222	0.246096	0.933316
P60953	-0.14173	0.931694
P25445	1.325223	0.931128
Q99569	6.45076	0.930758
P13726	-0.68981	0.929786
Q9NUJ1	-0.31315	0.927637

Q9Y2H0	0.27122	0.925914
P62750	-0.10737	0.923992
O60613	-0.6615	0.923664
O15160	0.21104	0.923501
P47985	0.11207	0.922843
O43684	-0.23591	0.92119
O95140	1.446373	0.919488
Q969S3	0.821291	0.918884
Q9Y605	-0.14155	0.917088
Q13123	0.242395	0.914632
P26640	-0.45179	0.913961
P17301	0.261552	0.911696
Q9ULC5	-0.36726	0.908285
Q6UXH1	-0.32498	0.907985
Q9NQG7	0.253302	0.907498
Q9P021	-0.16544	0.90347
P18887	0.229434	0.903332
P05787	0.573942	0.902649
Q9BX68	0.530403	0.9018
Q13443	-0.70105	0.901753
P11137	-1.00268	0.901001
Q9UHY7	-0.34394	0.900564
P55209	-0.15999	0.900508
P35610	0.775843	0.900229
P49257	0.177416	0.897781
P11310	-0.22762	0.896887
Q9NPA8	-0.19341	0.896439
O15143	-2.24319	0.89546
Q9NR31	-0.20172	0.890089
Q8WWV3	0.39975	0.88903
P55145	0.082661	0.888012

Q9NZ43	0.355826	0.886345
Q8IYS2	-0.50939	0.886254
Q712K3	-0.26552	0.886013
O43766	0.337482	0.884067
Q07021	-1.06261	0.883026
Q6WCQ1	0.230944	0.881914
Q9UMX0	0.385972	0.88162
Q14444	-0.36798	0.87948
P62879	-0.13924	0.879393
Q13596	0.177602	0.879305
O95573	-0.36686	0.879106
O43715	-1.38652	0.876274
O95336	0.951711	0.876189
Q9H0U4	-0.08906	0.874519
P33552	-0.89247	0.87413
Q9UHA4	1.490457	0.872049
Q9UPU7	-0.55829	0.871137
Q5QP82	0.115892	0.871029
P51149	-0.11154	0.869794
Q6WBX8	-0.15774	0.865739
P09382	0.265528	0.864431
Q12905	-0.38342	0.864243
Q16698	-0.25047	0.862191
Q53F19	0.22389	0.861913
Q03113	-0.12826	0.860251
P23634	0.280288	0.859678
P68431	-0.1163	0.859193
Q5QJE6	0.112579	0.857574
P62995	-0.20651	0.854731
Q01831	-0.52314	0.853997
Q9NPD3	-0.55703	0.853026

Q9NT62	-0.4465	0.853015
Q99961	-0.18878	0.852835
Q96RN5	0.156798	0.850433
Q15185	-0.11043	0.849447
P02765	1.404406	0.848775
P08047	0.235979	0.847496
P22061	0.145607	0.846732
Q8N684	0.920491	0.844221
Q9UBV8	0.327706	0.843654
Q8NBJ4	0.123958	0.843291
Q92688	-0.09903	0.842978
Q13948	0.294273	0.841681
P08134	-0.29675	0.840159
P14618	-0.40418	0.838502
O75348	-0.12182	0.83051
Q8TCJ2	0.127757	0.829755
Q9Y3E2	-1.2692	0.829302
P62851	0.19259	0.828686
Q7Z4W1	-0.22523	0.827533
Q12873	-0.20664	0.827256
Q96DA6	1.415067	0.825592
Q9Y2L1	-1.29438	0.823384
O95453	1.874941	0.822951
P63165	0.108047	0.822827
Q8WZA0	0.201994	0.821557
Q15006	0.662101	0.820897
Q9NUQ3	0.313205	0.818616
P41250	-0.2415	0.818197
P29966	-0.10257	0.817321
Q9NWB1	-1.49079	0.816878
Q9NPH2	-0.23931	0.816823

P62136	-0.21721	0.816766
P05386	-0.40472	0.815702
Q9BY43	-0.2819	0.814789
P28072	-0.14184	0.814106
Q8IWI9	-0.85059	0.813002
Q05707	-0.85059	0.813002
Q13547	-0.2573	0.812037
Q9NXE4	-0.39666	0.811163
Q92616	-0.25783	0.811053
Q9Y6A5	0.146625	0.809755
P30048	0.112967	0.809643
Q99798	-0.28178	0.809568
Q96EY1	0.118896	0.808918
P56381	0.12829	0.806029
O75822	0.12053	0.804774
P27348	-0.1018	0.80464
Q9BWU0	1.233627	0.803782
Q86W92	-0.17099	0.803686
Q15154	0.353029	0.802415
Q9UMR2	-0.84546	0.802238
Q9NQS1	0.279398	0.799867
P04004	1.058101	0.798011
Q9UHV9	-0.09541	0.795964
Q9Y2Q9	-0.14321	0.795843
Q9UH99	0.37287	0.794854
Q13724	-0.23861	0.790967
O95168	0.107645	0.790838
Q8WWY3	-1.31265	0.790545
Q96JJ7	0.133232	0.790484
O95229	0.159455	0.790359
Q969T9	-0.84922	0.789412

P04843	0.143745	0.788818
Q7Z7H8	-1.75419	0.784772
Q99829	-1.63535	0.784636
Q92665	0.343368	0.78331
Q16656	0.225033	0.781368
Q96G21	-0.40355	0.781145
O75380	0.122852	0.781084
Q8WXA9	0.204483	0.780761
O15514	0.161199	0.780425
Q9Y3D9	0.106435	0.777062
O60812	-0.09374	0.776732
B2RXH8	-0.09374	0.776732
P49792	-0.2735	0.775388
O75694	-0.1587	0.774014
Q15398	-0.21402	0.772216
P62330	0.80912	0.772213
Q00341	-0.24832	0.772158
P61964	-0.4425	0.771814
O95831	-0.23702	0.771178
P20674	0.077118	0.769397
P31040	-0.47723	0.769259
Q9Y6I9	-1.30574	0.769124
Q96MF7	0.651218	0.768918
O43172	-0.33005	0.76418
P78330	0.159415	0.760332
Q8TAD8	1.359241	0.759713
P56134	-0.21228	0.757172
P07900	-0.23274	0.756393
O96005	0.283695	0.754977
Q9BTD8	0.190431	0.754799
O75368	0.211567	0.752627

Q15121	-0.37007	0.749129
P08243	-0.26849	0.74452
P62312	0.145396	0.74389
Q9UHB9	-0.13705	0.740678
Q5T9A4	-0.14869	0.740396
Q9BRK5	0.090016	0.739586
O76071	0.951452	0.739136
Q6DKK2	1.005	0.738553
Q12931	-0.3175	0.73842
Q9ULF5	0.268363	0.738277
Q13601	0.216807	0.736923
O75475	0.148156	0.736901
P48556	-0.63323	0.736593
Q13151	0.263501	0.735935
P11388	-0.29066	0.733305
P23919	-0.12003	0.731753
Q13445	0.149459	0.72878
Q9Y2Y0	-1.28025	0.727941
Q7Z4H3	-0.21911	0.727194
Q15427	0.172941	0.726774
Q96AJ9	-0.30331	0.726459
P14859	0.513876	0.725425
P42229	-0.09357	0.725273
P51692	-0.09357	0.725273
P83916	0.098937	0.723529
Q9Y3E5	-0.14563	0.722327
Q15393	-0.09533	0.719761
Q9Y6Q5	-0.49981	0.717919
P62820	-0.07248	0.717443
Q9H3P2	-0.16364	0.717413
Q13901	0.780561	0.716652

Q14103	0.070318	0.716547
P00533	0.221179	0.715654
Q96A73	-0.80438	0.713186
O15182	0.094444	0.712857
Q92917	-0.16311	0.711038
Q9Y251	0.406987	0.710851
Q9H8H0	-0.66468	0.710604
Q15853	0.271647	0.710391
P49454	0.232336	0.710245
Q14739	-0.1667	0.70975
Q9NWB6	0.169064	0.709602
Q16822	0.227479	0.709251
Q9H1C7	-0.27775	0.709154
P56589	0.848531	0.709141
P62873	0.250519	0.708616
Q86XP3	-0.23438	0.708566
Q9UK53	1.886187	0.706445
Q9UHG3	-0.34926	0.705803
Q9H1K1	-0.276	0.704096
O43493	-0.17395	0.70358
Q96EL3	0.092662	0.703002
P61218	1.66575	0.702777
P31948	0.158957	0.702608
P61916	-0.12741	0.701028
Q96S97	0.141114	0.700826
P16422	0.162324	0.700007
Q96L50	-0.68425	0.699296
Q9UQ88	-0.23325	0.698652
Q92621	-0.29479	0.698026
O75431	0.261122	0.697136
O15427	-0.10403	0.697133

Q9BWT6	0.687147	0.696616
Q9Y6I3	-0.13787	0.696442
P04818	-0.34168	0.694529
P07437	0.7248	0.693134
Q9BUF5	0.7248	0.693134
Q9BVA1	0.7248	0.693134
P04350	0.7248	0.693134
P68371	0.7248	0.693134
Q96AY3	0.129363	0.691948
Q14764	-0.28189	0.690197
Q15907	0.079782	0.690174
Q9BRT9	-0.18662	0.689606
Q14683	-0.59626	0.689471
P11182	-0.23645	0.688635
Q96IZ0	0.265905	0.687517
P20700	0.164101	0.687119
Q13263	-0.079	0.68305
O15118	0.624977	0.68294
Q96P70	0.979501	0.68248
P22223	0.117868	0.681941
Q86Y46	-0.22773	0.681843
Q96RP9	-0.19375	0.681821
Q96KB5	-0.13105	0.681634
Q9Y2P8	-1.56935	0.679983
O15213	-0.13615	0.678715
Q9Y446	0.132148	0.678558
P61106	-0.10658	0.678312
Q53GS9	-0.22856	0.678174
P00403	-0.09873	0.677407
P22695	-0.21529	0.677274
Q9NWU2	0.177577	0.676108

Q8N0U8	0.536557	0.675851
Q8TAQ2	0.203525	0.675617
Q13561	-0.35197	0.67551
P08727	-0.11694	0.675479
O60869	-0.0771	0.674973
O75489	-0.11606	0.673329
Q9H299	0.079749	0.673214
P09543	-0.48099	0.672562
P31483	0.27923	0.671706
Q53H82	0.212297	0.6705
Q06210	-0.16161	0.669922
P52815	-0.38536	0.667978
O94906	-0.24103	0.667622
Q96SB3	0.133448	0.66739
P48735	0.171694	0.665744
P11047	0.125215	0.665636
Q96PD2	0.109935	0.665599
P29218	-0.43416	0.665538
Q15084	0.09071	0.66531
Q13148	-0.222	0.665268
Q99575	0.585796	0.665066
Q7Z6I8	0.159249	0.659011
P40121	-0.15868	0.65838
Q9Y5Z4	-0.55545	0.658273
Q9H832	-0.32563	0.658118
P00568	-0.14483	0.657923
Q5VT52	-0.67752	0.657371
A1L0T0	-0.24456	0.657344
P61289	-0.1118	0.656854
Q8WWC4	-0.64089	0.656812
P55789	0.19833	0.655147

Q9NX08	-0.35054	0.654738
Q92783	-0.13013	0.654143
P57088	-0.11997	0.653976
P55263	0.746705	0.651685
Q13232	-0.82777	0.651225
P10636	0.160126	0.651006
Q9Y6G3	0.07966	0.650901
Q9UJM3	0.215029	0.650594
Q96QK1	-0.81908	0.649229
Q9UBI1	1.303064	0.648852
Q9NXF7	0.555975	0.648398
Q9NX14	0.080621	0.648315
Q8N983	0.083945	0.646572
Q9H3P7	-0.1769	0.645568
Q8IXI1	-0.23645	0.644958
P03897	-0.74193	0.643494
Q9NRX1	0.414491	0.642807
Q15149	-0.41213	0.642656
P10620	-0.24585	0.641743
Q9UPN3	-0.0837	0.639831
P17029	0.676798	0.636731
Q9BRD0	0.204532	0.634596
Q13823	0.337498	0.632775
O95777	-0.12503	0.632759
Q08379	0.282284	0.630984
P49711	0.141891	0.630313
Q9UK45	-0.12076	0.628829
Q9BU61	0.220746	0.625726
Q5JWF2	-0.11097	0.625198
P63092	-0.11097	0.625198
P30049	0.451408	0.624917

Q969X5	-0.21225	0.62427
Q8IVS2	-1.04892	0.623103
Q6P1L8	-0.36444	0.622477
Q9NP84	0.332506	0.622031
P30519	0.164055	0.621918
P49756	-0.15582	0.617553
P78406	-0.29146	0.617373
P39880	0.367416	0.615852
Q6PI48	-0.48744	0.615641
Q9C0D2	1.165095	0.615112
Q96GQ5	-0.49156	0.615034
Q15847	-0.1162	0.614302
Q9NY93	-0.50696	0.614132
Q9P0S2	0.138	0.613055
P35659	0.082596	0.612923
Q9NP97	-0.11581	0.612304
Q8TF09	-0.11581	0.612304
Q8NE86	0.890517	0.611917
Q16854	-0.88591	0.610528
P56192	-0.48397	0.609204
P41091	-0.11884	0.608534
Q13698	0.591875	0.608025
Q9NR30	0.11934	0.607134
P13639	-0.38077	0.60702
Q9NV31	0.122038	0.606856
Q8IWZ8	-0.18287	0.606307
Q99661	0.927706	0.604572
P43686	0.11201	0.604215
P61421	0.163882	0.601107
Q9Y678	-0.41389	0.600347
Q9P287	-0.17147	0.600215

Q14116	-0.14701	0.599883
Q8TD16	-0.13534	0.598946
O43504	0.20756	0.596
Q99747	0.130265	0.594136
O15083	-0.66019	0.592665
Q92615	-0.57821	0.592425
Q5VT66	0.702064	0.589837
Q6L8Q7	-0.30279	0.589731
Q05519	-0.09597	0.588713
Q9ULW0	-0.0735	0.585656
Q99618	0.175586	0.585389
Q86UP2	0.213618	0.584433
Q96ST3	-0.28488	0.584423
P14550	-0.25458	0.583002
P15121	-0.25458	0.583002
Q9BT25	0.729731	0.582753
P62633	0.066132	0.581662
A8CG34	0.327775	0.581173
Q96HA1	0.327775	0.581173
Q9Y285	-0.18459	0.579365
P62899	0.075171	0.578188
O95202	-0.18469	0.577675
Q9NY59	0.87786	0.577128
P51553	-0.2233	0.573828
P63279	-0.0976	0.573105
P15170	-0.84872	0.572949
P51532	-0.23629	0.572739
Q8NE01	-0.40802	0.572544
P18084	-0.23809	0.571916
O95169	0.095672	0.570739
Q05682	0.372557	0.57049

Q9NX24	0.088647	0.568542
P31943	0.072861	0.568075
P62072	-0.19739	0.567946
Q96HR9	-0.27281	0.567763
P45880	0.092939	0.565975
Q13505	0.22832	0.564689
Q9UBM7	-0.36345	0.564594
Q12959	-0.55114	0.563183
Q9ULV3	0.628603	0.562429
O96019	-0.26434	0.562266
Q9BXR0	-0.86097	0.561871
Q8TD17	-0.38486	0.561242
Q6IN84	-1.24813	0.560281
Q9P013	0.165431	0.559561
Q96JP5	0.156636	0.557526
O00425	-0.12253	0.556694
Q9Y4Z0	-0.12517	0.556623
Q15654	-0.22122	0.55648
P18065	0.187911	0.556276
Q9P2I0	1.172148	0.556083
Q14160	0.118728	0.555576
O43676	0.120925	0.555489
Q96I25	0.098158	0.555251
Q86V81	-0.11925	0.554346
Q96AG4	-0.41391	0.554104
P20929	0.195219	0.553444
O43402	1.02471	0.55295
Q8WXH0	-0.91738	0.551547
Q9BSD7	0.174113	0.551263
O75691	0.445936	0.550562
Q9NW64	-0.88492	0.550024

Q9Y2R9	-0.09859	0.548736
P12277	-0.07317	0.547627
Q9HD20	-0.96982	0.546706
Q9Y5Y2	0.307995	0.545579
Q9NXG2	0.227785	0.544734
Q5VWK5	-0.77195	0.543279
Q99757	-0.12014	0.542157
P26232	0.10367	0.541874
Q969E2	0.106258	0.540507
Q5XKP0	-0.1429	0.539066
Q9Y4P3	0.378347	0.539022
Q8IY17	1.387927	0.538425
Q9BQB6	-0.17199	0.537542
P03928	-0.33825	0.537418
Q9BRR6	-0.18922	0.536807
Q9UI09	-0.12817	0.536411
Q9UBF2	-0.84342	0.535956
Q96E11	-0.09361	0.535827
Q86WR7	0.195992	0.535812
Q12800	0.514611	0.535084
O75438	-0.31782	0.534944
Q9Y5J7	0.13593	0.534832
O75410	-0.17451	0.532101
Q92839	-0.10499	0.531843
Q9H1B7	-0.48669	0.53178
P55011	-0.13251	0.530267
A0MZ66	0.182536	0.529244
Q96B97	-0.26013	0.529218
P06576	0.846006	0.528868
P49821	-0.19714	0.528499
P55735	-0.1725	0.526831

Q13049	-0.23757	0.523928
Q9Y3D6	0.384408	0.523524
Q96A08	0.086251	0.523523
P56270	0.283712	0.522468
Q9BSH5	-0.83921	0.522045
P55769	-0.12961	0.521453
Q5SRE5	0.539429	0.521399
Q7KZF4	-0.20104	0.520552
P48643	-0.19014	0.520413
O60701	-0.88327	0.52035
Q9GZY8	-1.18712	0.516241
Q96G01	-0.18946	0.515467
Q6PL18	0.193422	0.513384
P35613	-0.12583	0.513013
O60888	-0.36645	0.512713
O75506	-0.28646	0.512473
Q8WYA6	-1.06782	0.51025
P60981	-0.11947	0.51021
P16278	1.681846	0.508048
Q6UWU2	1.681846	0.508048
Q15392	0.589704	0.506886
Q9BQ52	-0.3258	0.506884
Q53S33	-0.16154	0.506835
Q9BT22	-0.37936	0.506576
Q9Y277	-0.08212	0.505514
Q9Y6X5	0.323147	0.504845
Q8NF37	0.36362	0.503884
O75367	0.129953	0.503691
Q9Y6E0	0.180183	0.502125
Q29983	0.926191	0.501507
Q8N8S7	-0.13168	0.501332

Q16836	-0.34139	0.500884
Q8N6S5	0.456139	0.500358
P35914	0.653475	0.495489
P35250	-0.2119	0.493265
Q9Y237	-0.13692	0.491304
Q9UL46	0.123234	0.491049
P38936	-0.71349	0.490515
P16989	-0.07419	0.490163
Q9NR45	-0.21336	0.489952
P51114	-0.42396	0.489365
P03891	-0.74551	0.489348
Q9Y2D8	0.468859	0.488882
Q86Y39	-0.63526	0.485836
Q8NEP3	-0.2163	0.485449
Q96CW1	-0.23479	0.483574
Q8TAT6	-0.87196	0.481523
O60832	-0.29318	0.481427
O14745	0.060416	0.480955
P46063	0.75	0.480105
O75208	-0.11399	0.480058
P43121	-0.10244	0.479542
Q99808	0.106628	0.479395
P04732	-0.10885	0.477198
Q9Y5K5	0.093504	0.476857
Q9UBX3	-0.25103	0.475673
P62191	0.068529	0.475566
Q9H1Y0	0.151915	0.475095
Q9UNP9	-0.08656	0.474413
P62308	0.195183	0.474248
Q9NV56	-0.33927	0.47274
O95926	0.452223	0.470353

Q9HCE1	0.614864	0.470269
Q9Y6K9	0.344088	0.468964
P0CB47	-0.31948	0.468902
Q9P289	0.193875	0.468896
Q96HS1	-0.05717	0.468312
Q9NX46	0.385679	0.467826
Q99595	0.57181	0.4643
P05141	0.060433	0.462738
O75964	-0.06323	0.46222
Q13541	-0.17969	0.461691
Q16763	-0.09751	0.461077
Q13523	0.322976	0.460112
P04632	0.110925	0.460029
Q9P031	0.667879	0.458897
P42285	-0.14917	0.458044
Q9Y4L1	-0.08932	0.457948
Q9P0L0	0.137206	0.457647
P39748	0.0652	0.457384
O76080	0.60315	0.456968
P13535	0.234289	0.455307
P62841	0.559559	0.454876
P82930	0.097113	0.454422
P60033	-0.06223	0.454008
Q9P0T7	0.191878	0.453991
P05455	-0.09708	0.452343
Q9Y3L3	0.19018	0.452219
Q9P0W2	0.329078	0.452181
Q9BQ39	0.072494	0.451526
Q9BWJ5	0.320764	0.450799
Q9H6T3	-0.18344	0.450551
P08779	0.05212	0.450518

Q8N4C6	-0.09629	0.450042
Q9GZS1	0.321425	0.449912
Q9NPJ3	0.19379	0.449655
Q9UHD8	-0.08778	0.447615
P33527	0.564484	0.44756
P02795	-0.08565	0.447463
Q9NQG5	0.252565	0.447437
Q29980	0.267654	0.44682
P08138	0.642605	0.445526
Q9BY32	-0.5975	0.445366
Q9Y383	0.055781	0.445347
Q9Y679	-0.25712	0.445175
P78310	0.129762	0.444628
Q8NCA5	-0.50554	0.444479
Q92538	3.583228	0.4423
Q8WUK0	-0.89128	0.44217
Q9Y657	0.457965	0.441633
P61081	-0.06158	0.441042
P61019	-0.08235	0.440905
P51659	-0.11508	0.440896
Q8IWA0	-0.28923	0.439957
O43852	0.117122	0.439869
P06865	-0.73606	0.439591
O43399	0.056844	0.438668
Q9Y6G9	-0.22847	0.438613
Q00765	0.169627	0.437912
Q9H0B6	-0.10646	0.437787
Q92922	0.151065	0.437739
Q9BQA1	-0.06371	0.437354
Q16740	-0.16199	0.436707
Q92797	-0.73166	0.436357

P09110	-0.29196	0.435422
O75521	-0.28199	0.432147
Q8N6T3	-0.14891	0.431775
O00764	-0.8839	0.431477
Q8N339	0.11835	0.431459
P80297	0.11835	0.431459
P13640	0.11835	0.431459
P17174	-0.22776	0.430207
P49916	0.238306	0.429797
Q9BW61	0.386871	0.429713
Q9BYD6	0.06525	0.428965
P09132	0.502993	0.428543
Q9P000	1.314099	0.426115
Q13794	0.789204	0.42552
Q15286	-0.06313	0.425095
P47813	0.153762	0.423377
P21127	-0.14592	0.419666
Q15269	-0.24098	0.418937
Q12929	0.204995	0.417598
Q9Y5K6	-0.09717	0.417071
P68402	-0.26924	0.41655
O75844	0.099653	0.416337
P78527	-0.55081	0.415686
P61006	-0.06027	0.41551
Q9UKJ3	-0.24858	0.415441
P11117	0.1444	0.414433
P84095	-0.07718	0.41193
Q96BK5	-0.08376	0.410075
O43488	-0.67272	0.408275
P09874	-0.05084	0.407458
Q92552	-0.14062	0.40652

A2RTX5	-0.89807	0.406121
Q92934	-0.13563	0.405532
Q15700	-0.46381	0.404005
O15460	0.426236	0.403263
Q8WWQ0	0.661051	0.402239
P27144	0.072333	0.400311
Q15061	-0.20361	0.399451
P09497	0.051611	0.39935
Q9UQR1	0.165096	0.397288
Q8NGY0	1.006692	0.396722
O75569	-0.06994	0.395747
Q08209	-0.27135	0.394773
Q86WX3	-0.12236	0.394482
Q12981	0.155903	0.393709
Q53GQ0	-0.24684	0.393636
Q8IY37	0.622503	0.392139
Q9NRL2	-0.06052	0.38989
P19404	-0.05469	0.389773
O95139	-0.25587	0.388838
P23229	-0.06585	0.38873
Q8WWI5	0.262514	0.387488
P30419	-0.063	0.386983
Q5VU43	0.235988	0.386801
Q8IZL8	-0.19199	0.386431
Q04695	0.067162	0.386408
Q9H074	-0.10807	0.38551
Q9C0B1	-0.1178	0.385274
Q8NEJ9	0.232996	0.384086
Q9Y2K7	0.613375	0.382516
P04181	-0.17177	0.382142
Q02218	-0.14509	0.381655

P38646	0.229524	0.381166
P08754	-0.05358	0.380683
Q96G25	0.192491	0.378767
Q9H3Q1	0.287599	0.377968
Q14011	0.05411	0.377932
P21291	0.49629	0.376351
O43264	-0.67564	0.37609
O00233	0.076871	0.375745
P79522	0.803349	0.375259
P43490	-0.11167	0.375059
Q14677	-0.059	0.375057
Q6P587	0.385138	0.374652
Q52LJ0	-0.21335	0.3742
P15514	-0.76935	0.374193
P26447	-0.05761	0.373782
P30085	-0.07174	0.373081
Q8IZP0	-0.15034	0.372295
O15067	0.533548	0.372188
O43175	-0.09194	0.37209
P49189	-0.29834	0.371738
P35555	-0.85565	0.370817
Q9BQI3	-0.98506	0.370584
O00487	-0.10275	0.370487
Q9Y6V0	0.504819	0.370395
P18615	-0.14263	0.369835
P30837	-0.20144	0.369428
P52294	0.332627	0.368903
Q3LXA3	-0.52297	0.368767
O95299	-0.15473	0.368619
Q16643	-0.1004	0.367655
O60684	0.246851	0.367365

P82979	0.049116	0.366898
P10586	-0.39767	0.365791
Q15365	-0.07034	0.365655
Q9Y2Q3	0.168973	0.36551
P52594	-0.18091	0.364708
O43583	0.048334	0.364228
Q9P0J0	-0.38208	0.364151
Q06033	-0.58737	0.362725
Q9UNE7	-0.27829	0.360505
Q96J84	0.131024	0.360399
P50579	0.067886	0.360321
P62318	-0.06734	0.359959
Q8IYU8	0.509177	0.358241
Q5UIP0	-0.11174	0.358026
Q13137	0.295882	0.35648
Q15714	0.134366	0.356207
P16070	-0.04056	0.355562
Q9H9B4	-0.09206	0.355021
O75340	0.092823	0.354021
P02538	0.141647	0.353416
Q99959	-0.18462	0.353398
Q3ZCQ8	0.150508	0.353207
Q05193	-0.25889	0.352944
P50570	-0.25889	0.352944
Q7KZI7	0.260086	0.35288
Q9UBV2	0.263589	0.351122
P15529	-0.06695	0.35042
Q9BW60	0.198559	0.35026
Q15554	-0.49749	0.350103
Q9BXK1	-0.10938	0.348677
Q9BPZ3	-0.17736	0.34681

Q00688	-0.10568	0.346471
P55084	-0.04738	0.346328
Q9Y305	-0.0966	0.343786
P46977	0.073932	0.343435
Q6PD62	-0.53708	0.343344
P49755	-0.05316	0.343113
Q96TA2	-0.05956	0.341862
Q15369	0.083381	0.341207
Q8IV08	0.136113	0.341154
P09429	0.225766	0.340972
Q9BTM1	0.206141	0.340925
Q99878	0.206141	0.340925
Q96KK5	0.206141	0.340925
P20671	0.206141	0.340925
P0C0S8	0.206141	0.340925
Q93077	0.206141	0.340925
Q7L7L0	0.206141	0.340925
P04908	0.206141	0.340925
P09651	-0.13352	0.340312
Q92572	-0.81425	0.339487
O75351	0.043639	0.337713
P36507	-0.26769	0.336117
Q02750	-0.26769	0.336117
O75874	-0.11376	0.335503
P32519	-0.23809	0.335281
P27695	-0.11078	0.335261
Q71RC2	-0.05008	0.334927
Q9UEU0	-0.08843	0.334732
Q9UHD9	-0.11494	0.334611
Q9Y289	-0.22902	0.334145
P15586	0.161381	0.333652

Q8TCD5	0.20687	0.332561
Q9BTX1	0.18373	0.332456
P23193	0.064906	0.33218
Q16881	0.526018	0.331464
O60264	-0.1442	0.331235
Q9Y508	0.104357	0.328197
Q6P1M0	0.411369	0.328036
Q9Y617	-0.09584	0.326975
Q9H0D6	-0.25215	0.32505
Q99615	-0.09725	0.32353
Q9Y5T4	0.209324	0.322019
Q96RU3	-0.64319	0.322013
Q13442	0.038443	0.321906
Q9Y314	-0.04538	0.320361
Q9UKM9	0.060224	0.319592
Q08945	-0.09816	0.319524
P49903	-0.59666	0.319397
P68366	0.302802	0.316317
O76003	-0.08303	0.315922
P12109	0.312595	0.315777
Q9H2D6	0.116866	0.315056
P16435	0.270102	0.314707
P56385	0.046271	0.312137
Q13185	-0.15743	0.311244
Q9P1U0	0.402634	0.310898
O95470	0.269345	0.310237
Q13409	-0.3099	0.309619
O43598	-0.09722	0.308339
Q9HD42	0.170252	0.307818
Q15738	-0.15974	0.305971
Q9Y6M9	0.116393	0.305866

O14949	0.266167	0.30477
P20340	-0.07032	0.304457
P42785	-0.44824	0.303556
Q9UNW1	-0.71034	0.301904
Q9NX20	0.34774	0.301638
Q14966	0.313805	0.300335
Q9BU89	-0.22112	0.300332
Q15293	-0.12184	0.299556
Q96T23	-0.06511	0.29938
O75880	0.107391	0.298093
Q9BVL2	0.072263	0.297769
Q9P2M7	0.106317	0.296117
Q8IWJ2	-0.37273	0.295873
O60739	0.044463	0.295865
P22570	-0.15327	0.295378
Q03111	0.170708	0.295365
O14548	0.277113	0.294326
Q8NBQ5	0.165892	0.293677
O60784	-0.35149	0.293166
P14625	0.368372	0.292527
P40939	-0.12334	0.292395
O15042	-0.05998	0.292324
Q8WUW1	0.095988	0.291791
Q9UK41	-0.26879	0.291762
Q9P2R7	-0.14518	0.291649
Q9Y4W6	-0.0953	0.291198
P30101	0.2581	0.288715
Q96N67	-0.36287	0.288494
Q03701	-0.85159	0.287336
Q6RW13	-0.40067	0.28646
P08708	0.176038	0.28632

Q9UKS6	0.041636	0.28383
P39687	-0.06742	0.28281
O95983	0.122826	0.282628
O75352	-0.33123	0.280859
Q01650	0.05274	0.278642
O75886	-0.607	0.277815
Q86YZ3	0.576223	0.277521
Q9UNQ2	-0.15717	0.277055
P55072	-0.09827	0.274317
Q9H0Z9	-0.32691	0.27316
P57740	-0.15052	0.272928
Q29RF7	0.1996	0.272515
P09661	-0.09932	0.271865
P10301	-0.06331	0.271461
P51665	0.523995	0.271402
P45954	-0.24202	0.270676
Q9UL25	0.150281	0.270478
Q8TED0	-0.12631	0.270307
O43707	0.247361	0.269934
Q9H4L5	0.667224	0.269704
Q01130	0.038084	0.269295
O00767	-0.66763	0.268851
P23381	-0.26783	0.268244
P07942	0.397435	0.26802
P11387	-0.03772	0.268012
Q8TAE8	-0.04327	0.266779
Q9H5Q4	0.135675	0.266001
P62310	-0.03822	0.26516
P48668	0.090346	0.264518
Q9BWF3	-0.07358	0.264444
Q8TEX9	-0.33251	0.264081

O43747	0.315013	0.26352
O60884	-0.07568	0.263504
Q07666	0.042537	0.263468
Q9UNL2	-0.07321	0.262898
Q9Y3C6	0.269113	0.26281
Q6P597	0.090057	0.26166
Q9UN37	0.032441	0.261164
Q9H0A0	-0.06475	0.260614
Q9BU76	0.113642	0.260009
Q9UFG5	0.223299	0.259578
Q9ULJ8	0.094083	0.25893
O75629	-0.41372	0.258498
Q9H0V9	0.385505	0.257966
P23588	-0.07123	0.257422
P61026	0.04535	0.257311
P61224	0.294743	0.257081
Q9BXV9	-0.23744	0.257011
Q9Y448	-0.08338	0.256834
P30536	-0.51939	0.256334
O94973	-0.29176	0.254619
P68104	-0.22194	0.254396
P27797	0.124025	0.254087
Q7Z434	0.102649	0.253701
P08133	0.064857	0.252422
Q99720	-0.14085	0.252316
Q9NPE2	0.12617	0.251726
Q15041	-0.14541	0.251442
Q9UII2	0.079083	0.25116
O75695	-0.34851	0.251029
P49137	0.564035	0.250768
Q9BYD1	-0.10395	0.24843

O95571	0.060257	0.24694
O60493	-0.08285	0.245582
Q01085	0.087945	0.245513
P21964	-0.13083	0.245286
O60762	-0.27386	0.245037
Q9BV79	0.798055	0.244277
P60660	0.050593	0.244232
Q96RE7	-0.47086	0.244105
Q92804	-0.07976	0.243861
O00217	-0.03335	0.243797
P82673	-0.10317	0.243143
Q49A26	-0.26927	0.242279
P00747	-0.57719	0.239592
Q8NI36	-0.11669	0.23954
O60220	-0.11768	0.238664
Q7Z5G4	0.100224	0.238101
P52701	-0.12839	0.237806
O60936	-0.46987	0.237675
P24752	-0.08101	0.237495
O00499	-0.11088	0.237439
Q9NQZ2	0.147311	0.236827
P35813	-0.25761	0.236477
Q9NR56	0.067044	0.234039
O00267	-0.25891	0.233223
Q8NI22	0.064441	0.232933
P24928	0.273316	0.232399
O00232	-0.14013	0.232163
Q16342	-0.09475	0.232098
O00411	-0.26164	0.231653
O75477	-0.10559	0.231476
O14681	-0.43687	0.229781

O43395	-0.18907	0.229328
O43143	-0.12374	0.229097
Q8IWC1	0.049688	0.226862
Q92890	0.395578	0.226617
Q13610	-0.13861	0.225898
Q9NQX1	-0.59778	0.225329
Q9Y606	-0.82025	0.225185
Q00839	-0.13275	0.224791
P61803	0.063732	0.223771
O60293	0.291329	0.223459
O60231	-0.10749	0.222836
P30825	0.282924	0.222551
Q9HB07	-0.2958	0.220996
P63241	0.070423	0.220487
O60925	-0.06431	0.220317
Q9NRR5	-0.23798	0.22031
Q9BRQ6	-0.08334	0.218978
Q9Y2Z4	-0.19032	0.218296
O94763	-0.5118	0.218144
Q92817	0.079963	0.217172
P62166	-0.08642	0.216583
Q13510	0.344622	0.216504
Q8N131	-0.05656	0.216362
P62861	0.035391	0.216157
O43292	0.258205	0.215639
O43447	-0.04792	0.215254
Q9HAV7	0.044441	0.215013
Q99436	-0.05567	0.214052
Q8N5M9	-0.36499	0.213876
P06727	-0.22052	0.211345
O94826	-0.0951	0.210065

O75746	-0.3084	0.208334
Q16890	-0.07989	0.208112
P51531	-0.20295	0.20801
Q8IXM2	-0.57414	0.207825
Q5RI15	-0.0964	0.207139
Q7Z2K6	-0.09551	0.206919
Q96J01	0.246889	0.206302
O95182	-0.05119	0.20387
Q15067	0.164071	0.203502
Q8NBS9	0.284636	0.203425
O43169	-0.48478	0.203225
Q9NW13	-0.10039	0.202821
P46783	-0.05808	0.20237
P84090	-0.03311	0.201627
Q6P1J9	0.24834	0.201335
Q9Y5M8	-0.06485	0.200883
Q9BQC6	-0.36692	0.200187
P02786	-0.02622	0.200137
P27694	-0.28762	0.199507
P25942	0.13325	0.19939
Q969V3	-0.12699	0.198813
Q8NFH4	-0.0909	0.198212
F5HG51	0.518444	0.198194
Q9H2K0	0.269306	0.197947
Q14690	-0.06823	0.197647
Q9NQS7	0.055724	0.197436
Q9BQ69	-0.17056	0.196994
Q9NUQ9	0.156689	0.196904
P78324	0.348405	0.196881
O94874	-0.15978	0.196607
P23786	0.337188	0.196488

P19387	0.169278	0.195302
P41208	0.101303	0.194766
P51571	-0.03153	0.194682
Q8TDP1	-0.38245	0.19393
P62942	-0.03917	0.193655
Q8WVJ2	-0.05422	0.193229
Q9NYP9	-0.14177	0.191986
Q8N4H5	-0.03157	0.19111
Q8N4V1	-0.09884	0.190293
P35251	0.272576	0.190157
Q9BUL5	0.415068	0.190012
P62993	0.041507	0.189765
Q8IXI2	-0.4198	0.189688
Q9NRP0	-0.0902	0.189147
Q9Y6A4	-0.35225	0.189021
Q9UQE7	0.102726	0.188898
P47755	-0.11788	0.18847
Q6DD88	0.161312	0.188086
Q5T0N5	-0.08345	0.187688
Q9BUL8	0.197781	0.18721
Q9BTV4	0.181536	0.184439
P61619	-0.09586	0.182361
Q9NZZ3	-0.09466	0.182287
P24844	0.02969	0.181679
Q9NUQ2	0.127694	0.181346
P55199	0.261115	0.17972
O43716	0.043368	0.178218
Q9UNM6	-0.13264	0.178174
Q8WVK2	-0.039	0.177126
Q9BZI7	-0.09879	0.176776
Q96AT9	-0.15111	0.176548

Q96GC5	-0.10886	0.176063
O75400	0.05531	0.1756
P63272	0.045759	0.174853
P49721	-0.14997	0.174657
Q9BQ48	-0.04206	0.17187
Q9NYK5	-0.16555	0.170943
Q9NR28	0.052261	0.170413
O75190	-0.11034	0.1702
P61586	0.070976	0.169889
O14777	-0.11664	0.169609
Q9UBQ0	0.357239	0.169516
Q9BSJ8	0.108888	0.16905
Q9BUA3	-0.12461	0.168709
Q93009	-0.14474	0.168586
Q9ULR0	0.084634	0.168544
Q96DV4	0.059612	0.167804
Q7Z2W9	0.390929	0.167745
Q9BQG0	0.149535	0.167671
Q8N4Q1	0.058607	0.167458
P61009	-0.04614	0.165711
Q9NYP7	-0.1857	0.16552
Q5SY16	0.504931	0.164801
Q63HN8	0.062835	0.163923
P53582	-0.04821	0.163781
P62328	-0.08192	0.163569
Q96I51	0.223107	0.162218
Q6NUM9	0.260068	0.161025
Q8N766	0.075104	0.157663
Q14318	-0.08253	0.157522
P62910	0.06401	0.15727
O95159	0.081017	0.156933

Q8WWM7	-0.03662	0.155951
O43688	-0.04005	0.155285
Q9NPF0	-0.15991	0.155221
Q14669	-0.07822	0.155148
Q99543	0.36473	0.154837
Q8WUM9	0.157577	0.15446
P46013	-0.07093	0.154102
P14314	-0.15854	0.153983
P28838	-0.04089	0.153743
P13693	0.067681	0.153682
Q08722	0.343963	0.153497
Q01628	0.394114	0.153305
Q01629	0.394114	0.153305
P13164	0.394114	0.153305
P53801	-0.02876	0.15316
O14773	-0.15759	0.152937
O15270	0.268207	0.152851
P18206	-0.07908	0.15208
P53597	-0.07797	0.150774
Q08752	-0.02697	0.149848
O15504	0.390826	0.148664
Q9HC36	0.119946	0.14856
A5D8V6	-0.08892	0.148124
P40855	0.178155	0.147775
P06746	0.323412	0.147748
P84103	-0.02256	0.147007
Q13576	0.054827	0.146986
Q96EY7	-0.0463	0.146945
Q9BW83	0.136315	0.146727
P47914	0.022786	0.146545
Q9Y2U8	0.095058	0.145926

P17480	0.042783	0.145473
P01889	0.037422	0.145338
Q9NR12	0.032913	0.145145
Q6PK04	-0.04174	0.144813
O00214	0.575592	0.144658
O43524	-0.32768	0.144484
P42766	0.022475	0.140933
Q96N66	0.131702	0.140504
Q9UDY2	0.44798	0.140302
O75915	-0.12991	0.139223
Q969G5	0.039982	0.138983
Q13200	-0.03274	0.138855
Q07817	0.090178	0.138453
Q5J8M3	0.298719	0.138269
Q92504	0.411971	0.138101
Q9NX70	0.092193	0.13804
Q5JTJ3	-0.0371	0.136611
P51116	-0.22253	0.135995
Q9NRR3	0.082745	0.135731
Q9UNK0	0.067861	0.135073
P49023	-0.11863	0.134364
O96013	0.310803	0.133654
Q9NUQ6	-0.24332	0.13364
P10768	-0.20582	0.131604
Q9NR46	0.059175	0.131529
P23511	-0.11063	0.131301
O00559	-0.25743	0.131039
Q6NVY1	-0.03549	0.130074
Q15942	0.034937	0.129384
P16144	0.057681	0.12928
P35268	0.021789	0.129063

Q96K17	-0.03039	0.128068
P24539	-0.02581	0.12748
Q9BYD2	-0.11873	0.12725
Q7Z3Z4	-0.19893	0.126813
P31689	0.022997	0.126542
Q15382	-0.18978	0.126314
P48960	-0.03386	0.124973
Q6RFH5	0.042502	0.124146
Q13509	-0.04114	0.123945
Q06587	-0.04246	0.123612
P41236	0.171073	0.123551
Q9BUR5	0.047214	0.123334
Q5SW79	0.027958	0.122829
Q9BUH6	0.093146	0.122563
P04792	0.068886	0.122019
Q7LGA3	-0.02849	0.121375
Q9BZL1	0.037957	0.120417
Q9P270	-0.06803	0.119864
Q8TCC3	0.08675	0.119782
Q8TC12	0.137071	0.119578
P54760	-0.04118	0.119257
O60749	-0.07267	0.118701
Q3ZCM7	-0.08592	0.118645
Q9NP90	0.02742	0.118621
Q8NBU5	0.145587	0.118526
Q9BYW2	-0.48627	0.117245
Q9UBQ7	-0.07826	0.116829
Q9Y3D3	-0.01864	0.116672
O60725	0.120228	0.11648
Q86UU0	0.146663	0.116254
P04179	0.069076	0.115482

P35637	0.031382	0.115075
Q8IWL3	0.03472	0.114884
Q9Y4B6	0.040742	0.11358
P67775	-0.0793	0.112023
P62714	-0.0793	0.112023
Q16864	-0.03535	0.111982
O94760	0.037706	0.111003
P52888	0.077927	0.110676
Q92973	-0.05709	0.110667
P04899	-0.03598	0.110451
O60716	0.048946	0.110144
P61011	0.053398	0.110069
P68036	-0.03421	0.109733
Q9Y2W2	0.022222	0.109541
O14618	-0.06228	0.108886
Q07866	0.018482	0.108678
Q96GN5	0.049957	0.108622
Q9NQW6	-0.06959	0.108579
O14662	0.286342	0.108239
Q14118	-0.12101	0.107898
O75027	-0.16731	0.107341
Q9BS26	0.066136	0.106492
Q0VDF9	0.275931	0.105128
Q9Y5A9	-0.05311	0.104995
Q8IY81	0.027678	0.104667
Q5T2T1	0.058468	0.104512
P63218	0.037	0.103917
P17544	-0.13766	0.103725
Q53H12	0.022742	0.102867
P62269	-0.01432	0.102864
A6NNZ2	-0.07064	0.102846

Q9H490	0.131691	0.1011
Q9BQE3	0.140718	0.099675
Q15629	-0.16121	0.099331
Q06265	0.022531	0.097953
Q9BY89	-0.04795	0.097836
P45877	0.327923	0.096564
Q14498	-0.03157	0.096504
P13073	-0.01515	0.096318
Q8TCT8	-0.01836	0.096133
P62273	-0.02239	0.095717
Q9NPF5	0.214813	0.095263
Q9H583	-0.19661	0.094328
P18859	-0.01378	0.093782
O14964	-0.01796	0.093663
Q9HBH0	0.137263	0.093558
Q8TBK6	-0.12906	0.093451
Q9BSH4	-0.07472	0.09336
Q16629	0.021372	0.093238
Q6IPM2	0.362704	0.09318
Q6PKG0	-0.06203	0.092671
Q15397	0.173277	0.092553
Q9BW27	0.040988	0.09237
Q13084	-0.0899	0.092046
P08582	-0.19547	0.091861
Q9NRH3	0.102107	0.090764
P23258	0.102107	0.090764
Q3ZAQ7	0.027344	0.090637
P54886	-0.04629	0.090218
Q9H6R4	-0.10155	0.08999
Q9Y490	-0.09609	0.089226
Q96EY4	0.016735	0.089015

Q96I99	-0.03144	0.088657
Q7Z3B4	0.072993	0.088645
Q14694	-0.06619	0.088082
Q99700	0.066862	0.087181
Q8WVM8	-0.05681	0.087165
Q96G23	0.069018	0.086544
Q15165	0.178462	0.086393
Q02447	-0.11606	0.086256
Q9BVC6	0.042887	0.086048
P52209	0.016364	0.08594
Q9NP79	-0.22347	0.085936
Q13247	0.01262	0.085796
Q96AA3	-0.07715	0.085194
O00592	-0.01588	0.085072
Q5JTH9	-0.03465	0.084393
Q9Y320	0.093806	0.084139
P55210	0.11697	0.08327
P62316	-0.01522	0.083199
Q9P2X0	0.093741	0.082946
Q7KZN9	0.120139	0.082125
Q12769	0.05398	0.07986
Q9UI30	-0.06088	0.079517
P35269	0.02131	0.079331
P46060	-0.12752	0.079216
Q9H444	-0.04104	0.07909
P82663	0.058443	0.078933
P00492	-0.02526	0.078408
O14828	0.026053	0.077001
P13861	-0.06748	0.076745
Q92896	0.06243	0.076591
P51648	0.045581	0.07644

P13647	0.034968	0.07605
P08240	-0.04028	0.075667
P49458	0.012796	0.075251
Q9HCU5	0.120069	0.075114
Q9NRV9	0.026145	0.074372
Q99614	0.014783	0.074224
P30405	0.040184	0.073171
Q96EQ0	-0.14503	0.073109
Q9Y3B3	-0.01942	0.072418
O94905	-0.03908	0.07241
O14776	0.016271	0.071714
O15049	-0.0416	0.071577
Q9H2W6	0.024294	0.071469
P51858	-0.01631	0.070742
P09884	-0.1815	0.070418
Q96B23	-0.10774	0.070069
P40616	-0.01778	0.070033
P21579	-0.05505	0.069579
P22033	-0.05662	0.06908
Q9Y221	0.069536	0.068712
P09417	0.109958	0.068319
P09001	0.098783	0.068317
P51636	-0.17009	0.067938
Q96CS3	-0.01598	0.067859
P52756	-0.03554	0.067662
Q9Y3X0	0.026366	0.067296
Q92882	-0.01629	0.066808
Q96NB3	0.077245	0.066189
P07954	0.029567	0.065661
Q8N3X1	-0.05627	0.065653
Q96CS2	0.04412	0.065239

P22059	0.065296	0.06438
Q5T6F2	0.026426	0.064213
P09104	-0.01164	0.06389
Q8TDN6	0.054162	0.063651
P15153	-0.01459	0.063647
Q15370	0.011315	0.063415
P20810	-0.02172	0.063413
Q7Z2W4	0.030885	0.063332
Q99986	0.017378	0.062799
O43166	0.113086	0.061878
Q15029	0.046132	0.06179
Q07157	-0.01664	0.061378
Q15599	-0.03008	0.061162
P19525	-0.10442	0.061003
Q06136	-0.07671	0.060243
Q15024	-0.1144	0.058703
O00443	-0.51264	0.058099
Q96EH3	-0.03433	0.05748
Q8NFH5	-0.02024	0.057294
Q9Y6K0	0.158612	0.056467
P51610	-0.02317	0.056118
Q96MU7	0.17511	0.056109
Q9UKL0	-0.11722	0.054854
Q9P2K3	-0.11722	0.054854
P16615	0.042151	0.054024
Q8N9E0	-0.0489	0.053383
P49748	-0.01007	0.05281
Q13347	-0.03083	0.050966
Q9UIF9	-0.18128	0.05076
Q96DF8	0.02859	0.04965
P11413	0.065148	0.049225

Q92530	0.073163	0.048587
Q9Y3Y2	0.020317	0.048359
P61978	-0.03599	0.048254
P50443	0.041463	0.047361
O00139	-0.09464	0.047269
Q13586	0.08842	0.047182
O75531	0.021866	0.046499
P62070	-0.03749	0.046241
Q96SB4	-0.02095	0.046212
Q6P2Q9	0.023611	0.046133
Q13595	0.014053	0.046087
P50897	-0.01441	0.045756
P06756	0.010411	0.045102
P50402	0.020498	0.044389
P29692	-0.01638	0.044348
Q9UM54	-0.01862	0.044308
O75394	-0.08017	0.042805
Q6ZSY5	-0.14968	0.042351
O43795	-0.0269	0.04178
P55809	0.018406	0.041602
Q9BTT6	0.009135	0.04152
Q6ZMU5	0.024542	0.040741
Q13813	-0.02394	0.040714
Q8N9R8	0.099201	0.038807
Q6NZ67	0.013498	0.03872
Q6P582	0.013498	0.03872
Q1ED39	-0.01307	0.03871
Q96A49	0.00994	0.038159
O00161	0.017155	0.037806
P62834	0.037384	0.03749
O15347	-0.02625	0.037441

Q9Y6A9	0.062358	0.036412
P54578	-0.0095	0.035848
Q8TDD1	0.03503	0.03559
O95429	0.070853	0.035578
O75396	-0.00934	0.035541
Q6NXS1	0.055981	0.035239
Q9BQE4	0.052961	0.035201
Q96GA3	0.01014	0.035172
P07741	0.013377	0.035147
O60437	-0.00987	0.034786
Q9BQ04	-0.01063	0.034471
Q13098	-0.06073	0.034102
Q5VT06	0.089368	0.033807
Q969N2	-0.01254	0.033271
O75592	-0.00776	0.033003
O14957	-0.11729	0.032043
Q15785	-0.01645	0.031247
Q15363	-0.00834	0.031177
Q14807	0.008167	0.031069
Q569H4	-0.06934	0.029445
O75940	-0.00606	0.029179
Q02338	0.041913	0.028628
Q14165	-0.01651	0.028278
Q9H7B2	-0.02016	0.027782
O95249	-0.0671	0.027124
O60763	0.014862	0.026005
O75306	-0.00893	0.025267
P54756	0.014891	0.02512
O75947	-0.02184	0.024253
Q6NZI2	0.004356	0.023598
P21283	0.01459	0.021537

Q9BZE1	-0.03315	0.02121
Q9Y5S9	-0.01061	0.020862
Q9Y3D0	-0.00739	0.02066
P30038	0.187225	0.020493
Q6IQ22	0.005104	0.020046
P48739	-0.01319	0.019903
Q15070	0.015527	0.019862
Q92643	-0.02042	0.019592
P35916	-0.18504	0.019484
P34130	-0.00707	0.01948
Q8WXI7	-0.00707	0.01948
Q8WUD4	-0.00555	0.019332
O00488	-0.00978	0.018759
P25325	-0.04144	0.018571
Q13308	-0.00365	0.018267
O75323	0.008987	0.018255
O15126	-0.01682	0.018145
Q99496	0.011158	0.017677
Q96DA2	0.00451	0.017447
Q8NCW5	-0.01729	0.016922
O95372	0.014311	0.016746
P20020	-0.00362	0.016634
P53701	-0.00572	0.016502
Q92820	0.007727	0.016323
P51795	-0.04218	0.016305
Q92733	-0.00914	0.015717
Q13011	-0.00991	0.015469
Q53EZ4	0.021845	0.014848
Q8NCN5	0.022393	0.014223
P20337	-0.00354	0.01332
Q14554	-0.0246	0.013097

Q9BWM7	0.009241	0.012474
O43390	0.002688	0.012016
P0C0S5	-0.00219	0.010494
Q71UI9	-0.00219	0.010494
Q32P28	0.006368	0.010285
Q9NX62	-0.01089	0.009666
Q9NPE3	-0.00704	0.009488
Q969X6	0.010835	0.008681
Q9HAF1	0.002521	0.007724
Q7Z7F7	0.002755	0.0066
Q14257	0.004326	0.006305
P61769	0.002239	0.006219
Q9BRU9	0.005835	0.005835
O43678	-0.00081	0.005388
Q8NAV1	0.002902	0.005308
Q8N5P1	0.01744	0.005228
Q9BRX5	-0.00322	0.004694
Q02127	0.001707	0.004445
O94901	-0.00124	0.002925
Q96TC7	-0.0008	0.001633
P13804	-0.00036	0.001561
O15226	-0.00262	0.001365
P54727	9.80E-05	0.000389
P10412	-3.55E-15	0

CURRICULUM VITAE

NAME	Jeeraprapa Siriwaseree
DATE OF BIRTH	22 August 1992
BIRTH PLACE	Kanchanaburi
ADDRESS	45 Village No.5, Ta Khram En Sub-district, Tha Maka District, Kanchanaburi 71130
EDUCATION	MS in the field of Bio-systems Sustainability, Hokkaido University, 2018 BS in Biomedical Science, Rangsit University, 2015
WORK EXPERIENCE	National Blood Center, Bangkok, 2015-2016 Scientist (temporary)
AWARD RECEIVED	The Professor Dr. Tab Nilanidhi Foundation Award in 2015 Biomedical Science in Bachelor's degree of Science, first-class honors at Rangsit University.
PUBLICATION	Siriwaseree, J., et al., Synchrotron Fourier Transform Infrared Microscopy Spectra in Cellular Effects of Janus Kinase Inhibitors on Myelofibrosis Cancer Cells. ACS Omega, 2022. 7. Paemanee, A., et al., Mass spectrometry and synchrotron-FTIR microspectroscopy reveal the anti-inflammatory activity of Bua Bok extracts. Phytochemical Analysis, 2022. 33. Wongkhieo, S., et al., In vitro cholesterol lowering activity of Ganoderma australe mycelia based on mass spectrometry, synchrotron Fourier-transform infrared analysis and liver-spheroid bioactivity. Scientific Reports, 2023. 13. Siriwaseree, J., et al., Exploring the Apoptotic-Induced Biochemical Mechanism of Traditional Thai Herb (Kerra™) Extract in HCT116 Cells Using a Label-Free Proteomics Approach. Medicina, 2023. 59: p. 1376. Ratanabunyong, S., et al., Exploring the apoptotic effects of sericin on HCT116 cells through comprehensive nanostring transcriptomics and proteomics analysis. Scientific Reports, 2024. 14.
SCHOLARSHIP	the Royal Golden Jubilee Ph.D. Program between the National Research Council of Thailand (NRCT) and the Synchrotron Light Research Institute (SLRI)